The Cardenas Formation in East-Central Mexico (Maastrichtian): Stratigraphy, Depositional Environment and Rudist Decline

Zur Erlangung des akademischen Grades eines

Doktors der Naturwissenschaften an der

Fakultät für Bauingenieur-, Geo- und Umweltwissenschaften

der Universität Fridericiana zu Karlsruhe (TH)

genehmigte

Dissertation

von

Armin Schafhauser

aus

Bamberg

2006

Tag der mündlichen Prüfung: 14.12.2005
Referent: Prof. Dr. rer. nat. Wolfgang Stinnesbeck
Korreferent: Priv.-Doz. Dr. rer. nat. Eberhard Frey

Erklärung

Hiermit erkläre ich, die vorliegende Arbeit selbstständig und nur unter Verwendung der angegebenen Hilfsmittel erstellt zu haben. Alle Zitate wurden im Literaturverzeichnis gekennzeichnet.

Karlsruhe, den 15.08.2005 Armin Schafhauser

Acknowledgements

This thesis was prepared at the Geological Institute at the University of Karlsruhe and supervised by Prof. Dr. Wolfgang Stinnesbeck. I am much indebted to him for imparting his knowledge to me and for providing training, encouragement, advice, and funding, as well as for improving my English writing.

A very special thanks goes to Dr. Stefan Götz, Geological Institute, University of Karlsruhe, for his excellent introduction into the fascinating "world of rudists", as well as for his steady support, advice and encouragement. He imparted his knowledge in paleontology and sedimentology to me and provided crucial impulses for the success of the thesis.

For biostratigraphic work, I would like to thank Prof. Dr. Gerta Keller, Department of Geosciences, Princeton University, for determinating the planktic foraminifera, and Christina Ifrim, Geological Institute, University of Karlsruhe, for the determination of the ammonites.

I gratefully acknowledge Dr. Manuel Palacios-Fest, Terra Nostra (Tucson), for the classification of the ostracods, and Dr. Rosemarie Baron-Szabo, Smithsonian Institution (Washington), for the elaboration of the coral taxonomy.

I would like to thank Dr. Thomas Steuber, Institute of Geology, Mineralogy and Geophysics, Ruhr-University (Bochum), for the analyzes of the Sr-isotopes, and Dr. Zsolt Berner, Institute for Mineralogy and Geochemistry, University of Karlsruhe, for the geochemical measurements.

I would like to thank particularly Stefan Unrein for the careful preparation of the fossils and rock samples.

I would like to thank particularly my former colleague Dr. Peter Schulte, Institute of Geology, Mineralogy and Geophysics, Ruhr-University (Bochum), for many constructive and stimulating discussions.

I am grateful to the people who supported me during the field work. A special thanks goes to the Calderon family and José Miguel Díaz. Especially, I would like to thank Juan, Rafael and Victoria, who introduced me into the society of Cardenas and created an atmosphere of well-being. In addition, I would like to thank Prof. Dr. López-Oliva for support.

I am grateful to the DFG (projects STI 128/7, GO 1021/2-1), DAAD (Kurzstipendium für Doktoranden), and AAPG (Grants-In-Aid Program) for funding my work.

I would like to thank my parents, Uta and Siegfried Schafhauser, my sister and her husband, Petra and Sigmar Leyer, for the support of my decision to write this thesis.

Last but not least, a very special thanks goes to Sandra Schwemmle and our son Levi for their essential tolerance, patience, love, and interest.

Abstract

12 sections of the Cardenas and Tabaco formations in east-central Mexico have been analyzed by means of bio-, Sr-isotope, sediment, and sequence stratigraphy in order to reveal the age and depositional facies of the sediment sequence, and to evaluate the age and mode of decline of rudist assemblages in this region.

The Cardenas and Tabaco formations are exposed near the town of Cardenas in the eastern part of the state San Luis Potosí. The Cardenas Formation is 1200 m thick and consists of conglomerate, arenite, siltstone, marl, and limestone. 3 lithologic members are distinguished by the occurrence of coral and rudist-bearing limestone in the lower and upper members and their absence in the middle member. Continental red beds of the Tabaco Formation conformably overlie the Cardenas Formation and reach a visible thickness of approximately 20 m.

Ammonites (*Pachydiscus neubergicus, Sphenodiscus pleurisepta, Coahuilites sheltoni*) and planktic foraminifera (e.g., *Globotruncanita stuarti, Archaeocretacea cretacea, Globotruncanella petaloidea, Gansserina gansseri, Globotruncana linneiana*) indicate an early Maastrichtian age for the middle member of the Cardenas Formation, corresponding to the foraminiferal zones CF5 and CF6. Sr-isotope stratigraphic data suggest an early late Maastrichtian age (67.98 Ma) for the last rudist assemblage in the upper member of the Cardenas Formation, coinciding with the foraminiferal zone CF4. 18 parasequences (4^{th} order cycles) and 3 depositional sequences (3^{d} order cycles) are recognized in the Cardenas and Tabaco formations, and correlation of these depositional sequences with the global sea level chart indicates a late Maastrichtian age for the exposed part of the Tabaco Formation. In consequence, ages for the Cardenas and Tabaco formations range from the early to middle late Maastrichtian.

Depositional environments of the Cardenas and the Tabaco formations represent a wave-dominated shoreface delta system in the foreland belt of the Sierra Madre Oriental. Facies encompass the lower and upper shoreface, and the offshore transition to offshore. Upper shoreface facies consist of conglomerate and arenite, with oysters and actaeonellid gastropods. Mono- to paucispecific rudist reefs occur in lagoonal areas of the upper shoreface and are characterized by the predominance of a single rudist species. In proximal environments of the upper shoreface, rudist species include *Durania ojanchalensis, Macgillavryia nicholasi,* and *Biradiolites* sp., whereas *Praebarrettia sparcilirata* predominates in the distal part. Lower shoreface facies are characterized by arenite, siltstone, and marl, and contain diverse molluscan assemblages consisting of ammonites, gastropods, plagioptychids and non-rudist bivalves. In addition, coral-rudist bioherms characterize high-energy environments of the lower shoreface. Rudists in these environments include *Hippurites ceibarum, Hippurites muelleriedi, Tampsia floriformis, Bournonia cardenasensis, Coralliochama gboehmi,* and *Biradiolites rudissimus.* In contrast, coral-dominated bioherms in protected areas of the lower shoreface contain only rare rudist individuals (*Bournonia cardenasensis, Coralliochama gboehmi, Hippurites* ?*perkinsi*). The rudist- and coral- assemblages reach only minor thickness and extension, probably as a result of high (re-)sedimentation rates and frequent reworking of the reef fauna in the shallow depositional area. In the offshore transition zone, reefs are absent, and lithologies are predominated by siltstone and marl. The fauna includes *Pachydiscus neubergicus, Exogyra costata,* branching bryozoans, as well as abundant orbitoidacean foraminifera (*Lepidorbitoides minima*). Offshore facies consist of siltstone and marl with

abundant planktic foraminifera and calcispheres. The red conglomerate, arenite, silt-, and claystone of the Tabaco Formation represent the most proximal environments in the upper shoreface. Paleosoil in the red-colored sediments indicates subaerial emersion of the depositional area, caused by the progradation of the foreland belt and a decrease in sea level. This emersion resulted in the total loss of rudist habitats in east-central Mexico during the late Maastrichtian.

Kurzfassung

In der vorliegenden Arbeit wurden 12 Profile der Cardenas und Tabaco Formation (Ost-Zentralmexiko) biostratigraphisch und sedimentologisch untersucht sowie sequenzstratigraphisch interpretiert. Ziel der Arbeit war es, Daten zu Alter und Ablagerungsbedingungen der Cardenas und der Tabaco Formation zu gewinnen, um den Zeitraum und die Ursachen für das Rudistenaussterben in Ost-Zentralmexiko zu erfassen.

Die Cardenas Formation und die Tabaco Formation sind im östlichen Teil des zentralmexikanischen Bundesstaates San Luis Potosí aufgeschlossen. Die Cardenas Formation besteht aus einer ca. 1200 m mächtigen sedimentären Sequenz aus Konglomerat, Arenit, Siltstein, Mergel und Kalkstein. Sie wird in drei lithologische Einheiten (Members) unterteilt. Das Untere und Obere Member sind durch rudisten-und korallenführende Kalksteine charakterisiert, die im Mittleren Member fehlen. Die Cardenas Formation wird konkordant von den kontinentalen Rotsedimenten der Tabaco Formation überlagert, welche im Untersuchungsgebiet eine sichtbare Mächtigkeit von ca. 20 m erreicht.

Ammoniten (*Pachydiscus neubergicus*, *Sphenodiscus pleurisepta*, *Coahuilites sheltoni*) und planktonische Foraminiferen (u.a. *Globotruncanita stuarti*, *Archaeocretacea cretacea, Globotruncanella petaloidea*, *Gansserina gansseri*, *Globotruncana linneiana*) ergeben ein spätes Unter-Maastricht Alter (Foraminiferen Zonen CF5 oder CF6) für das Mittlere Member der Cardenas Formation. Sr-Isotopen Daten zeigen ein frühes Ober-Maastricht Alter für die letzten Rudisten Assoziation im Oberen Member an. 18 Parasequenzen (Zyklen 4. Ordnung) und 3 Sequenzen (Zyklen 3. Ordnung) wurden in der Cardenas und Tabaco Sedimentfolge unterschieden. Ihre Korrelation mit der globalen Meeresspiegelkurve ergibt ein Ober-Maastricht Alter für die Tabaco Formation.

Die sedimentäre Abfolge der Cardenas Formation und der Tabaco Formation repräsentiert ein wellendominiertes Küsten-Delta System im Vorlandgürtel zur Sierra Madre Oriental. Sie enthält Fazies des oberen (flachen) und unteren (tiefen) Subtidal, eine Subtidal-Becken Übergangsfazies sowie Beckensedimente. Das obere Subtidal ist charakterisiert durch Konglomerat und Arenit, die Austern und actaeonellide Gastropoden enthalten. In lagunären Bereichen treten mono- bzw. paucispezifische Rudistenassoziationen auf, die jeweils durch eine einzelne Rudistenart dominiert werden, bsw. *Durania ojanchalensis, Macgillavryia nicholasi* oder *Biradiolites* sp. In distalen Bereichen des flachen Subtidal dominiert ?*Praebarrettia sparcilirata*. Arenit, Siltstein und Mergel des unteren Subtidal enthalten Ammoniten, Gastropoden, Plagioptychiden und andere (Nicht-Rudisten) Bivalven. Bereiche mit erhöhter Wasserenergie sind außerdem durch diverse Korallen-Rudistenbioherme charakterisiert, mit den Rudistenarten: *Mitrocaprina* cf. *tschoppi, Coralliochama gboehmi, Tampsia floriformis, Tampsia poculiformis, Bournonia cardenasensis, Biradiolites rudissimus, Hippurites perkinsi*. In geschützten Bereichen mit niedriger Wasserenergie wird die Biohermfauna von Korallen dominiert, wohingegen Rudisten (*Bournonia cardenasensis, Coralliochama gboehmi, Hippurites perkinsi*) zahlenmäßig zurücktreten. Wegen der hohen (Re-)Sedimentationsraten und häufiger Aufarbeitung der Riff-Fauna erreichen die rudisten- und korallenführenden Kalke in dem seichten Ablagerungsraum nur geringe Mächtigkeiten und laterale Ausdehnung. In der Übergangszone zwischen Subtidal und Becken dominieren Siltstein und Mergel. Sie enthalten *Pachydiscus neubergicus, Exogyra costata,* verzweigte Bryozoen und orbitoide Foraminiferen (*Lepidorbitoides minima*). In der Beckenfazies dominieren Siltstein und Mergel mit planktonischen Foraminiferen und Calcisphären. Die kontinentalen Rotsedimente der

Tabaco Formation (Konglomerat, Arenit, Silt- und Tonstein) werden als Delta-Sedimente interpretiert. Paläoböden zeigen wiederholtes Auftauchen des Ablagerungsraumes an, das auf Progradation des Vorlandgürtels sowie eustatischen Abfall des Meeresspiegels zurückgeführt wird. Dieses Auftauchen und das sukzessive Verschwinden ihres Lebensraumes führte im Obermaastricht zum Niedergang der Rudisten in Ost-Zentralmexiko.

Content

1 Introduction

During the Upper Cretaceous, a significant change in facies took place in northeast and east-central Mexico, leading from the extended lower and "middle" Cretaceous carbonate platforms (e.g., Cupido Platform, Valles-San Luís Potosí platform) to clastic-dominated environments (e.g., Sohl et al., 1991; Moran-Zenteno, 1994; Goldhammer and Johnson, 2001). This change was caused by the uplift of the Sierra Madre Oriental, and clastic sediments were deposited in the newly developed foreland (e.g., Lopez-Ramos, 1985; Ye, 1997; Goldhammer and Johnson, 2001). In northeastern Mexico, shallow water environments are represented by the delta complex of the Difunta Group (Figure 1) exposed in the Parras and La Popa basins (e.g., McBride et al., 1974; Soegaard et al., 1997; Lawton et al., 2001; Soegaard et al., 2003). In east-central Mexico, the Cardenas Formation was deposited in the Tampico-Mizantla Basin (Myers, 1968; Goldhammer and Johnson, 2001). Deeper water environments are represented by the marls of the Mendez Formation (e.g., Sohl et al., 1991; Moran-Zenteno, 1994; Goldhammer and Johnson, 2001).

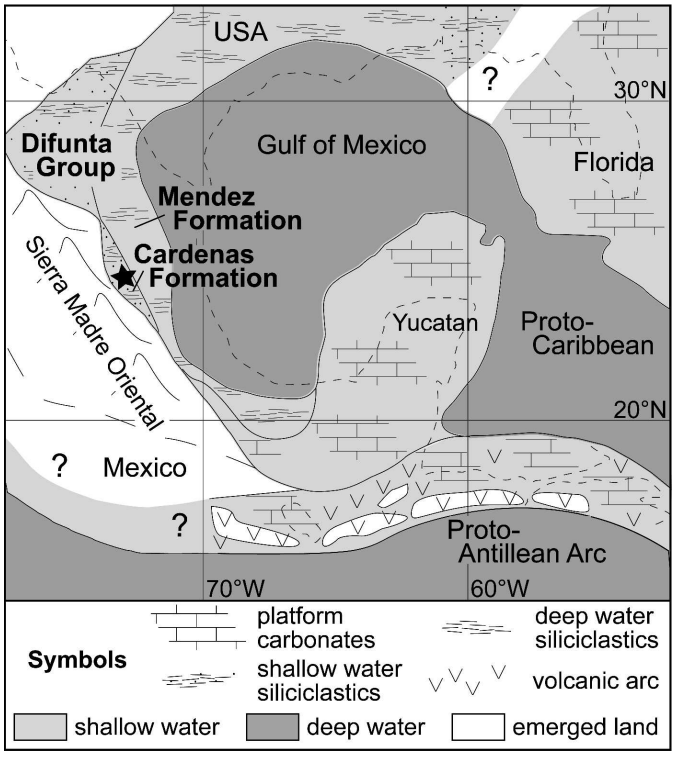

Figure 1: Maastrichtian palaeogeography of the Gulf of Mexico and northern Caribbean (after Pindell et al., 1988; Sohl et al., 1991; Goldhammer & Johnson, 2004). Asterisk marks the location of the studied area.

Rudist assemblages, characteristic elements of lower and "middle" Cretaceous carbonate platforms (e.g., Basáñez-Loyola et al., 1993; Wilson and Ward, 1995; Alencáster and Oviedo-García, 1998; Alencáster and Pantoja-Alor, 1998) are also abundant in the clastic shallow water sediment units of the Difunta Group and the Cardenas Formation (McBride et al., 1975; Johnson and Kauffman, 1996) and are even known from the Mendez Formation (Stephenson, 1922). In recent years, composition and stratigraphy of the Difunta Group (e.g., Vega and Perrilliat, 1995; Soegaard et al., 1997; Vega et al., 1999; Lawton et al., 2001; Soegaard et al., 2003), and Mendez Formation (Ifrim et al., 2004) have been analyzed in some detail, and many studies focused on complex sediment units spanning the Cretaceous/Paleocene (K/P, formerly K/T) boundary (e.g., Stinnesbeck et al., 1993; Stinnesbeck and Keller, 1996; Stinnesbeck et al., 1996; Stinnesbeck et al., 2001; Keller et al., 2002; Schulte, 2003; Schulte et al., 2003; Lawton et al., 2005). In contrast, stratigraphic data on the Cardenas Formation are scarce. Outcrop data and macrofossils as well as benthic foraminifera indicate Campanian(?) to Maastrichtian ages (Myers, 1968; Aguilar et al., 2002; Caus et al., 2002; Ifrim et al., 2005), but stratigraphic marker fossils pro-

viding precise age data are not known. Nevertheless, due to the description of Myers (1968) rudists of the Cardenas Formation have been considered as some of the last known assemblages worldwide, and a gradual extinction pattern has been suggested by Johnson and Kauffman (1996). I agree with these authors that the Cardenas Formation is an excellent outcrop area to study the mode of rudist extinction. However, the gradual extinction pattern is based only on the vague description of rudist assemblages provided by Myers (1968), and timing of the extinction is questionable. Moreover, environmental conditions (e.g., siliciclastic input, water depth, current energy) have not been considered by Johnson and Kauffman (1996) as controlling factors of composition and structure of the various rudist associations.

The present research intents to document the age, depositional facies and sequence stratigraphic framework of the Cardenas Formation and overlying Tabaco Formation, in order to delineate the geological evolution of the Cardenas area and its relation to the geological history of eastern Mexico. In addition, the evolutional pattern of rudist assemblages within the Cardenas Formation and its controlling factors are documented. Special attention has been paid to:

1) Stratigraphy (see chapter 2). A stratigraphic framework of the Cardenas and Tabaco formations is developed, which allows determining the age of rudist assemblages within the Cardenas Formation and their evolution.

2) Depositional facies and environments (see chapters 4 and 5), as well as their variations within the Cardenas and Tabaco formations. These data are necessary to reconstruct the geological evolution of the Cardenas area during the Maastrichtian, to develop a sequence stratigraphic framework, and to recognize compositional variations in rudist assemblages caused by environmental changes.

3) Structure and composition of rudist assemblages (see chapter 4), to distinguish different types of reefs and to detect the causes and controlling factors of their development.

4) Sequence stratigraphic framework (see chapter 6), to correlate the Cardenas Formation with the Maastrichtian sea level chart provided by Hardenbol and Robaszynski (1998). This set of data yields additional information regarding the age and stratigraphy and helps to detect compositional changes of rudist assemblages caused by changes of the sea level.

1.1 Geological setting

The Cardenas Formation is a 1200 m thick mixed siliciclastic-carbonate sedimentary sequence of the Campanian(?) to Maastrichtian age and is exposed close to the city of Cardenas in the State of San Luis Potosí in east-central Mexico (Figure 2). The Cardenas Formation conformably overlies the Tamasopo Formation that consists of shallow water carbonates of Santonian to Campanian(?) age (Figure 3; Basáñez-Loyola et al., 1993).

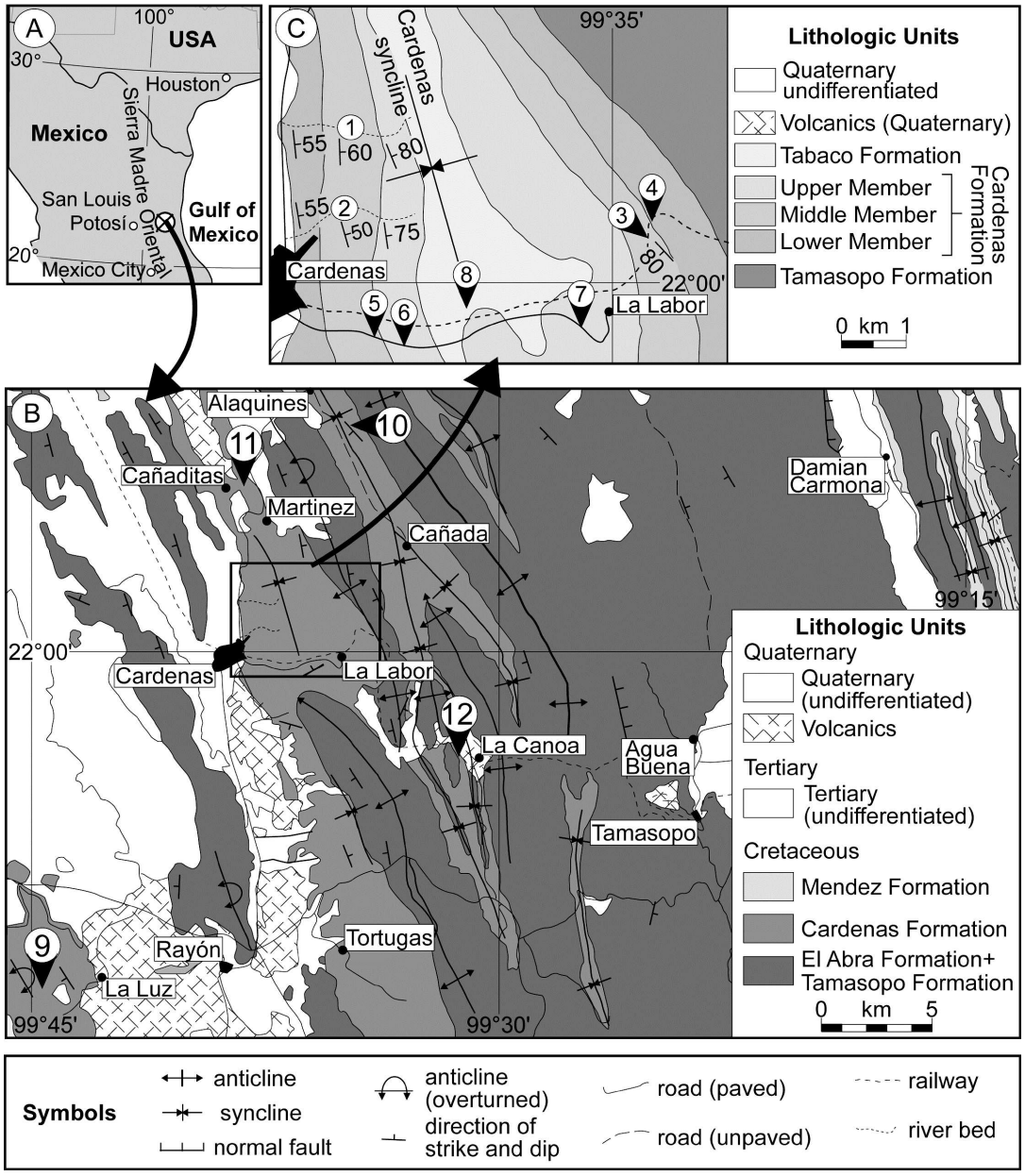

Figure 2: Location and geologic map of the studied area in east-central Mexico (A) and position of the sections investigated here (1–12), with enlargement of the Cardenas syncline (C). Sections: (1) Arroyo de la Atarjea, (2) Cardenas, (3) Railway I, (4) Railway II, (5) Cerro Mocho II, (6) Cerro Mocho I, (7) La Labor, (8) La Presa, (9) La Luz, (10) Morales, (11) Cañaditas, (12) Estación Canoa. After the geologic maps of the Comisión de Estudios del Territorio Nacional (sheet F-14-5, Ciudad Mante, scale 1:250 000; sheet F-14-8, Ciudad Valles, scale 1:250 000; sheet F-14-A88, Alaquines, scale 1:50 000), Smith (1986), Myers (1968), and own observations.

Towards the east, the Cardenas Formation passes into the deep-water marls of the coeval Mendez Formation, which in turn overlie marls and limestones of the Coniacian to Campanian San Felipe Formation (e.g., Lopez-Ramos, 1985; Sohl et al., 1991; Basáñez-Loyola et al., 1993). Upsection, continental red beds of the Tabaco Formation conformably overlie the Cardenas Formation (Myers, 1968). No fossils are known to exist in the Tabaco Formation. Nevertheless, Myers (1968) suggested an Upper Cretaceous or Lower Paleocene age. Tectonically, the Tamasopo, Cardenas, and Tabaco formations are part of the fold and thrust belt of the Sierra Madre Oriental of eastern Mexico, whereas marls of the Mendez Formation

were deposited in the corresponding foredeep to the east (e.g., Sohl et al., 1991; Moran-Zenteno, 1994; Goldhammer and Johnson, 2001).

The transition from the carbonate platform sediments of the Tamasopo Formation to the mixed siliciclastic-carbonate sediments of the Cardenas Formation took place during the Campanian and Maastrichtian and documents a change in facies from carbonate to clastic dominated environments, (Sohl et al., 1991; Moran-Zenteno, 1994; Goldhammer and Johnson, 2001). In northeastern Mexico, similar clastic environments of Campanian to Maastrichtian age are represented by the deltaic to prodeltaic Difunta Group, which passes eastwards into the basin sediments of the Mendez Formation (Figure 1). The beginning of clastic sediment input is attributed to early orogenetic phases of the Sierra Madre Oriental (Sohl et al., 1991; Ye, 1997; Goldhammer and Johnson, 2001). Due to this orogenetic uplift, underlying older lithostratigraphic units were eroded and sediments redeposited in the foreland basin east of the Sierra Madre Oriental (Ye, 1997). Subsequently, during the main orogenic phases in the Paleocene, the foreland belt prograded and sediments of the Cardenas Formation were folded to broad anticlines and synclines (Fuente-Navarro, 1964; Torre, 1964; Suter, 1987).

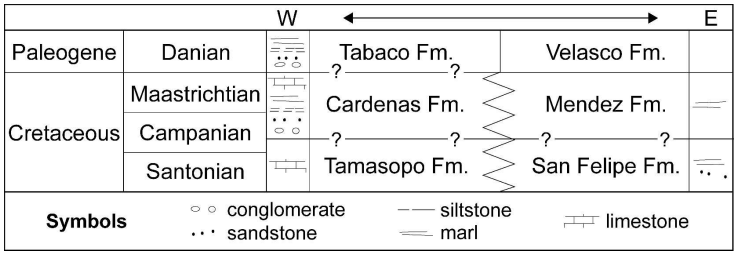

Figure 3: Stratigraphy and lithology of the Santonian to early Paleogene formations exposed adjacent to the Cardenas Formation in east-central Mexico. Marl and sandstone of the San Felipe and Mendez formations represent deep water equivalents to the shallow water carbonates of the Tamasopo Formation and the mixed siliciclastic-carbonate Cardenas Formation. Age ranges are not well defined in central Mexico (after Sohl et al., 1991 and Basañez-Loyola et al., 1993).

1.2 Applied nomenclature and symbols

In the following, the nomenclature used in this research is listed and defined, if controversy about the meaning and significance exists in the literature.

Lithology: The description of carbonate microfacies is based on the classification of Wright (1992), who revised the classification of Dunham (1962) and Embry and Klovan (1971) and expanded it to diagenetically altered limestones. Clastic sediments are subdivided by grain-size into conglomerate, arenite, siltstone, and marl. The term “arenite” describes a fine-grained sandstone, which is framework supported and consists of approximately 50% carbonate rock fragments and siliciclastic grains (Flügel, 2004).

Reefs: Rudists generally grew in biogenic assemblages of various compositions and structures. In recent years, a debate arose about the applicability of the term “reef” for these assemblages, but also about a general definition of the term “reef”. A detailed overview about the history and diversity of reef definitions is provided by Höfling (1997) and will not be repeated here. In the present investigation, the classification scheme recently presented by Riding (2002) is used, and reefs are defined as “calcareous deposits created by essentially in place sessile organisms” (Riding, 2002, p. 165). This simple scheme tries to avoid reef classification by subjective interpretations, such as wave resistance, which can hardly be tested in the geologic record (Riding, 2002). Instead, classification is based on observable reef struc-

tures, which is easy to apply on biogenic frameworks of the geological past (Riding, 2002). Within a reef, rudists occur as “isolated individuals”, without any connection to adjacent specimens, or in small groups of few individuals called “bouquet” (Cestari and Sartorio, 1995). “Clusters” are bigger groups of a few dozens of specimens, and “thickets” contain several dozens to hundreds of rudists (Cestari and Sartorio, 1995). This scheme does not consider rudist diversity or interactions between rudist individuals, such as point contacts or coalesced individuals, which are often difficult to observe in the field.

Rudists: Palecological morphotypes of rudist individuals are classified by using the scheme provided by Skelton and Gili (1991), who distinguished elevator, clinger and recumbent morphotypes (Figure 4).

Elevator morphotypes grew perpendicular to the bedding plane. Their conical right valve stacked into the substrate and stabilized the rudist shell allowing a stable upward growth. Elevators were thus able to settle in environments, where sedimentation rates almost reached their growth rates (Skelton and Gili, 1991). Clinger morphotypes were not able to persist high sedimentation rates. They grew upon the sediment surface or the lower part of the attached valve anchored within the sediment (Skelton and Gili, 1991). Clingers thus settled on hard substrate or in areas, which were only sporadically or never affected by sediment input (Skelton and Gili, 1991). The recumbent growth mode permitted rudists to settle in high-energy environments with mobile and coarse substrate, but required the absence of any sediment accumulation (Skelton and Gili, 1991).

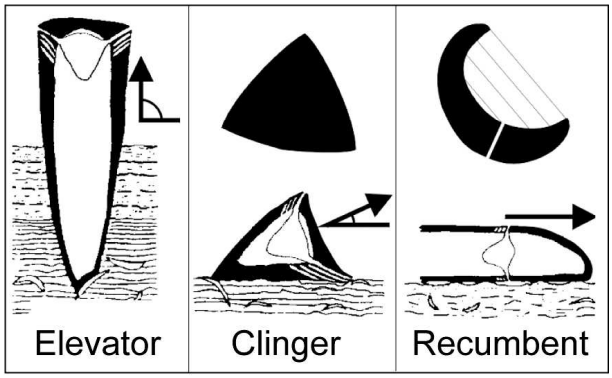

Figure 4: Rudist morphotypes defined by Skelton & Gili, (1991). Arrows mark the direction of growth relative to the sediment surface. In the plan views, the area of contact between shell and substratum is labeled in black. Together with the lined field (only in recumbent type), it marks the effective zone providing stabilisation on mobile substrate (after Skelton & Gili, 1991).

Sequence stratigraphy: The terminology recently provided by Coe (2003) was employed, who summarized the vast number of articles on sequence stratigraphy published in recent years (e.g., Vail and Mitchum, 1977; Van Wagoner et al., 1988; Wilgus et al., 1988; Galloway, 1989a, b; Van Wagoner et al., 1990; Vail et al., 1991; Van Wagoner, 1995; Miall, 1997; Strasser et al., 1999). The sequence stratigraphic terms used in the present research are presented in chapter 6.

Sections: Each section is described in terms of sedimentary facies. Sections are illustrated in 10 m intervals. Only if sections are less than 100 m thick, 1 m intervals have been used and, for comparison, illustrations in 10 m intervals are added.

Each section figure contains 7 columns, which include: age (stage and – if possible – substage), lithostratigraphic unit (formation and member), scale, litholog, fossil content, environmental interpretation, and sequence stratigraphic interpretation.

Explanation and abbreviations to symbols used in the figures are given in Figure 5. Unless figures contain separate explanations, this legend is valid for all figures of the investigation.

1.3 Methods

The geologic maps Ciudad Mante (sheet F-14-5, scale 1:250 000), Ciudad Valles (sheet F-14-8, scale 1:250 000), Alaquines (sheet F-14-A88, scale 1:50 000) and Rio Verde (sheet F-14-C17, scale 1:50 000) of the Comisión de Estudios del Territorio Nacional (CETENAL) were used for orientation in search of new outcrops. For every section studied here, all rock types were sampled for microfacies analysis, and reefs have been described in terms of geometry, lithology (macro- and microfacies), and faunal composition. Reef sediment has been prepared by large-sized thin sections (7 cm x 5 cm), to document the various microfacies within a reef limestone; for homogenous arenite, marl, and siltstone, small-sized thin sections (4.5 cm x 2.8 cm and 4.5 cm x 4.5 cm) have been used. For biostratigraphic and environmental analysis, microfossils (ostracods, foraminifera) have been picked from siltstones and marls, but have also been analyzed in thin sections. Taxonomy of corals and rudists has been determined by using thin sections and polished sections.

Samples, used for Sr-isotope stratigraphy (see chapter 2.3), were drilled with tungsten instruments from well preserved areas of the outer shell layer of *Coralliochama*. The state of preservation was analyzed in thin sections, and the absence of diagenetic alteration in the selected samples was verified by measuring Mn, Fe, Sr, and Mg concentrations with inductively couplet plasma-mass spectrometry (ICP-MS). Sr was separated by standard ion-exchange methods, and isotope ratios were analyzed on a Finnigan MAT 262 thermal-ionization mass spectrometer.

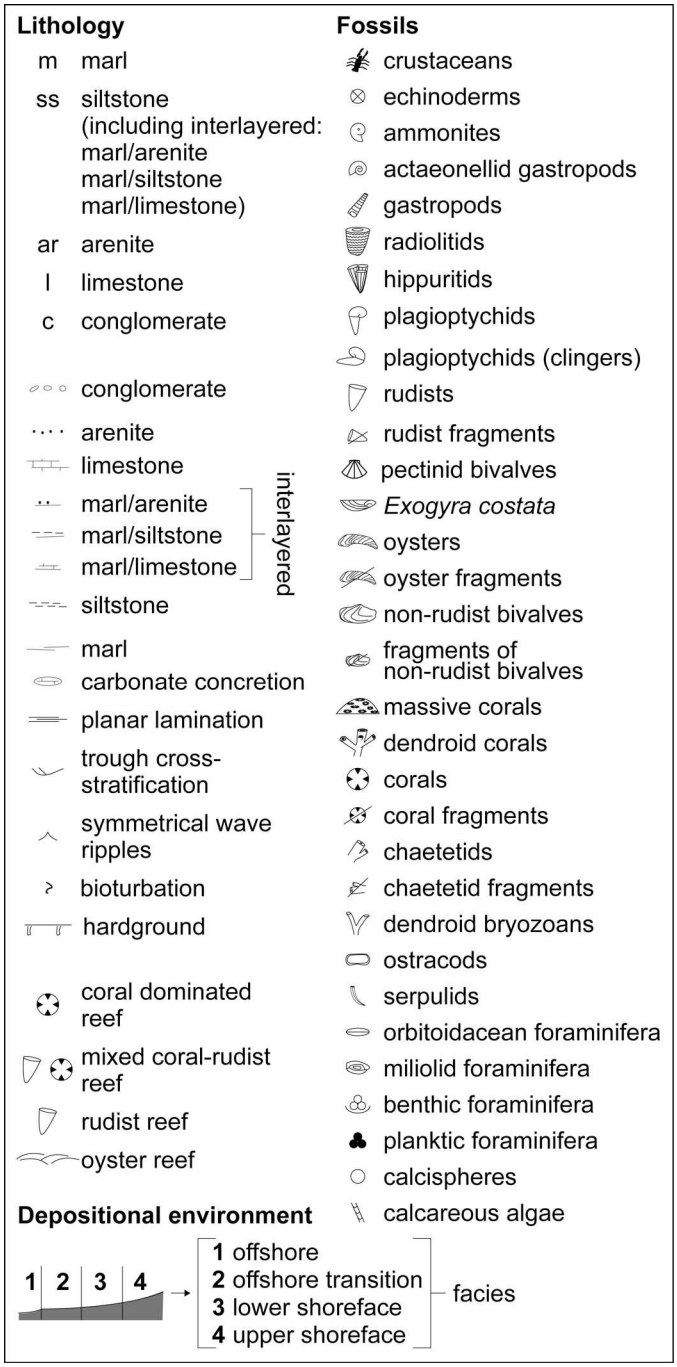

Figure 5: Key to symbols and abbreviations used in the stratigraphic columns.

1.4 State of Research

The fauna of the Cardenas Formation is relatively well known, and numerous new species have been described in the past 40 years, such as the crustacean *Branchiocarcinus coronatus* (Vega and Feldmann, 1991), several gastropods and non-rudist bivalves (e.g., *Turritella guionae*, *Cardium cardenasensis*; Böse, 1906), as well as the foraminifer *Lepidorbitoides minima* (Douvillé, 1927). Vega and Feldmann (1991) emphasized the similarity between the molluscan fauna of the Cardenas Formation and the Difunta Group of northeastern Mexico, an aspect, already recognized by Böse (1906) and recently supported by comparative studies of the ammonite fauna (Ifrim et al., 2005). Moreover, the Cardenas Formation is the type localitiy of several rudist species, such as *Biradiolites aguilerae*, *Bournonia cardenasensis*, *Coralliochama gboehmi*, *Hippurites perkinsi*, *Tampsia floriformis*, and *Durania ojanchalensis* (Böse, 1906; Myers, 1968). Their depositional environment, as well as the structures and compositions of various rudist reefs of the Cardenas Formation, have recently been described by Schafhauser (2003). Johnson and Kauffman (1996) suggested, that a stepwise extinction pattern of rudists prior to the K/P boundary is documented for the Cardenas Formation.

Since the first publication on the Cardenas Formation by Böse (1906), biostratigraphy and age have been discussed (Böse and Cavins, 1927; Burckhardt, 1930; Heim, 1940; Mueller-ried, 1941; Imlay, 1944). A Campanian to Maastrichtian age was proposed by de la Torre (1964), de la Fuente-Navarro (1964) and Carrillo-Bravo (1971) based on benthic foraminifera. Recently, Caus (2002) and Aguilar (2002) analyzed ostracods and foraminifera in the type section of *Lepidorbitoides minima*. They assume an isochronic occurrence of *Lepidorbitoides minima* in the central and western Tethys and suggest a late Campanian age for the lower Cardenas Formation.

In a comprehensive study, Myers (1968) subdivided the Cardenas Formation. Based on lithological differences, he distinguished in the Arroyo de la Atarjea a lower, middle, and upper member (Myers, 1968). The lower and upper members consist of sandstone, shale, and limestone and contain abundant rudist assemblages (Figure 6). The middle member is dominated by shale, whereas limestone is scarce and rudist assemblages absent. However, the boundaries between the members are not well defined, and determination of their precise position in the field is difficult. In addition, Myers (1968) separated 3 biozones in the Cardenas Formation (from below to above): the *Durania ojanchalensis*, the *Arctostrea aguilerae*, and the *Tampsia floriformis* zone (see Figure 6; Myers, 1968). The extensions of the members and biozones almost coincide. According to Myers (1968), depositional facies of the *Arctostrea aguilerae* and the *Tampsia floriformis* biozones are similar,

and terrigenous sediments predominate. In the *Durania ojanchalensis* zone, on the other hand, terrigenous sediment is less abundant, and limestone prevails (Myers, 1968). Myers (1968) concluded that the absence of *Durania* in the *Arctostrea aguilerae* and *Tampsia floriformis* biozones is a result of this change in depositional facies. Consequently, Myers (1968) suggested, that the disappearance of *Exogyra costata* in the upper *Arctostrea aguilerae* biozone, should be a result of its extinction, because environmental conditions stayed constant from the *Arctostrea aguilerae* to the *Tampsia floriformis* biozones.

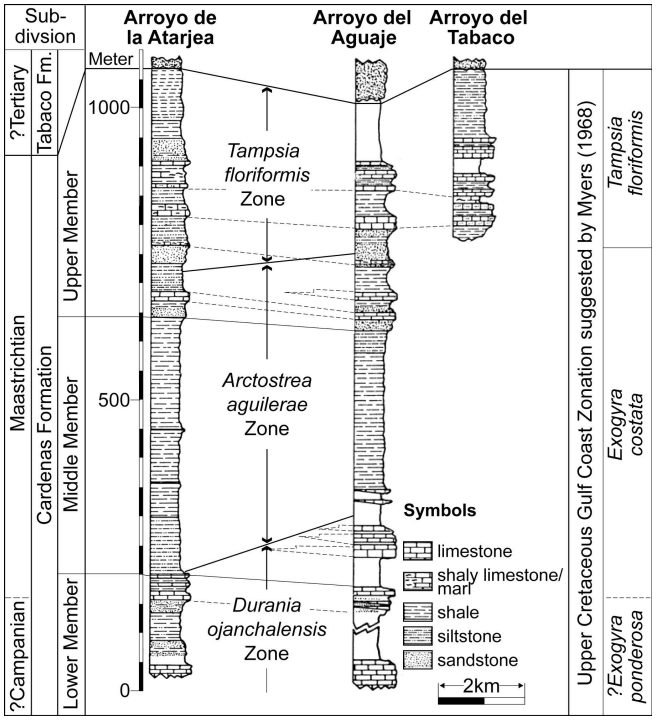

Figure 6: Subdivision of the Cardenas Formation after Myers (1968). See text for discussion.

Myers (1968) correlated these biozones of the Cardenas Formation to the Upper Cretaceous zonal scheme for the Northern Gulf of Mexico, which was introduced by Wade (1926) and Stephenson (1941). According to Myers (1968), the upper *Durania ojanchalensis* and the *Arctostrea aguilerae* biozones correspond to the Maastrichtian *Exogyra costata* zone. The lower part of the *Durania ojanchalensis* biozone is correlated with the Campanian to Maastrichtian *Exogyra ponderosa* zone and the *Tampsia floriformis* zone considered as a new Maastrichtian biozone above the LAD of *Exogyra costata* (Myers, 1968). For the overlying unfossilifereous Tabaco Formation, Myers (1968) suggested a latest Cretaceous to early Paleocene age.

2 Subdivision and Stratigraphy

2.1 Lithologic members

Myers (1968) separated 3 lithologic members in the Cardenas Formation (see chapter 1.4). However, the lack of precise defined boundary layers makes determination of the members in the field difficult and hamper correlation of the sections. According to my observations, the subdivision of members by the presence or absence of rudist reefs is more practical (and roughly corresponds to Myer`s subdivision). Hence, I define the boundary between the lower and middle member immediately above the last reef-bearing limestone that occurs below the thick siltstone and marl unit characterizing the middle member. Consequently, the boundary between the middle and upper member is defined at the base of the first reef limestone that occurs upsection from the thick siltstone and marl unit of the middle member. Reef limestone of the lower member is characterized by mono- to paucispecific rudist assemblages predominated by *Durania*, *Macgillavryia*, and *Praebarrettia* (see chapters 4.1.1 and 4.1.2). Reef limestone of the upper member contains abundant coral-rudist and coral-dominated reefs, whereas rudist reefs are sparse (see chapters 4.2.1 and 4.2.2).

2.2 Biostratigraphy

The Cardenas and Tabaco formations mainly consist of shallow water deposits, which lack widely used biostratigraphic index fossils. The occurrence of *Exogyra costata*, which I found

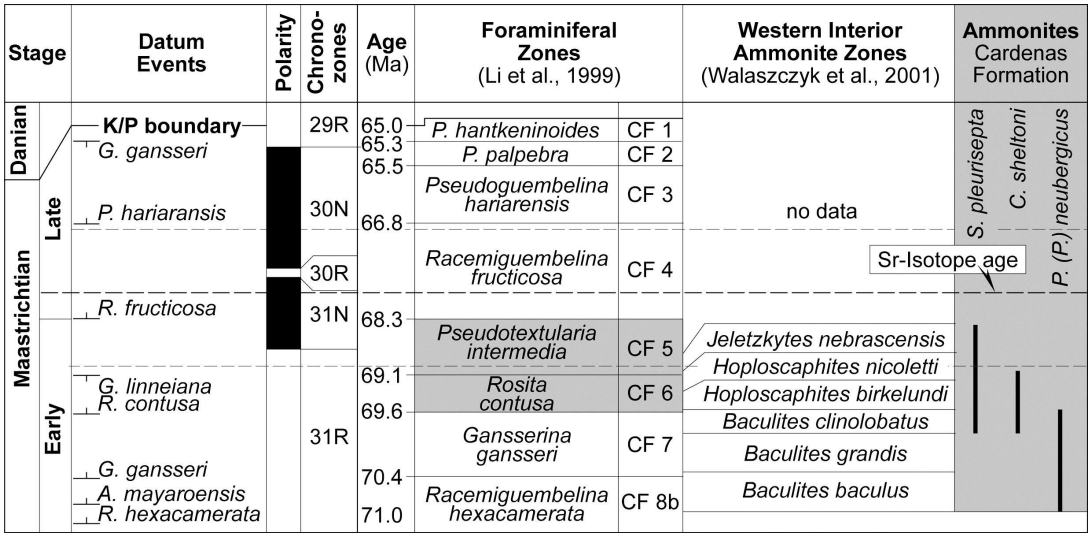

Figure 7: Calibration of bio- and Sr-isotope data of the Cardenas Formation (grey) based on ammonites, planktic foraminifera, and Sr-isotopes. Maastrichtian time scale provided by Li et al. (1999). Western Interior ammonite zones defined by Walaszczyk et al. (2001). Correlation of ammonite and foraminiferal zones after Ifrim et al. (2005) and of chrono- and foraminiferal zones after Li & Keller (1998). Grey dashed lines indicate Sr-age ranges due to limits of analytical precision and statistical uncertainty of seawater curve. See text for discussion.

in the middle member and in the lower part of the upper member, indicates a Maastrichtian age for these units.

Pachydiscus (Pachydiscus) neubergicus is present in marls of the upper part of the lower member exposed in the Railway II section. This species defines the early Maastrichtian (Gradstein et al., 2004; Ifrim et al., 2005). Its LAD is correlated with the LAD of *Baculites clinolobatus* in the Western Interior (Ifrim et al., 2005), which almost corresponds to the upper boundary of the foraminiferal zone CF7 in the Maastrichtian zonation provided by Li (1999). In addition, *Sphenodiscus pleurisepta* co-occurs with *Coahuilites sheltoni* in a siltstone layer in the lowermost middle member of the Arroyo de la Atarjea section (see chapter 3.1). Sediments containing *Sphenodiscus pleurisepta* and *Coahuilites sheltoni* cannot be older than the *Baculites clinolobatus* zone of the Western Interior (Figure 7; Ifrim et al., 2005). In consequence, an early Maastrichtian age is assigned to the upper lower and basal middle member of the Cardenas Formation based on the Maastrichtian zonation provided by Li (1999).

In addition, in the Arroyo de la Atarjea section a diverse planktic foraminiferal assemblage was identified in a 15 m thick siltstone unit in the middle part of the middle member, 170 m upsection of the layers containing *Sphenodiscus pleurisepta* and *Coahuilites sheltoni* (see Figures 8 and 27). The following species are present (Plate 12): *Globotruncana arca*, *Globotruncana aegyptiaca Globotruncana dupeublei*, *Globotruncanita stuarti*, *Archaeocretacea cretacea*, *Globotruncanella petaloidea*, *Gansserina gansseri*, *Rugoglobigerina rugosa*,

Rugoglobigerina rugosa pennyi, *Hedbergella monmouthensis*, *Globigerinelloides aspera*, *Heterohelix globulosa*, *Guembelitria cretacea*, and *Globotruncana linneiana* (pers. comm. Gerta Keller). The foraminiferal assemblage is assigned to foraminiferal zones CF5 or CF6 (Li and Keller, 1998b), resulting in a late early Maastrichtian age of the middle member within an interval of 70.4 Ma to 68.1 Ma.

2.3 Sr-isotope stratigraphy

$^{87}Sr/^{86}Sr$-isotope ratios were analyzed in the outer low-Mg calcite shell layer of well preserved plagioptychids (*Coralliochama*), to determine the age of the uppermost rudist reef in the Cardenas Formation. The method is well established and described in detail by numerous authors (e.g., McArthur, 1994; Crame et al., 1998; McArthur et al., 2000; McArthur et al., 2001; Steuber, 2001; Steuber et al., 2002; Steuber, 2003).

4 samples from 4 different specimens were analyzed, which were collected from the uppermost rudist reef in the Arroyo de la Atarjea section (see chapters 3.1 and 6). The absence of covariations of Mn, Fe and Sr concentrations, and the small range of $^{87}Sr/^{86}Sr$ values in the samples, testify to a good preservation of original isotope ratios in the samples selected (see Table 1). Diagenetically altered low-Mg calcite is frequently indicated by high concentrations of Mn and Fe and low Sr-concentrations (Veizer, 1983), which was not observed in the samples.

The resulting Sr-value of 0.707788 in the rudist shells determines an age of 67.98 Ma for the last rudists of the Cardenas Formation (pers. Comm. Thomas Steuber, 2004), corresponding to the lower part of foraminiferal zone CF4 (Figure 7). The limit of analytical precision, statistical uncertainties (2 s. e.), and the uncertainty related to the strontium isotope curve span a lower and upper age limit of 66.93 Ma and 68.96 Ma, respectively (e.g., Howarth and McArthur, 1997; Steuber, 2001; Steuber et al., 2002 for details).

Table 1: Analytical results of low-Mg calcite of plagioptychid rudists from the uppermost reef of the Cardenas Formation:

Sample no.	$^{87}Sr/^{86}Sr$	$\pm$ 2 s.e. (x 10^{-6})	Sr (µg/g)	Mg (µg/g)	Fe (µg/g)	Mn (µg/g)
NCT 120-1	0.707754	7	1260	2534	450	19.8
NCT 120-2	0.707766	6	1373	3408	356	17.4
NCT 120-3	0.707766	7	1316	1609	208	18.3
NCT 120-4	0.707745	7	1375	2335	450	49.8
EN-1 (Standard)	0.709151	7				
EN-1 (Standard)	0.709138	7				
Mean	0.707758	7	Age (Ma): > 66.93		67.98	< 68.96

3 Sections

The exposed combined thickness of the Cardenas and overlying Tabaco formations is approximately 1220 m. The 1200 m thick Cardenas Formation includes conglomerate, arenite,

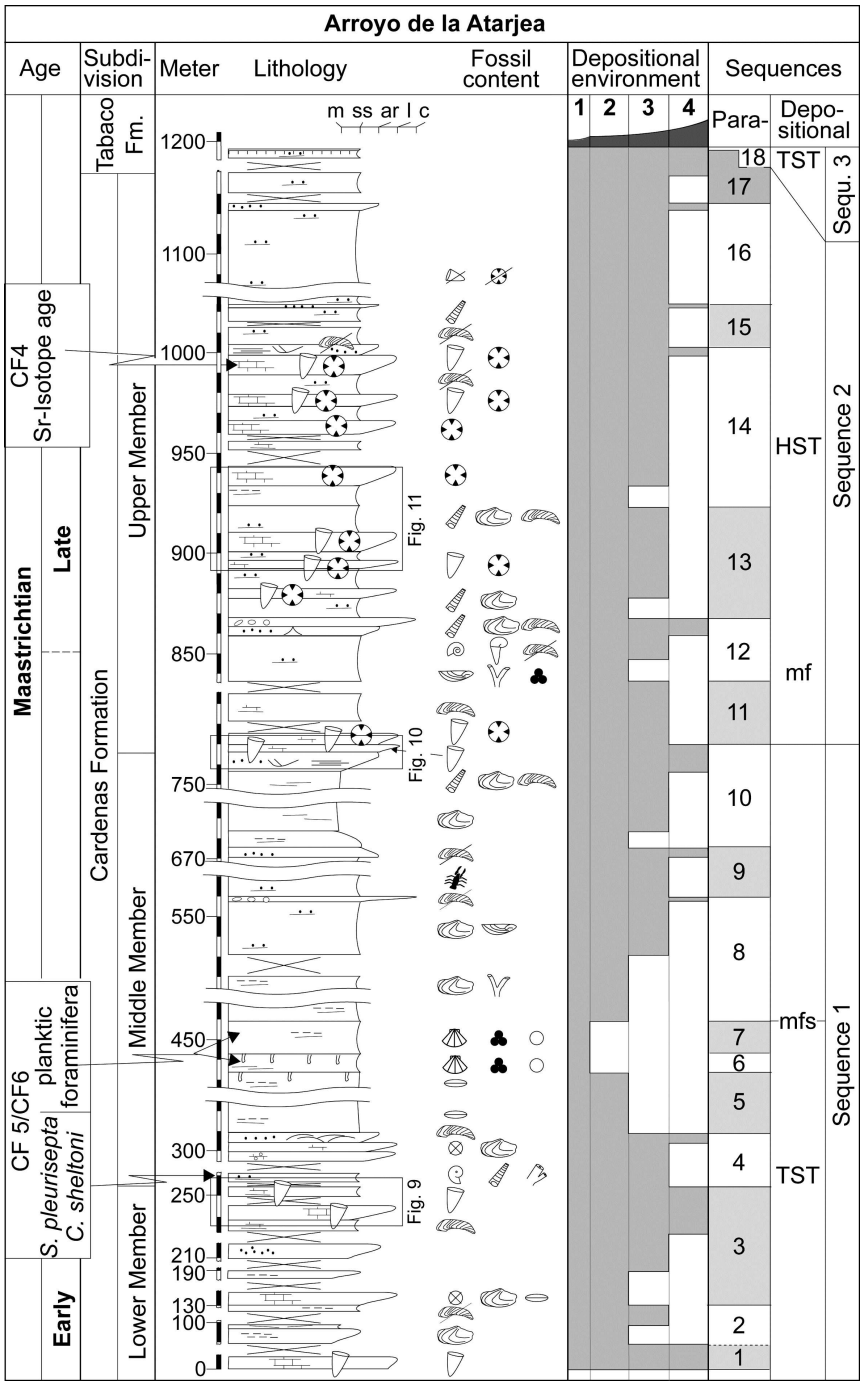

Figure 8: Section Arroyo de la Atarjea. Ammonites (*Sphenodiscus pleurisepta, Coahuilites sheltoni*) at 260 m and planktic foraminiferal assemblage between 435 m and 450 m (foraminiferal zones CF5 or CF6) indicate an early Maastrichtian age for the middle member (see chapter 2 for details). A late Maastrichtian age for the upper member is indicated by Sr-isotope stratigraphy (see chapter 2.3) and sequence stratigraphic correlation (see chapters 6 and 7.2 for details).

siltstone, and marl, as well as reefal and non-reefal limestone. The Tabaco Formation is about 20 m thick and consists of conglomerate and red colored arenite, silt-, and claystone. In contrast to the resistant and widely exposed limestone units of the Valles-San Luis Potosí carbonate platform of Valanginian to Campanian age, the clastic sediments of the Cardenas and the Tabaco formations are easily weathered and eroded and provide only few outcrops. The best exposures are in riverbeds and roadcuts in the vicinity of Cardenas, a town located about 200 km east of San Luis Potosí. To the north and west of Cardenas only arenite and marl of the middle member crop out. 12 sections of the Cardenas and Tabaco formations have been measured in the type area near Cardenas (Figure 2) and are described in detail.

3.1 Arroyo de la Atarjea

The Arroyo de la Atarjea section represents the type section of the Cardenas Formation (Myers, 1968) and is exposed in the riverbed of the Arroyo de la Atarjea crossing the road Cardenas-Ciudad del Maíz, approximately 2.5 km north of Cardenas (Figure 2). According to my data, Myers (1968) underestimated the thickness of this section. The sediment sequence is 1200 m thick and forms part of the western limb of the Cardenas syncline (Figure 8).
The Arroyo de la Atarjea section encompasses all three members of the Cardenas Formation and a thin interval of the Tabaco Formation. Though the Arroyo de la Atarjea section is the best exposed section of the Cardenas Formation, significant parts – especially of the lower member – are covered by soil and calcretes. The sediment succession consists of interbedded conglomerate, arenite, siltstone, marl, and limestone, as well as several reef units.

3.1.1 Lower Member

The lower member is 255 m thick. A 6 m thick rudist limestone forms the base and contains *Durania* cf. *ojanchalensis* (see chapter 4.1.1). Upsection, 83 m are covered. Overlying this covered interval siltstone and marl contains *Trigonia* sp. The interval between 99 m and 129 m lacks outcrops. At 129 m, a 1 m thick oyster-bearing marl underlies a 2 m thick limestone that contains echinoderms, gastropods, bivalves, and orbitoidacean foraminifera (130 m to 132 m). Upsection (132 m to 238 m), outcrops are sparse and sediment exposed consists of unfossiliferous arenite and siltstone.
A 16 m thick unit of interlayered siltstone, marl, and limestone is present between 238 m and 253.5 m (Figure 9). The limestone contains *Durania* cf. *ojanchalensis*, actaeonellid gastropods, and benthic foraminifera (*Quinqueloculina*, *Cuneolina*, *Gaudryina*, haplophragmoidal foraminifera). In the lower part of the unit (238 m to 243 m), siltstone and marl layers are between 0.1 m and 0.3 m thick and contain gastropods, bivalves, sparse oysters, whereas limestone layers are between 0.1 m and 0.8 m thick. At 243 m, a 0.2 m thick oyster layer is intercalated. Upsection (243.2 m to 253.5 m), thickness of limestone layers increases from 0.3 m to 1.1 m, whereas siltstone and marl units are between 0.08 m and 1.1 m thick and contain abundant actaeonellid gastropods. At 253.5 m, a 1 m thick rudist rudstone containing *Durania* cf. *ojanchalensis* terminates the lower member.

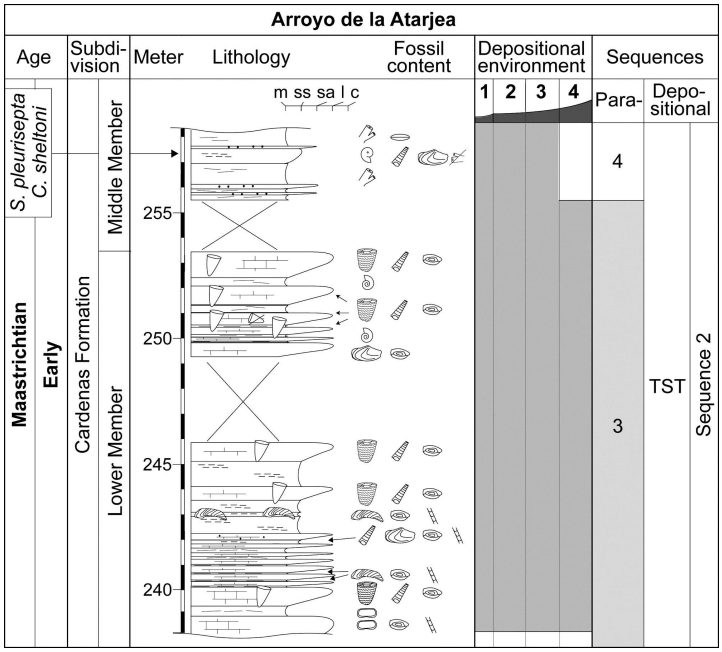

Figure 9: Lower part of the Cardenas Formation in the Arroyo de la Atarjea containing *Durania* cf. *ojanchalensis* reefs (complete section see figure 8). Ammonites (*Sphenodiscus pleurisepta, Coahuilites sheltoni*) indicate an early Maastrichtian age of the lower part of the middle member (see chapter 2 for details).

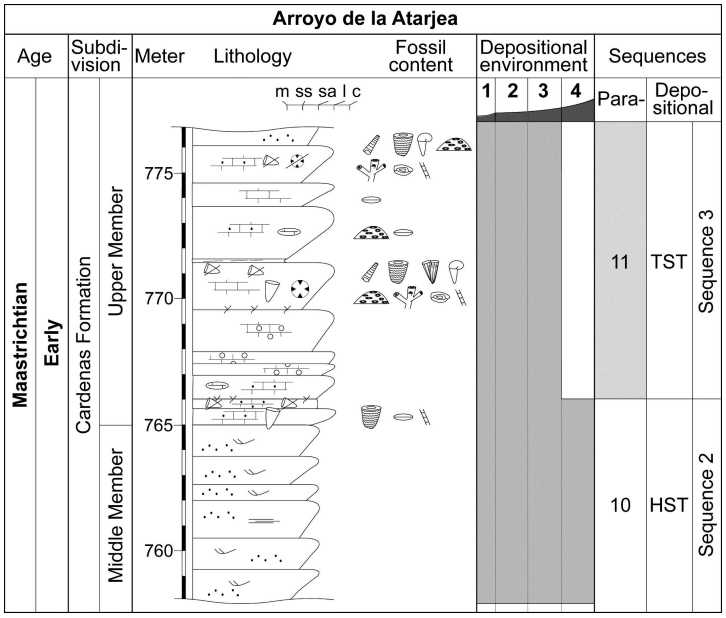

Figure 10: Detailed litholog of the boundary between the middle and upper member of the Cardenas Formation in the Arroyo de la Atarjea (complete section see figure 8). The boundary is located at the base of the first rudist assemblage, above the predominantly clastic sediments characterizing the middle member.

3.1.2 Middle Member

The middle member is approximately 510 m thick. The lowermost unit, between 255.5 m and 258 m, consists of marl, which is intercalated by 0.05 m to 0.6 m thick layers of arenite and siltstone (Figure 8). The fauna is well preserved and includes ammonites (*Sphenodiscus pleurisepta*) indicating a Maastrichtian age, gastropods (*Pugnellus densatus*, *Longoconcha* sp., *Gyrodes* sp.) and chaetetids.

Upsection, above a 40 m thick covered interval (258 m to 298 m), a 3 m thick oolitic packstone (see chapter 4.2 for details) is sharply overlain by a 3 m thick bioclastic packstone (298 m to 304 m). At 304 m, a 3 m thick oyster biostrome is intercalated. Upsection (308 m to 520 m), a 212 m thick monotonous unit consists of alternating 0.1 m to 0.5 m thick siltstone and marl and rare layers of arenite. The arenite is 0.3 m to 0.4 m thick and hummocky cross-bedded in the lower part of the unit. Fauna comprises pectinid bivalves, branching bryozoans, and orbitoidacean foraminifera (*Lepidorbitoides minima*). At 442 m and 460 m, hardgrounds, characterized by the accumulation of pectinid bivalves and iron crusts, separate 5 m and 15 m thick marl units, which contain pectinid bivalves as well as abundant serpulids (*Hamulus* ?*angulatus*).

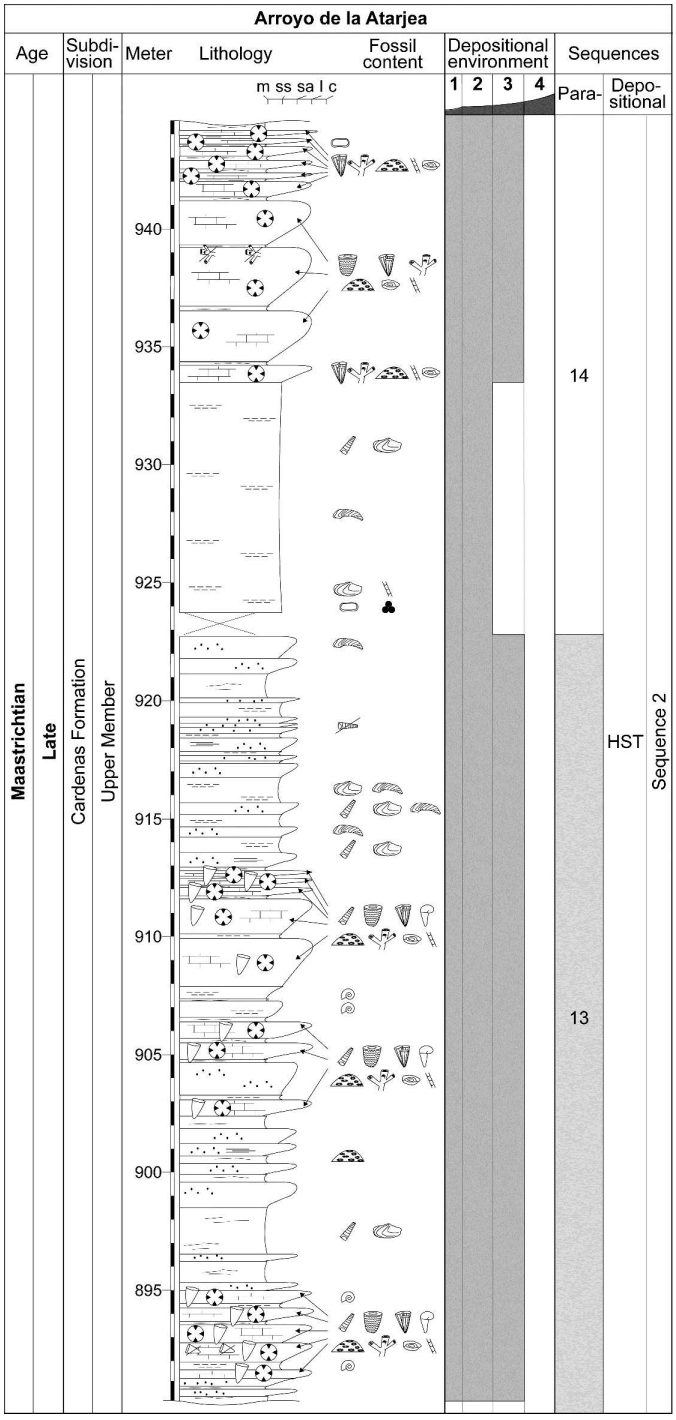

Figure 11: Detailed litholog of the upper member of the Cardenas Formation in the Arroyo de la Atarjea (see also figure 8).

The interval between 520 m and 530 m is not exposed. Between 530 m and 559 m, arenite layers increase in abundance and *Exogyra costata* is common. At 559 m, a 1 m thick conglomerate is present containing pebble- and cobble-sized chert and lime clasts as well as oyster fragments (see chapter 4.1 for details). The conglomerate underlies an 110 m thick interval (560 m to 670 m) of 0.2 m to 1 m thick layers of interlayered arenite, siltstone, and marl, which contain crustaceans.

At 670 m, a 5 m thick arenite interval is exposed containing oyster fragments. Upsection (675 m to 758 m), siltstone and marl forms an 80 m thick unit, which contains in the uppermost part non-rudist bivalves, including oysters, and turritellid gastropods. The topmost unit of the middle member (758 m to 765 m) is 7 m thick and consists of trough cross-bedded and planar laminated unfossiliferous arenite (Figure 10). The arenite layers are between 0.4 m and 1.3 m thick.

3.1.3 Upper Member

The exposed part of the upper member is 375 m thick (Figure 8), but a 60 m thick interval between the uppermost Cardenas Formation and the Tabaco Formation is covered by soil. A 2 m thick rudist limestone at 765 m (Figure 10) marks the base of the upper member. It contains bouquets of small radiolitids (see chapter 4.1.1 for more details). Upsection (767 m to 769.8 m), a 2.8 m thick oolitic limestone is present.

The topmost layer of the oolitic limestone is bioturbated and sharply overlain by an 6.3 m thick coral-rudist reef unit (see chapter 4.2.1 for more details), which consists of 1 m to 2 m thick reef rudstone intercalated by 0.1 m thick marl (769.8 m to 776.1 m). A 1 m thick arenite overlies the reef unit. The interval between 777.1 m and 780 m is not exposed.

From 780 m to 795 m, limestone of varying thickness interlayers with arenite, siltstone and marl. The clastic sediments contain oysters, and layer thickness reaches from 0.08 m to 0.4 m. The limestone consists either of skeletal grainstone, which is 1.1 m to 2.1 m thick, or of coral-rudist packstone, forming layers from 0.1 m to 0.4 m thick.
The interval between 795 m and 838 m is covered. The sediment unit above (838 m to 863 m) consists of interlayered arenite, siltstone, and marl. Upsection, the amount of arenite layers increases. The topmost part (859 m to 863 m) consists only of unfossiliferous arenite, which forms symmetric wave ripples. Thickness of individual layers reaches from 0.4 m to 4 m. In the lower part of the unit (838 m to 850 m) fossils consist of *Exogyra costata*, branching bryozoans, and serpulids as well as sparse planktic foraminifera. Upsection (850 m to 859 m) actaeonellid gastropods and miliolid foraminifera are abundant and *Coralliochama* sp. is sparse. The arenite passes into a 0.6 m thick oyster-bearing conglomerate. The uppermost part contains reworked gastropods and non-rudist bivalves were found.
From 870 m to 1000 m, arenite, siltstone, and marl are interlayered. In addition, coral-rudist reefs are present at 880 m, 895 m, 905 m, 975 m, 990 m (see chapter 4.2.1 for more details) and coral-dominated reef units at 935 m and 960 m (see chapter 4.2.2 for more details). The clastic sediments form layers between 0.05 m and 3 m thick (Figure 11) and contain diverse assemblages of gastropods, plagioptychids (*Coralliochama* sp.) and non-rudist bivalves (e.g., *Exogyra costata* SAY, *Pycnodonte mutabilis* (MORTON), *Lopha* sp., *Trigonia* sp., *Pholadomya* sp., *Cardium* sp.). At 900 m, one branched coral was found in the marls.
The reefs consist of 0.2 m and 2 m thick coral-rudist rudstone or coral framestone (Figure 11), which interlayer with actaeonellid bearing siltstone and marl. Limestone thickness in the reef units gradually decreases upsection and thickness of the siltstone and marl increases. The topmost reef unit (990 m to 1000 m) underlies laminated and trough cross-bedded arenites, which are 2 m thick.
Upsection, from 1002 m to 1140 m, arenite, siltstone, and marl are interlayered and form 0.8 m to 2 m thick layers. Faunal diversity is low. The lower part of the interval (1002 m to 1012 m) contains fragmented oysters. At 1040 m, a 0.3 m thick coquina contains abundant turritellid gastropods. The upper part (1012 m to 1140 m) is poorly exposed and contains ostracods and benthic foraminifera. At 1090 m, sparse rudist and coral fragments have been identified in thin sections.

3.1.4 Tabaco Formation

The topmost 8 m of the Arroyo de la Atarjea section (1191 m to 1199 m) correspond to the Tabaco Formation. The boundary between the Tabaco and the Cardenas Formation is not exposed and the interval between the uppermost exposed layers of the Cardenas Formation, at 1140 m, and the lowermost layers of the Tabaco Formation, at 1191 m, is covered by soil. Strike and dip of the Tabaco Formation coincide with the Cardenas Formation and no angular unconformity appears to be present.

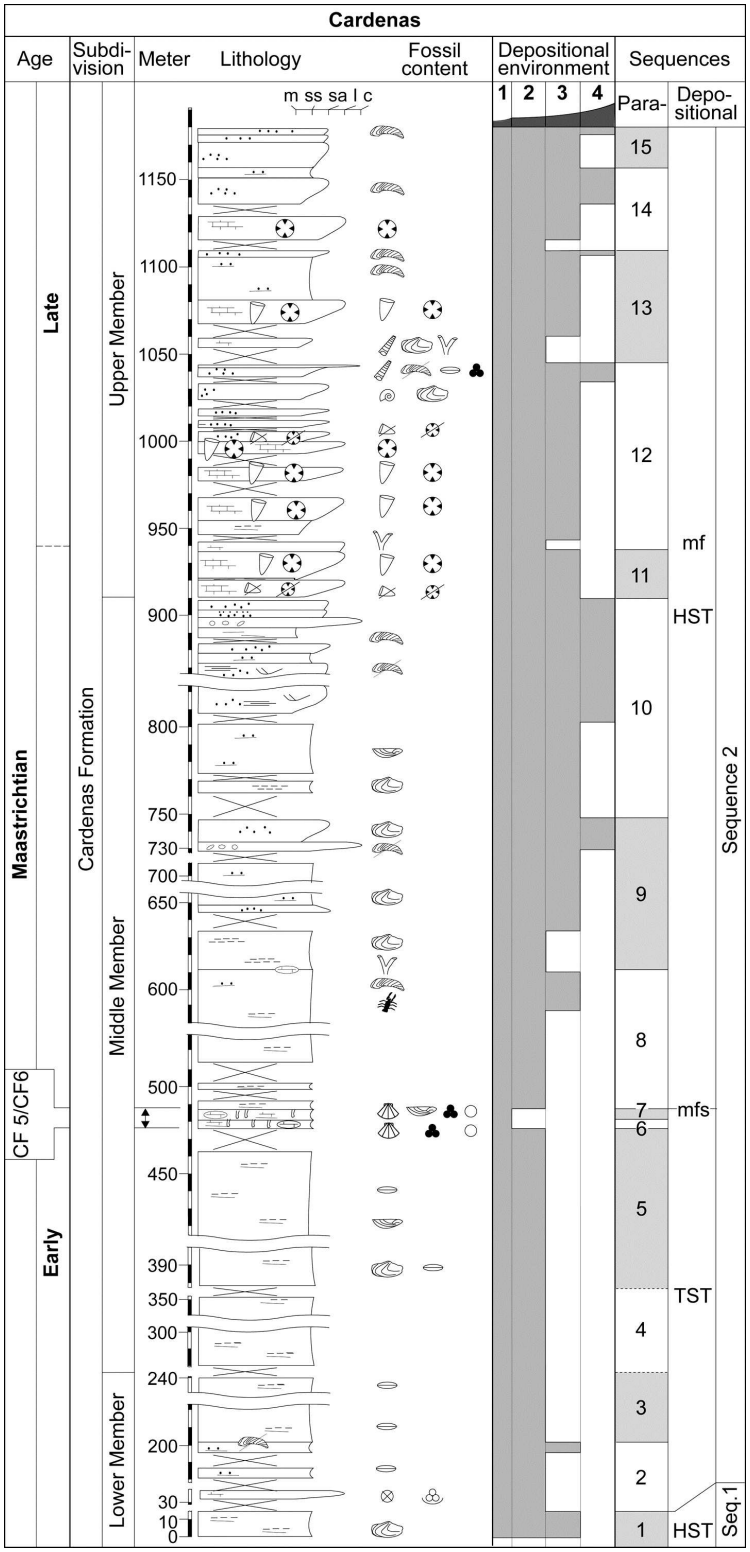

Figure 12: Cardenas section. Planktic foraminiferal assemblages between 475 m and 488 m (foraminiferal zones CF5 or CF6) indicate an early Maastrichtian age for the middle member (see chapter 2 for details). A late Maastrichtian age for upper member is indicated by sequence stratigraphic correlation (see chapters 6 and 7.2 for details).

The Tabaco Formation consists of unfossiliferous red silt- and claystone, which is intercalated by fine-grained arenite. The silt- and claystone layers are between 0.5 m to 2 m thick and arenite layers between 0.2 m and 0.6 m. In the claystone, a 0.01 m to 0.05 m thick layer of calcrete is present at 1196 m and is interpreted to represent a palaeosoil horizon (Plate 5/4).

3.2 Cardenas

The Cardenas section is 1180 m thick (Figure 12) and exposed in a canyon on the northern outskirts of Cardenas.
A trail along the southern flank of the canyon leads to the village El Tulillo. The section forms part of the western limb of the Cardenas syncline, similar to the Arroyo de la Atarjea section, which is located 1 km to the north (Figure 2).

3.2.1 Lower Member

The lower member of the Cardenas Formation has a visible thickness of approximately 260 m, but outcrops are sparse.
At the base of the section, from 0 m to 12 m, siltstone, marl, and sparse arenite in layers of 0.1 m to 3 m thickness are interlayered and contain *Trigonia* sp. The overlying interval, from 12 m to 32 m in the section, is covered by soil. At 32 m, a 1 m thick packstone contains echinoderms, ostracods and miliolid foraminifera and underlies a 148 m thick covered interval reaching from 33 m to 181 m. Upsection, between 181 m and 240 m, interlayered arenite, siltstone and marl contain orbitoidacean foraminifera. At 203 m, a 1 m thick hash layer is intercalated and contains reworked oysters.
Assignation to the lower member of the Cardenas Formation is based on the spatial correlation of the individual sediment layers with that of the Arroyo de la Atarjea section and correlation of the depositional sequences (see chapter 6.2). Rudist reefs are probably covered by soil, but transported *Durania* are present in the riverbed.

3.2.2 Middle Member

The middle member of the Cardenas Formation is approximately 650 m thick, but the base of the member, between 260 m and 280 m is not exposed. The lower part (280 m to 475 m) consists of interlayered siltstone and marl, but the interval between 350 m and 390 m is covered by soil. Sediment layers are between 0.2 m and 0.8 m thick and faunal elements include turritellid gastropods, non-rudist bivalves (*Arctostrea aguilerae*, *Exogyra costata*) and orbitoidacean foraminifera (*Lepidorbitoides*).
Between 475 m and 493 m, marly limestone interlayers with sandy marl. Thickness of layers in this interval increases upsection from 0.7 m at the base to 4 m at the top. Hardgrounds on the upper limestone bedding planes are characterized by iron crusts and are covered by pectinid bivalves. The limestone contains non-rudist bivalves (*Neithea*, *Exogyra*), abundant serpulids (*Hamulus* ?*angulatus*) and orbitoidacean foraminifera.
From 493 m to 499 m, the section is covered by soil. Overlying siltstone and marl (499 m to 590 m) contain *Exogyra costata* and sparse crustaceans. Layers are from 0.1 m to 0.5 m thick. Upsection (590 m to 611 m), oyster-bearing arenite layers, up to 0.5 m thick, are intercalated.

Between 611 m and 635 m, a 24 m thick siltstone unit overlies the arenite with an abrupt contact. Thickness of the siltstone layers reaches from 0.5 m to 2 m and the basal layer contains calcareous concretions. Branching bryozoans and non-rudist bivalves are common in the entire unit. The following 10 m of the section (635 m to 645 m) are covered. Interlayered arenite, siltstone and marl overlie the covered interval (645 m to 709 m) and layers reach thicknesses between 0.5 m and 3 m. Sparse non-rudist bivalves (*Cardium*) are present, and the arenite contains escape burrows. Upsection, a 20 m thick covered interval (709 m to 729 m) underlies a 2 m thick conglomerate (729 m to 731 m) with oyster fragments. The overlying 17 m thick arenite (731 m to 748 m) contains sparse non-rudist bivalves.
The interval between 748 m and 771 m is mostly covered and only between 761 m and 769 m, a siltstone unit is exposed, which contains non-rudist bivalves. Between 771 m and 801 m, interlayered arenite, siltstone and marl in layers between 0.2 m and 1 m thick contain *Exogyra costata*. Upsection, the number of arenite layers increases. Between 804 m and 872 m, a 68 m thick arenite unit with layer thickness of 7 m in the lower part decreasing to 5 m in the upper part shows trough cross-stratification and planar lamination. Abundant oyster fragments are present in the uppermost layer. Between 872 m and 893 m, 0.05 m to 1.3 m thick interlayered arenite, siltstone, and marl contain oysters. A 2 m thick conglomerate overlies the unit with an abrupt contact and passes into 0.5 m to 1.5 m thick layers of unfossiliferous arenite (895 m to 910 m).

3.2.3 Upper Member

The upper member of the Cardenas Formation is 270 m thick, but the top is not exposed. A 28 m thick coral-rudist reef unit marks the base of the upper member (910 m to 938 m), and coral-rudist reef units predominate in the section, up to 1000 m. Siltstone and marl is interlayered between the reef units, as well as sparse arenite and sandy packstone and layers reach thicknesses from 0.25 m to 4 m. At 990 m, the packstone contains non-rudist bivalves, as well as abundant branching bryozoans. Individual reef units are 4 m to 13 m thick. Each unit consists of 0.2 m to 2.5 m thick layers of marly coral-rudist rudstone, which are separated by 0.05 m to 0.5 m thick marl interlayers. At 1000 m, the coral-rudist rudstone passes into a 2 m thick arenite, containing rudist and coral fragments. Upsection, from 1002 m to 1042 m, outcrops are mostly covered by soil; arenites exposed contain turritellid gastropods and non-rudist bivalves. At 1042 m, a 0.8 m thick conglomerate overlies the arenite. Clasts consist of arenite, and limestone with orbitoidacean and planktic foraminifera, and fossils in the matrix

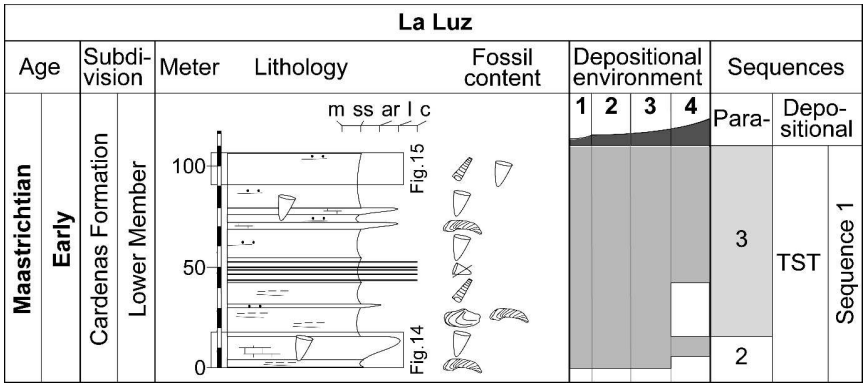

Figure 13: La Luz section. An early Maastrichtian age is indicated by sequence stratigraphic correlation (see chapters 6 and 7.2 for details).

include oysters and turritellid gastropods.

The interval between 1043 m and 1070 m is mostly covered; only a 3 m thick packstone is exposed at 1056 m, containing turritellid gastropods, non-rudist bivalves and branching bryozoans.

An 11 m thick reef unit is present between 1070 m and 1081 m and consists of marly coral-rudist rudstone (see chapter 4.2.1), and marl with actaeonellid gastropods. The reef unit gradually passes into a unit of oyster-bearing interlayered arenite, siltstone and marl forming layers between 0.1 m to 1 m thick (1081 m to 1111 m). The interval between 1111 m and 1118 m is covered by soil. A second 11 m thick reef unit is located between 1118 m and 1129 m and represents the topmost reef unit in the Cardenas section. It consists of 0.5 m to 2 m thick coral-dominated framestone (see chapter 4.2.2), which interlayers with 0.05 m to 0.5 m thick marl. Upsection, 9 m are covered (1129 m to 1138 m). Between 1138 m and 1180 m, interlayered arenite and marl with oysters represent the uppermost sediments exposed in the section.

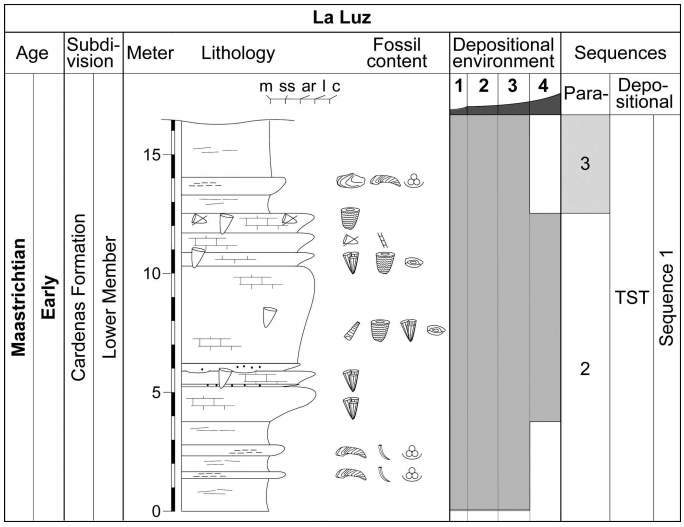

Figure 14: Detailed litholog of the lowermost part of the La Luz section (see also figure 13).

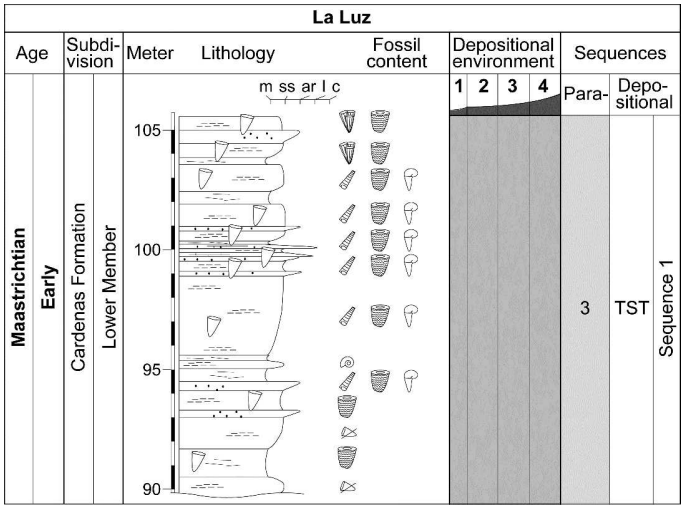

Figure 15: Detailed litholog of the uppermost part of the La Luz section (see also figure 13).

3.3 La Luz

The La Luz section is 105 m thick and located at a water reservoir, approximately 3 km southwest of the village La Luz (Figure 2). It is a composite section with the lower part exposed at the southeastern, and the upper part at the southwestern flank of the reservoir. Sediment consists of interlayered arenite, siltstone, marl, and limestone (Figure 13). Reef limestone containing *Durania ojanchalensis* and weathered arenite and shale with *Arctostrea* and *Exogyra costata* exposed east of the measured section and correlated with the middle member, indicate that the lower member of the Cardenas Formation is present in the section.

The lower 5 m of the La Luz section consist of marl and intercalated siltstone, which is 0.2 m to 0.3 m thick. The fossil assemblage consists of abundant oysters, serpulids (*Pentaditrupa*), benthic foraminifera and shell fragments (Figure 14).

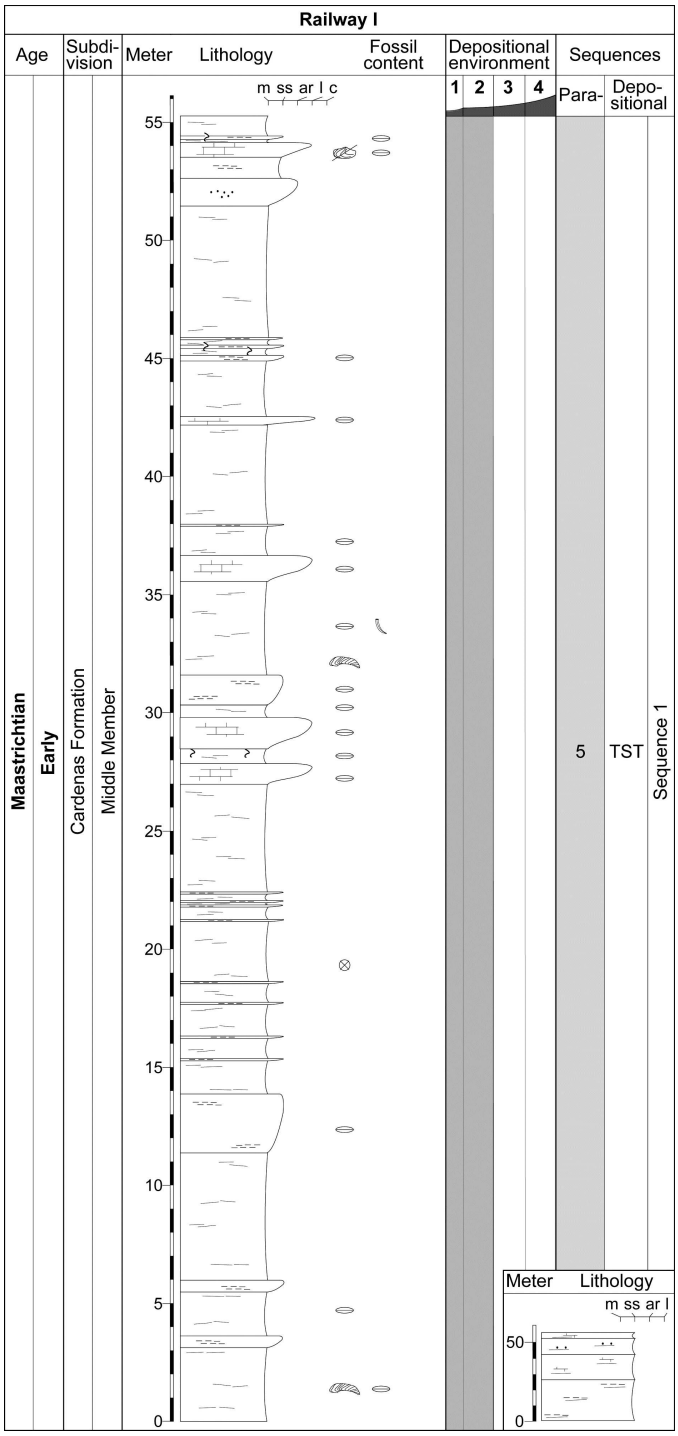

Figure 16: Railway I section. An early Maastrichtian age is indicated by sequence stratigraphic correlation (see chapters 6 and 7.2 for details).

A 7.5 m thick reef unit overlies these sediments (5 m to 12.5 m) and is almost exclusively composed of *Praebarrettia sparcilirata*, associated only with few small radiolitids (see chapter 4.1.2 for more details). The internal sediment consists of marly packstone. Two 0.1 m and 0.3 m thick arenite layers are intercalated at 5.2 m and 6 m. Within the uppermost 2.5 m of the reef unit *Praebarrettia sparcilirata* is gradually replaced by *Durania ojanchalensis*. At 12 m, this latter species reaches > 95% of the fossil assemblage.

Overlying the rudist reef unit, an 18.5 m thick marl interval is present (12.5 m to 31 m) and intercalated by 0.1 m to 0.3 m thick siltstone. The faunal assemblage comprises gastropods, non-rudist bivalves, and oysters. At 31 m, a 1.2 m thick unfossiliferous arenite overlies the marl. Upsection, between 31 m and 43 m, siltstone interlayers with marl, and layer thickness reaches from 0.1 m to 0.3 m. Between 43 m and 52 m, marl is absent and siltstone layers reach a maximum thickness of 3 m. 0.05 m to 0.15 m thick conglomerate layers containing coquinas of *Durania* fragments intercalate the siltstone.

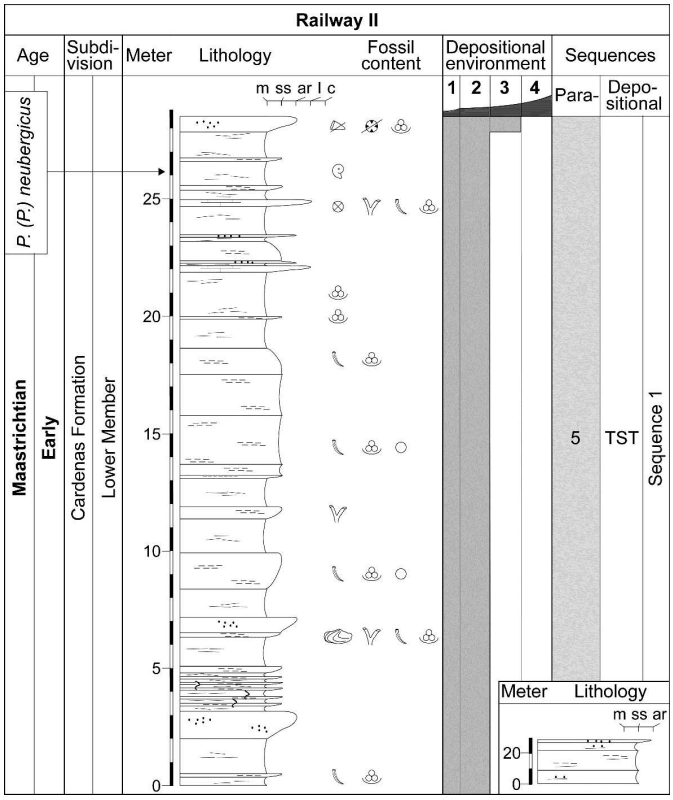

Figure 17: Railway II section. The ammonite *Pachydiscus* (*Pachydiscus*) *neubergicus* indicates an early Maastrichtian age (see chapter 2 for details).

From 52 m to 104 m, *Durania* assemblages are abundant in interlayered arenite, siltstone, marl, and limestone. Layers are from 0.1 m to 0.6 m thick, and occasionally, individual lime- and siltstone layers reach a thickness of 3 m. At 60 m and 72 m, two oyster reefs occur in the limestones. The abundance and thickness of *Durania* reefs increase upsection (Figure 15). From 94 m to 104 m, *Durania* is associated with *Coralliochama* (see chapter 4.1.1 for more details) and in the topmost section, from 104 m to 105 m, with *Praebarrettia sparcilirata*.

3.4 Railway I and Railway II

The Railway I and Railway II sections are exposed along the railway line from Cardenas to Estación Canoa, between Kilometers 419 and 420, approximately 6 km east of Cardenas (Figure 2). They are separated by an 110 m thick covered interval and belong to the western limb of the Cardenas syncline. The sections are assigned to the middle member of the Cardenas Formation, as indicated by lithologies, fossil content (absence of rudist reefs), and correlation of the depositional sequences with other sections analyzed in this study (see chapter 6.2). Aguilar (2002) and Caus (2002) suggested a middle to late Campanian age of these sections. However, the presence of the ammonite *Pachydiscus neubergicus* (Ifrim et al., 2005) indicates a Maastrichtian age.

Section Railway I (Figure 16) is 55 m thick. The lower 27 m consist of marl intercalated by siltstone. Upsection (27 m to 55 m), 0.4 m and 4.5 m thick marl interlayer with arenite, siltstone and limestone, which reach a thickness between 0.1 m and 2 m. The fossil assemblages consist of echinoids, rare non-rudist bivalves, serpulids, and orbitoidacean foraminifera.

Section Railway II is 29 m thick (Figure 17). 0.1 m to 2 m thick marl units interlayer with arenite, siltstone, and limestone. Fossils include non-rudist bivalves, serpulids, and branching bryozoans. Near the top of the section, at 26 m, *Pachydiscus neubergicus* is present, and the overlying arenite contains sparse fragments of radiolitids.

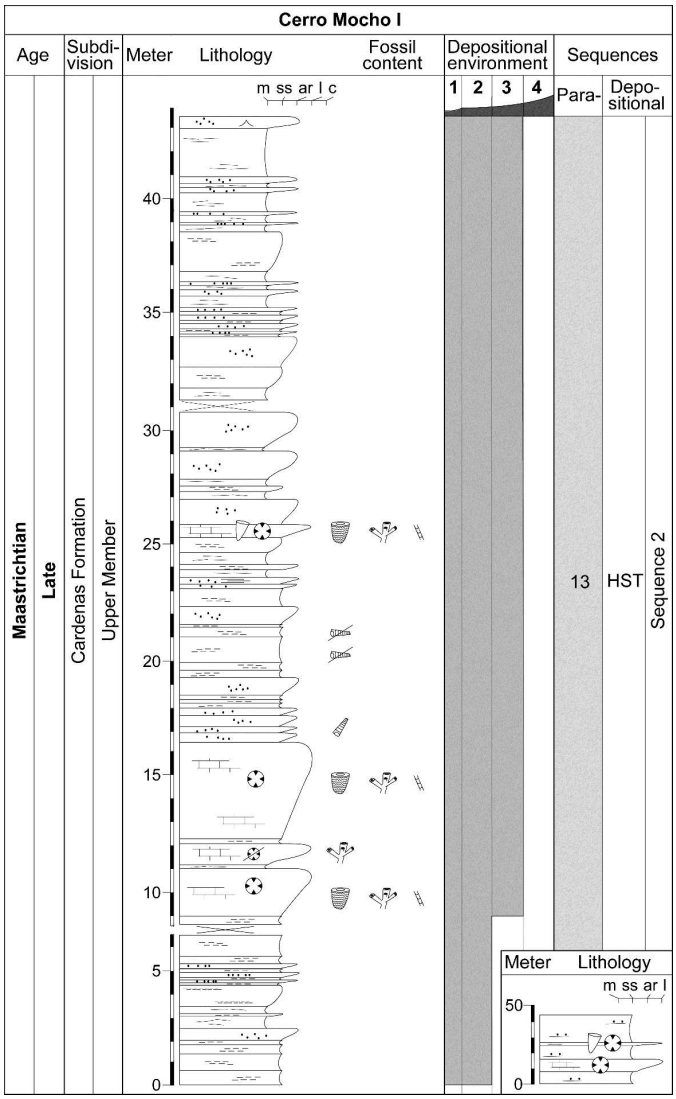

Figure 18: Cerro Mocho I section. A late Maastrichtian age is indicated by sequence stratigraphic correlation (see chapters 6 and 7.2 for details).

3.5 Cerro Mocho I and Cerro Mocho II

The Cerro Mocho I and II sections are exposed along the road Cardenas-La Labor, approximately 2 km east of Cardenas on the western limb of the Cardenas syncline (Figure 2). The two sections are separated by a covered interval of approximately 440 m thickness.

The Cerro Mocho I section (Figure 18) is 43 m thick and assigned to the upper member of the Cardenas Formation based on the presence of *Tampsia*. The section is formed by interlayered arenite, siltstone, and marl, which reach a layer thickness from 0.1 m to 1.6 m. Between 9 m and 16 m, a coral-dominated reef unit is exposed (see chapter 4.2.2), consisting of 1 m to 4 m thick coral-rudist rudstone and intercalated 0.1 m to 0.2 m thick siltstone and marl. In addition, a 0.8 m thick coral-rudist rudstone (see chapter 4.2.1) is intercalated at 25 m. The topmost arenite, at 43 m, contains symmetrical wave ripples.

Section Cerro Mocho II (Figure 19) is almost 19 m thick. Interlayered arenite forms layers 0.1 m and 0.8 m thick, and siltstone varies in thickness between 0.2 m and 3.2 m. Between 6 m and 9.7 m, a 3.7 m thick arenite is exposed. At 0.5 m, a coquina consisting of gastropod fragments and, *E*xogyra *costata* contains the only fossils found in the section near the top of the section. The Cerro Mocho II section is tentatively correlated with the middle member of the Cardenas Formation based on lithology, absence of rudist reefs, and the presence of *E. costata*.

3.6 La Labor

The La Labor section is 28 m thick (Figure 20) and exposed along the road Cardenas-La Labor, 2 km west of the village La Labor (Figure 2) on the eastern limb of the Cardenas syncline (Myers, 1968). Interlayered arenite, siltstone, and marl form layers between 0.1 m and

3 m thick. These sediments are unfossiliferous, except for a 1.2 m thick arenite, at 22 m, which contains reworked radiolitids (*Bournonia*). This section is assigned to the upper member of the Cardenas Formation based on the presence of *Bournonia cardenasensis*, which is a characteristic faunal element in the coral-rudist reefs of the upper member of the type section (Arroyo de la Atarjea).

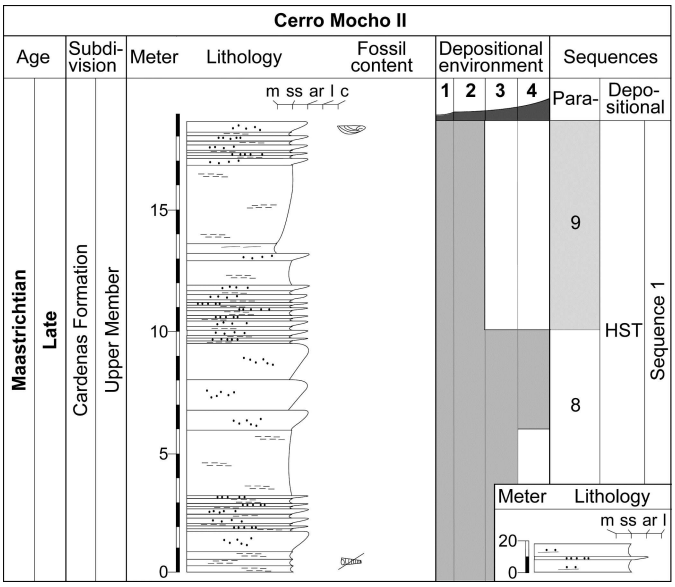

Figure 19: Section Cerro Mocho II. An early Maastrichtian age is indicated by sequence stratigraphic correlation (see chapters 6 and 7.2 for details).

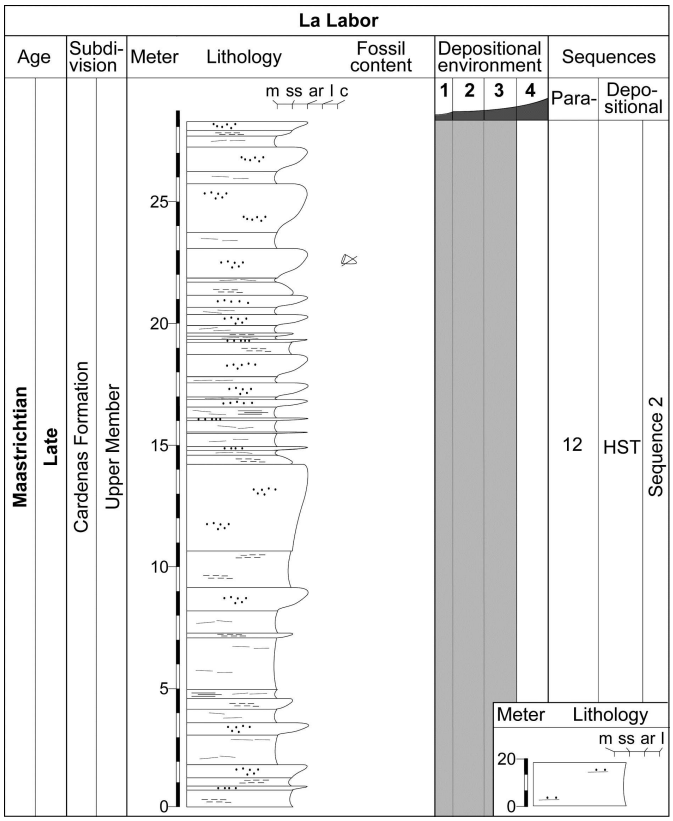

Figure 20: Section La Labor. A late Maastrichtian age is indicated by sequence stratigraphic correlation (see chapters 6 and 7.2 for details).

3.7 Morales

The Morales section forms part of the western limb of the Cardenas syncline. This 262 m thick section is exposed in the hamlet Morales, approximately 20 km north of Cardenas (Figure 2), and encompasses the upper member of the Cardenas Formation and the lowermost Tabaco Formation (Figure 21).

The base of the section (0 m to 12 m) consists of 0.75 m to 3 m thick coral-rudist rudstone layers that interlayer with 0.2 m to 0.4 m thick layers of siltstone and marl. Upsection, from 50 m to 100 m, siltstone and marl, form layers between 0.08 m and 2 m thickness. At 90 m, a 1 m thick packstone is intercalated in the siltstone-marl sequence and contains reworked corals and rudists.

Upsection from a 30 m thick covered interval (100 m to 130 m), interlayered siltstone and marl contain non-rudist bivalves and abundant orbitoidacean foraminifera. At 155 m, a 7 m thick unit consisting of 0.25 m to 1.25 m thick amalgamated arenite layers contains abundant molluscan shell fragments. Overlying the arenite, between 162 m and 180 m, interlayered arenite, siltstone and marl, 0.1 m to 2 m thick, pass into a marl and siltstone unit

(180 m to 215 m). Between 215 m and 223 m, the section is covered and, from 223 m to 227 m, interlayered arenite, siltstone, and marl overlie the covered interval.

The topmost 12 m of the Morales section (250 m to 262 m) consist of red arenite, siltstone, and a 2 m thick conglomerate. These sediments are assigned to the Tabaco Formation, which overlies the Cardenas Formation conformably. The contact between the Tabaco Formation and the Cardenas Formation is not exposed, and the two are separated by a 30 m thick covered interval. The fine to medium-grained arenite of the Tabaco Formation contains oyster fragments. The conglomerate consists of pebble- to cobble-sized rounded clasts of limestone, as well as of red arenite and siltstone (see chapter 5).

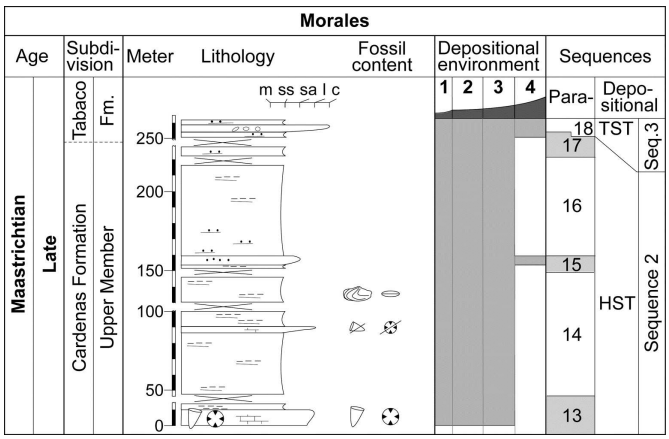

Figure 21: Morales section. A late Maastrichtian age is indicated by sequence stratigraphic correlation (see chapters 6 and 7.2 for details).

3.8 Cañaditas

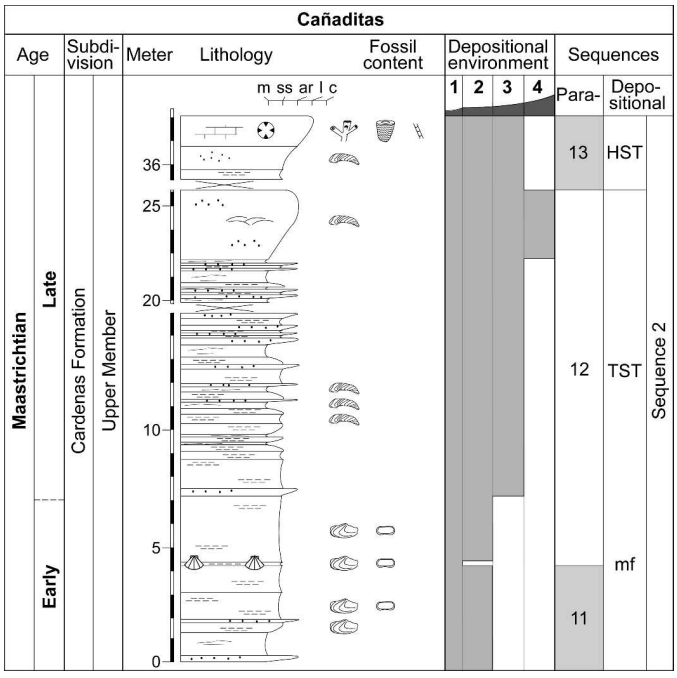

Figure 23: Section Cañaditas. The early and late Maastrichtian age is indicated by sequence stratigraphic correlation (see chapters 6 and 7.2 for details).

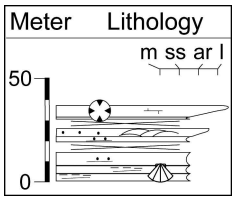

Figure 22: General view of the section Cañaditas

The lower 11 m of this section (Figures 22, 23) consist of siltstone and marl, forming layers of up to 3.2 m thickness. They are intercalated by 0.1 m to 0.2 m thick layers of arenite. At 4.2 m, omission surfaces are marked by the accumulation of pectinid bivalves.

In the overlying interval, from 11 m to 25.5 m, arenite increases and layers reach a maximum thickness of 2.5 m. Faunal diversity is low, but oysters are common in the arenite and siltstone. At 23 m, a 2.5 m thick oyster reefs is exposed within the arenite unit.

Above a covered interval between 25 m and 35 m, 0.25 m thick siltstone, a 0.9 m thick arenite, and a 1.2 m thick coral framestone (see chapter 4.2.2) complete the uppermost 2.35 m of the Cañaditas section (35.8 m to 38.15 m).
The Cañaditas section is assigned to the upper member of the Cardenas Formation, based on the presence of a coral-dominated reef, which is a characteristic element of the upper member of the Cardenas Formation in the type section (Arroyo de la Atarjea),

3.9 La Presa

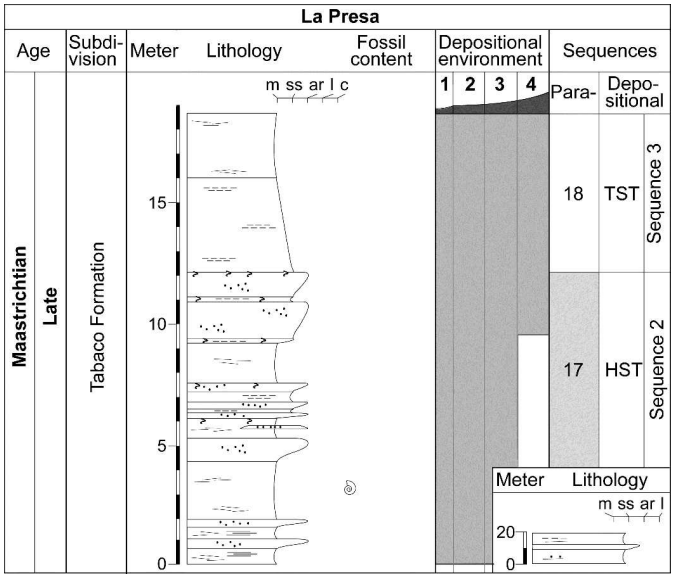

Figure 24: Section La Presa. A late Maastrichtian age is indicated by correlation with other sections (see chapters 6 and 7.2 for details).

Red arenites and claystones of the Tabaco Formation are exposed in the 18 m thick La Presa section located at a water supply reservoir approximately 3 km east of Cardenas (Figure 2). Layers are 0.3 m to 1.3 m thick and are intensively bioturbated (Figure 24; Plate 5/6).

3.10 Estación Canoa

The Canoa section is located along the railway Cardenas-Estación Canoa, approximately 1 km east of the La Canoa station. The area is covered by dense tropical vegetation, and only a 2 m thick isolated rudist reef crops out (Plate 2/3, 4). Rudists consist of *Macgillavryia nicholasi* that reach maximum diameters of 490 mm and heights of up to 180 mm (see chapter 8). Their irregular conical right valves are in situ, whereas fragments of the left valves are distributed within the marly packstone. The absence of index fossils hampers correlation with other analyzed sections. However, the presence of *Macgillavryia nicholasi* indicates a Campanian–Maastrichtian age, and comparable monospecific rudist reefs are common in the lower member of the Cardenas Formation; in consequence, the Estación Canoa section is tentatively correlated with the lower member of the Cardenas Formation.

4 Depositional facies of the Cardenas Formation

Lithologies in the Cardenas Formation include conglomerate, arenite, siltstone and marl, as well as non-reefal and reefal limestone. Sediments are interpreted to represent upper shoreface/lagoonal, lower shoreface, offshore transitional, and offshore environments (Figure 25). In this chapter, these depositional facies are described by lithofacies (macro- and microfacies) and faunal content. These characteristics are summarized in table 2, and a depositional model is illustrated.

4.1 Upper shoreface facies

Shoreface environments are divided into high-energy/upper shoreface and low-energy/lagoonal and environments. The latter consist of conglomerate and arenite. Siltstone, marl, and limestone with rudist reefs are interpreted to represent lagoonal environments.

The conglomerate layers representing high-energy/upper shoreface environments reach a maximum thickness of 0.8 m. Clasts are well rounded (Plate 1/2), granule- to cobble-sized, and include chert and limestone (Plate 6/5), as well as fragments of gastropods and oysters (Plate 7/5). The lime clasts are reworked from shoreface to offshore transition environments. The matrix consists of unfossiliferous fine-grained arenite with occasional orbitoidacean foraminifera (Plate 7/5). The arenite units reach a maximum thickness of 65 m (see chapter 3.2.3), and individual layers are up to 4 m thick. Some layers are amalgamated and characterized by trough cross stratification (Plate 1/4), overlain by planar or slightly inclined laminated layers (Plate 1/1). The sediment is generally fine-grained and contains abundant subangular to subrounded and well-sorted quartz and non-skeletal lime clasts, as well as sparse bioclasts (Plate 8/2, Plate 10/7). Pore spaces are usually absent in the arenite. If present, then they are filled by silt (Plate 7/1), mud, or calcite cement. Locally isolated oysters and oyster fragments as well as benthic foraminifera are present.

Lagoonal environments are represented by marl, silt-, wacke- (Plate 6/2), and packstone (Plate 6/1). In the lower member of the Arroyo de la Atarjea section, the micritic packstone matrix is recrystallized into poikilotopic blocky spar (Plate 6/3), or pseudospar (Plate 6/6) causing cementstone. Occasionally, unfossiliferous arenite is intercalated in the siltstone or marl. This arenite corresponds to the arenite described for the high-energy shoreface. Faunal diversity in lagoonal environments of the Cardenas Formation is generally low and includes rudists, actaeonellid gastropods, and isolated oysters. In thin sections, lagoonal microfacies are characterized by miliolid and textulariid foraminifera (e.g., *Cuneolina, Dicyclina, Gaudryina, Quinqueloculina, Textularia, Trochammina*), and dasycladacean algae (Plate 7/4, 7).
Locally, up to 2.5 m thick oyster reefs are present. The internal sediment of the oyster reefs consists of siltstone or marly packstone, with ostracods, miliolid and textulariid foraminifera (*Cuneolina, Dicyclina*) (Plate 6/7). High amount of detrital quartz indicates terrigenous input. Oyster reefs are interpreted to characterize the transition from high-energy to lagoonal environments.

4.1.1 Rudist reefs of lagoonal environments

Mono- to paucispecific rudist reefs are interpreted to represent lagoonal environments. Reefs with *Durania ojanchalensis* and *Macgillavryia nicholasi* occur in the lower member of the Cardenas Formation, whereas small *Biradiolites* sp. prevails in rudist reefs of the upper member. In the reefs, elevator rudist morphotypes are isolated or form bouquets between 4 to several tens of rudist individuals. Associated fauna is low in diversity.
In the lower member, rudist reefs are from 1 m to 5 m thick, and consist of 0.3 m to 5 m thick rudist-bearing marl and rudist rudstone. These lithologies interlayer with 0.1 m to 1 m thick lagoonal marls, siltstones, and arenites, as described in the previous chapter (Figure 9, 15).

Within the reef units, right (attached) valves are preserved in growth direction (Plate 1/3). Fragments of the left valves are frequently distributed in the reef sediment and locally form imbrication structures (Plate 1/5). Only at La Luz, reworked right valves have been observed in arenites, but shell fragmentation is low and indicates minor transport (Plate 1/6).
In the reefs, specimens form “rudist meadows” of limited extend. Commonly, a single rudist species (e.g., *Durania ojanchalensis*, *Macgillavryia nicholasi*) prevails in a reef. However, in the La Luz section, between 93 m and 103.5 m, *Durania ojanchalensis* is associated with *Coralliochama gboehmi* and sparse corals (Figure 15). At the base of this reef, clinger morphotypes of *Coralliochama gboehmi* predominate, and *Durania ojanchalensis* is scarce. Towards the reef top, elevators replace clinger morphotypes of *Coralliochama gboehmi*, and the abundance of *Durania ojanchalensis* increases significantly. Increasing water depth likely caused the higher faunal diversity and the presence of corals in this reef at La Luz, which is interpreted to represent the transition from the proximal to the distal upper shoreface.
Sediment of the rudist reefs consists of foraminiferal packstone that contains actaeonellid gastropods, as well as miliolid and textulariid foraminifera (*Cuneolina*, *Quinqueloculina*, *Textularia*; Plate 7/3). Locally, weakly rounded detrital quartz is common. In the Arroyo de la Atarjea section, the micritic matrix is recrystallized, and poikilotopic blocky spar cement fills the pores (Plate 6/4). In the Estación Canoa section, packstone contains encrusting fora-

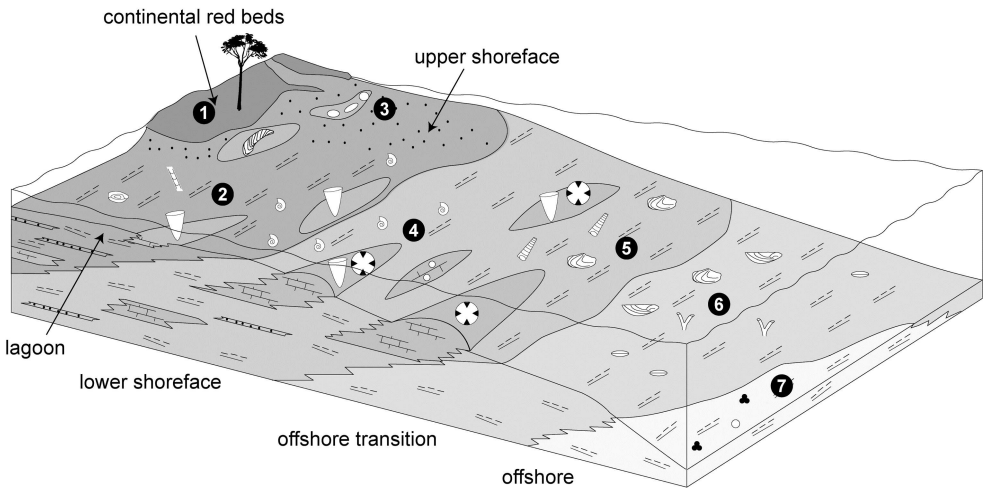

Figure 25: Depositional model of the Cardenas Formation as a progradational sequence (see also text for discussion): (1) land, (2) lagoon (rudist reefs, miliolid foraminfera, calcareous algae), (3) high-energy upper shoreface (wave-dominated deltas, conglomerate sand bodies, oyster reefs), (4) proximal lower shoreface (coral-rudist reefs, oolitic shoals, actaeonellid gastropods), (5) distal lower shoreface (coral-dominated reefs, diverse molluscan fauna), (6) offshore transition (*Exogyra costata*, branching bryozoans, orbitoidacean foraminifera), (7) offshore (planktic foraminifera, calcispheres).

minifera (*Placopsilina*, ?*Bullopora*) and abundant corallinacean and peysonneliacean algae (*Sporolithon*, *Pseudolithothamnium album*), which are arranged as rhodoliths around pelsparitic nuclei (Plate 7/8). In the wackestone, dasycladacean algae are sparse, but *Lithocodium* has been identified on some rudist shells.

Small radiolitid individuals with a maximum height of 50 mm characterize rudist reefs in the upper member of the Arroyo de la Atarjea section (Figure 10). Sparse miliolid foraminifera

are the only bioclasts in the radiolitid float-, and rudstone (Plate 9/1). Sediment in the radiolitid cavities consists of calcimudstone. A sandy radiolitid floatstone is intercalated at 766 m, containing reworked, but weakly fragmented, radiolitids (Plate 1/7). Reworking of the radiolitids was probably caused by shallowing of the depositional area, resulting in an increasing exposure to storm events and water currents.

4.1.2 Rudist reefs at the transition from upper to lower shoreface

Praebarrettia reefs of the Cardenas Formation are more diverse than the rudist reefs described in the previous chapter and are interpreted to thrive at the transition from lagoonal to lower shoreface environments. They are 0.5 m to 7 m thick (Plate 2/1, 2). In addition to *Praebarrettia sparcilirata*, small radiolitids (?*Biradiolites*) and *Coralliochama gboehmi* are present. Reef sediment consists of marly packstone, which contains rudist fragments (*Praebarrettia*, radiolitids, plagioptychids), abundant miliolid, textulariid (e.g., *Dicyclina, Textularia;* Plate 8/1, 3), and sparse encrusting foraminifera (e.g., *Placopsilina*; Plate 7/10, Plate 8/3), as well as *Lithocodium*, dasycladacean (Plate 7/9) and red algae that arranged as rhodoliths. Sparse 0.1 m to 0.3 m thick packstone layers are intercalated in the reef and are interpreted as storm deposits. Bioclasts in the packstone are well sorted and comprise recrystallized rudist fragments, orbitoidacean foraminifera and calcareous algae (Plate 8/5).

4.2 Lower shoreface facies

Lower shoreface facies are predominated by clastic sediments, but limestone is also present including coral-rudist and coral-dominated reefs (see chapter 4.2.1 and 4.2.2). In comparison to the upper shoreface facies, the amount of arenite is low, and conglomerates are absent, whereas faunal diversity is significantly higher.

Arenite, siltstone, and marl of the clastic lower shoreface (Plates 8/3, 4) contain a diverse assemblage of crustaceans (*Dakoticancer)*, sphenodiscid ammonites (*Sphenodiscus, Coahuilites*), gastropods (turritellids, actaeonellids), non-rudist bivalves (*Veniella, Cardium, Venericardia),* plagioptychids (*Coralliochama*), sparse oysters (*Arctostrea, Lopha*), benthic foraminifera (e.g., *Ayalaina*, *Quinqueloculina*, orbitoidacean foraminifera), and chaetetids. The marl contains abundant ostracods (*Antibythocypris* sp., *Cytherelloidea* cf. *austinensis, Haplocytheridea* cf. *dilatipuncta*, *Platycosta* cf. *lixula*, *Xestoleberis* sp., *Cytherella* sp.; pers. comm. Manuel R. Palacios-Fest), and benthic foraminifera.

Limestone of the lower shoreface includes marly actaeonellid floatstone and bioclastic packstone (Plates 4/6, 8/6), which interfinger with coral-rudist reefs (see chapter 4.2.1), as well as with oolithic and bioclastic grainstone (Plate 8/7).
The matrix of the marly actaeonellid floatstone consists of wacke- or packstone with miliolid and textulariid foraminifera, as well as dasycladacean algae. Detrital quartz is common.
Bioclasts in the bioclastic packstone encompass echinoderms, gastropods, rudists (*Coralliochama*), corals, ostracods, benthic foraminifera, and dasycladacean algae, as well as abundant detrital quartz (Plate 8/6). Boreholes of lithophagid bivalves are common in the shell fragments.

The oolithic grainstone consists of superficial ooids with a radial microframe and well-rounded and sorted coated grains (Plate 8/7). Molluscs, miliolid foraminifera, and quartz form ooid nuclei. Interstitial spaces are filled by blocky calcite cement.
The bioclastic grainstone is well sorted and contains molluscan fragments (echinoids, gastropods, rudists, non-rudist bivalves, oysters), benthic foraminifera (*Ayalaina, Sulcoperculina, Lenticulina*), calcareous algae (*Sporolithon*), and detrital quartz. Micritic coatings are common around the bioclasts and pore spaces are filled with blocky calcite, but rare patches of micritic matrix also exist.

4.2.1 Coral-rudist reefs

The presence of mixed coral-rudist patch reefs characterizes the upper member of the Cardenas Formation (Schafhauser et al., 2003). They contain the most diverse coral and rudist assemblages within the Cardenas Formation and are best exposed in the Arroyo de la Atarjea (Plate 3/1) and Cardenas sections, but are also present at the Rancho Morales section (Figures 8, 12, 21). 1 m to 11 m thick bioherms reach a maximum lateral extension of 14 m and consist of 0.5 m to 2 m thick coral-rudist rudstone, which is often interlayered by 0.1 m to 0.5 m thick marl and siltstone, or rare arenite of up to 1.5 m thickness (Figure 11). Laterally, reef flanks slope gently and interfinger with arenite, siltstone, and marl (Plate 3/3, 5) of the lower shoreface (Figure 26). In the marl, actaeonellid gastropods and plagioptychids are common faunal elements.
Reef units usually overlie siltstone or marl. In reef units overlying arenites, clinger morphotypes of *Coralliochama gboehmi* are common faunal elements, which settled in scour marks that are incised into the arenites below (Plate 2/5; Schafhauser et al., 2003). Corals and rudists in the reefs are usually well preserved and appear to be in growth position. Small branched plocoid (*Multicolumnastraea cyathiformis*) and meandroid corals (*Dictuophyllia conferticostata*), clusters and bouquets of hippuritids (*Hippurites* cf. *perkinsi*), and isolated specimens of *Coralliochama gboehmi* characterize the faunal assemblage near the base (Figure 26). Spheroidal and hemispheroidal growth forms of *Actinacis haueri* and one “skullcap-shaped” (sensu Höfling, 1989) *Siderastrea adkinsi* are also common. This “pioneer” fauna not only predominates at the reef base (Plate 3/6), but also near the reef margins and transition towards the adjacent arenite, siltstone, and marl (Plate 2/6). In the reef core, *Multicolumnastraea cyathiformis* and *Dictuophyllia conferticostata* are characterized by massive morphotypes and columnar *Multicolumnastraea cyathiformis* are rare. The reef core comprises a diverse coral assemblage of spheroidal and hemispheroidal growth forms and meandroid,

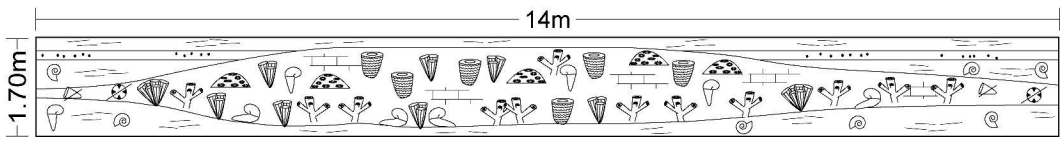

Figure 26: Structure of a coral-rudist bioherm. See text for discussion.

cerioid, phaceloid, and plocoid polyparia arrangements (e.g., *Meandroria oceani, Siderastrea vancouverensis, Cladocora gracilis, Dermosmiliopsis orbignyi*; Plate 3/4). Coral height generally ranges from 0.2 m to 0.6 m, but specimens >1 m are also present. Single elevator rudists (e.g., *Mitrocaprina* cf. *tschoppi, Coralliochama gboehmi Tampsia floriformis, Tampsia poculiformis, Bournonia cardenasensis,*) predominate in the reef core, but clusters and thick-

ets of hippuritids (*Hippurites muellerriedi*, *Hippurites* cf. *perkinsi*) and sparse clingers (*Coralliochama gboehmi*) are also present. The biggest rudists are *Tampsia* and *Coralliochama*, which reach a maximum height of approximately 400 mm. Reef binders are coralline algae (*Sporolithon*), peysonneliacean algae (*Pseudolithothamnium album*), and encrusting foraminifera.

Reef sediment consists of marly coral-rudist rudstone with packstone matrix (Plate 9/5). Microfossil constituents in the packstone matrix comprise ostracods, benthic foraminifera (*Cuneolina*, *Nummoloculina*), and calcareous algae including recrystallized, mostly fragmented, dasycladacean algae. In addition, sorted fragments of gastropods, rudists, non-rudist bivalves, corals, sparse stromatoporids, as well as detrital quartz are common and abundant near the reef margins (Plate 9/6). In the Cardenas section, between 910 m and 938 m, coral-rudist rudstone, contains sparse ooids and a minor amount of detrital quartz as compared to other coral-rudist reefs (Plate 3/2).

Schafhauser (2003) distinguished a “hippuritid-dominated reef type” consisting of branched corals and hippuritids (Plate 2/6). However, our recent studies indicate that these “hippuritid-dominated reefs” represent reef margins of coral-rudist reefs or early stages in reef development.

4.2.2 Coral-dominated reefs

Coral-dominated reefs are restricted to the upper member of the Cardenas Formation, similar to coral-rudist reefs. Units are 4 m to 11 m thick and consist of 0.15 m to 2 m thick coral-bafflestone (Plate 4/5), which interlayer with 0.01 m to 0.25 m thick marl (Plate 4/3).

Faunal diversity is considerably lower than in the coral-rudist reefs. Colonial branching corals are the main reef builders (Plate 4/1) and construct a rigid framework consisting of *Multicolumnastraea cyathiformis* and *Dictuophyllia conferticostata*. Specimens of *Neithea* are abundant and grew on the corals. Rudists are generally small (<100 mm in height) and comprise *Bournonia cardenasensis*, *Coralliochama gboehmi*, *Biradiolites* sp., and sparse hippuritids (e.g., *Hippurites* cf. *perkinsi*). In the core of thicker reef units, massive growth forms of *Antiguastrea cellulosa* and bigger elevator rudists (*Tampsia floriformis*) are present (Plates 4/2, 5/1). Encrusters are corallinacean (*Sporolithon*) and peysonneliacean algae (*Pseudolithothamnium album*), as well as placopsilinid foraminifera.

The bafflestone matrix consists of a packstone that contains scarce fragments of gastropods, abundant miliolid foraminifera, rhodoliths of peysonneliacean algae (Plate 10/1), as well as abundant dasycladacean or gymnocodiacean algae (Plate 9/4).

The marl interlayered with the reef bafflestone contains a diverse, but poorly preserved ostracod fauna (*Haplocytheridea* cf. *dilatipuncta*, *Paracypris* cf. *angusta*, *Platycosta* cf. *lixula*, *Bairdoppilata* sp., *Brachycythere* sp., *Cythereis* sp., *Cytherella* sp., *Neonesidea* sp., *Xestoleberis* sp., ?*Antibythocypris* sp., ?*Trachyleberidea* sp., ?*Limburgina* sp., ?*Escharacytheridea* sp., ?*Veenia* sp., ?*Phacorhabdotus* sp.; pers. comm.. Manuel R. Palacios-Fest), and miliolid foraminifera.

Table 2: Depositional facies of the Cardenas Formation:

Depositional environment		Lithology	Description	Characteristic Fossils
Upper Shoreface	high-energy shoreface	conglomerate	clasts: chert and limestone, well rounded, granules to cobbles, shell fragments; matrix: fine-grained arenite	oysters
		arenite	clasts: quartz, carbonate, fine-grained, subangular to subrounded, well-sorted; matrix: generally absent, rarely pore space filled by silt, mud, or spar calcite cement; sedimentary structures: (slightly inclined) lamination, trough cross-stratification	oysters
	lagoon (low-energy upper shoreface)	marl	sedimentary structures: lamination	miliolid and textulariid foraminifera, dasycladacean algae
		siltstone	clasts: quartz, carbonate, subangular to subrounded, well-sorted; matrix: absent or mud; thick oyster-reefs	actaeonellid gastropods, oysters
		foraminiferal wackestone/ packstone	± detrital quartz	sparse actaeonellid gastropods, ostracods, miliolid and textulariid foraminifera, dasycladacean algae
		foraminiferal cementstone	original matrix recrystallized into pseudospar, ± detrital quartz	sparse actaeonellid gastropods, ostracods, miliolid and textulariid foraminifera, dasycladacean algae
		rudist limestone	rudist floatstone or rudstone; matrix: wackestone (matrix locally recrystallized into pseudospar); ±detrital quartz	rudists, miliolid foraminifera, ± calcarerous algae
Lower Shoreface	sand shoal	oolitic-grainstone	ooids, well-sorted coated grains; nuclei of the ooids: miliolid foraminifera, shell fragments, quartz	
		bioclastic-grainstone	well-sorted coated grains, shell fragments, detrital quartz, patches of foraminiferal packstone	benthic foraminifera, red algae
	middle to lower shoreface	arenite	clasts: quartz, carbonate, fine-grained, subangular to subrounded, well-sorted; matrix: generally absent, silt, or mud	actaeonellid gastropods
		siltstone	clasts: quartz, carbonate, subangular to subrounded, well-sorted; matrix: absent	sphenodiscid ammonites, actaeonellid and turritellid gastropods, bivalves, ostracods, benthic foraminifera
		marly limestone	packstone, shell fragments; abundant detrital quartz	actaeonellid gastropods, miliolid foraminifera, dasycladacean algae
		coral-rudist limestone	coral-rudist rudstone; matrix: packstone with sorted bioclasts; ± detrital quartz	corals, rudists, gastropods, ostracods, miliolid foraminifera, calcareous algae

Depositional environment		Lithology	Description	Characteristic Fossils
Lower Shoreface	lower shoreace	coral-limestone	coral-bafflestone; matrix: foraminiferal packstone	branched corals, small rudists, calcareous algae
		marl		sphenodiscid ammonites, crustaceans, turritellid gastropods, bivalves, ostracods, benthic foraminifera
	lower shoreface	packstone	foraminiferal packstone	echinoderm fragments, ostracods, benthic foraminifera
		siltstone	quartz, carbonate; sedimentary structures: symmetrical ripples	branched bryozoans, orbitoidacean foraminifera, serpulids
		marl	sedimentary structures: lamination	ammonites, gastropods, single oysters, ostracods, benthic foraminfera, sparse planktic foraminifera, serpulids, sparse calcispheres, chaetetids
Offshore	offshore	siltstone	clasts: quartz, carbonate, subangular to subrounded, well-sorted matrix: absent	sparse benthic foraminifera, planktic foraminifera, calcispheres, serpulids
		marl/marly limestone		sparse benthic foraminifera, planktic foraminifera, calcispheres, serpulids

4.3 Offshore transition facies

The offshore transition facies is characterized by arenite, siltstone, marl, and foraminiferal packstone (Plate 11/1). The faunal assemblages include echinoids, rare ammonites (e.g., *Pachydiscus neubergicus*), gastropods, bivalves (*Exogyra costata, Lopha* sp., *Arctostrea* sp.), abundant branching bryozoans (Plates 5/2, 5; 10/4), abundant benthic foraminifera, (*Ayalaina, Lepidorbitoides, Sulcoperculina*; Plates 10/5; 11/1, 5, 7), calcified (serpulid and spirorbid) and aggregated (sabellariid) worm tubes (Plates 4/4; 10/3, 4), as well as abundant ostracods (*Haplocytheridea* sp., *Cytherella* sp., *Cytheridea* sp. cf. *mytiloides*, *Polylophus asper*, *Xestoleberis* sp., *Cytherelloidea* cf. *austinensis*, *Brachycythere* sp.; pers. comm. Manuel R. Palacios-Fest), and sparse planktic foraminifera.

4.4 Offshore facies

Offshore lithology consists of siltstone, marl, and marly limestone, whereas arenite is characteristically absent. The faunal assemblages include echinoids, pectinid bivalves, ostracods, abundant orbitoidacean and planktic foraminifera, as well as calcispheres (Plate 11/ 2, 3). Offshore facies mark the highest water depths in the Cardenas Formation. Transgression led to sediment starvation and hardgrounds. These discontinuities are marked by the accumulation of pectinid bivalves, iron crusts (Plate 5/2), and carbonate nodules (see chapter 6).

4.5 Depositional setting

Lithologies of the Cardenas Formation are predominated by fine-grained clastic sediment (arenite, siltstone, marl) with uniform grain-sizes and good sorting, whereas conglomerate layers are thin and sparse. These lithologic characteristics, as well as sediment structures in the arenite, such as trough cross-stratification and overlying planar lamination, indicate deposition in a wave-dominated shoreface delta system (Elliott, 1986; Howell and Flint, 2003).

The thin and sparse conglomerate layers are intercalated in arenite units, but lack characteristics of channel deposits, such as channel morphology, trough cross bedding, or fining upward sequences. Conglomerates are hence interpreted to represent proximal sediment bodies or bars of the upper shoreface (Figure 25), which have been redistributed by storm events or longshore currents. Oysters, which settled in the upper shoreface, were ripped off during these periods and reworked into the conglomerates after transport (Einsele, 1992). Cherts are resistant residues and suggest sediment erosion from a nearby carbonate platform (Pettijohn et al., 1984). They probably result from the weathering and erosion of older limestones of the Valles-San Luis Potosí platform. These rocks have been exposed during the uplift of the Sierra Madre Oriental, west of Cardenas (see chapter 1.1). Trough cross-stratified and laminated arenite associated with the conglomerate has also been deposited in the upper shoreface zone, above fair-weather wave base (Howell and Flint, 2003). These areas have likely been affected by continental runoff and fluctuating salinities. In consequence, oyster biostromes developed in the shallow turbid waters and faunal diversity is generally very low.

Miliolid foraminifera and dasycladacean algae in siltstone, marl, and limestone characterize lagoonal areas, almost unaffected by terrigenous input. Under these environmental conditions mono- to paucispecific rudist patch reefs existed in the Cardenas Formation and are also well known to exist from lagoonal and inner platform environments of the whole Tethyan realm (e.g., Masse and Philip, 1981; Scott et al., 1990; Gili et al., 1995; Sanders and Baron-Szabo, 1997; Sanders and Pons, 1999; Götz, 2001). In the *Durania ojanchalensis* and radiolitid reefs, the predominance of miliolid foraminifera, and absence of calcareous algae, suggests low light intensity. The low faunal diversity may also indicate fluctuating water salinities as suggested for *Durania* assemblages from central Oman (Schumann, 2000). *Durania ojanchalensis* settled in extremely shallow environments of the Cardenas Formation and formed patchy “rudist meadows” above the fair-weather wave base. In this environment the fine sediment was reworked by wave action and storm events leading to turbid water and low light intensity. Parautochthonous *Durania ojanchalensis* assemblages in arenites in the La Luz section appear to be reworked by storm events, and subsequently covered by clastic sediments. In a slightly deeper water, reef thickness increased and *Durania* is associated with *Coralliochama* and sparse corals.

In contrast, abundant calcareous phylloid and corallinacean algae in the *Macgillavryia nicholasi* reefs of the Estación Canoa section indicate well-illuminated environments. This interpretation is supported by the lateral expansion of the right (attached) valve of *Macgillavryia nicholasi,* leading to an umbrella-like morphology (see chapter 8). Expansion of the upper margin of the attached valve is described from several radiolitid taxa (e.g., *Durania*) and is often considered as evidence for an expanded mantle that acted as a host tissue for light-dependent symbiotic zooxanthellae. The giant clam *Tridacna* is thought to represent a recent counterpart (Kauffman and Sohl, 1973; Vogel, 1975; Skelton, 1979). On the other hand, abundant rhodoliths in the fine-grained reef sediment indicate a mobile substrate. In this shift-

ing sediment, umbrella-like structures of *Macgillavryia nicholasi* may also have provided stabilization. The extended upper part of the right valve rested on the substrate and prevented toppling; hence this elevator rudist mimics the growth mode of clinger and recumbent rudist morphotypes (see chapter 1.2) by extension of the contact area between shell and substratum.
In the *Praebarrettia* reefs, the abundance of calcareous algae and absence of detrital quartz suggest well-illuminated environments and reduced terrigenous input. In addition, favorable environmental conditions are indicated by an increased faunal diversity, a lower abundance of miliolid foraminifera, and an increasing thickness of the reef bodies as compared to the *Durania* reefs. *Praebarrettia* reefs hence developed in more distal areas and deeper waters as compared to the *Durania* reefs, at the transition between the lagoon and lower shoreface. Upsection, *Praebarrettia* associations are replaced by *Durania*. In addition, reworking of the rudists increases upsection in these reefs. These changes are interpreted as a shallowing-upward sequence (see chapter 6.1).

Towards the lower shoreface**,** faunal diversity increases. The transition between upper and lower shoreface is characterized by the abundance of actaeonellid gastropods and miliolid foraminifera. Distally, these faunal elements decrease in number, whereas turritellid gastropods and non-rudist bivalves increase.
In areas of low terrigenous input and high current energy, mobile sediment bodies were deposited consisting of oolitic and skeletal grainstone (Flügel, 1978; Tucker, 1990; Simone et al., 2003). The grainstones are interpreted to represent shoals and bars. They were deposited on the lower shoreface as indicated by a mixture of components derived from shoreface (dasycladacean algae, miliolid foraminifera) and offshore environments (orbitoidacean foraminifera). Micritic coatings around the bioclasts are caused by endolithic microorganisms (Wright, 1990) and suggest the absence of significant sediment accumulation and longer periods, in which bioclasts remain unburied (Greenstein and Pandolfi, 2003). The high-energy setting prevented the deposition of fine-grained sediment. Only short episodes of lowered energy permitted the deposition of mud (Samankassou et al., 2003), as indicated by patches of foraminiferal packstone in the oolitic grainstone (Plate 8/7).
Storm-generated oolitic packstone is sporadically intercalated. It consists of single superficial and compound ooids, gastropods, benthic foraminifera (*Lepidorbitoides, Ayalaina*), intraclasts, and detrital quartz (Plate 10/8). Ooids generally develop in shallow agitated waters, whereas packstones indicate low-energy conditions. However, the mixture of bioclasts in the packstone derived from deeper (orbitoidacean foraminifera) and shallow environments (miliolid foraminifera, ooids, detrital quartz) indicates a storm-induced deposition. During these events, ooids and detrital quartz were transported from shallow water environments into sheltered areas of deeper water (Scholle and Ulmer-Scholle, 2003).
The coral-rudist reefs interfinger with clastic sediments of the lower shoreface, and most reefs evolved from siltstone, marl, and marly limestone. At the base of the reefs, the pioneer fauna consists of branching corals, clinger rudists and rudist frameworks. The low variety of coral growth forms, the predominance of branching corals, the occurrence of *Actinacis* and of "skullcap-shaped" corals (sensu Höfling, 1989), and the abundance of rhodoids suggest an unstable soft substrate and moderate to high sedimentation or resedimentation rates (Chappell, 1980; Höfling, 1989; Baron-Szabo, 1997). Composition of this pioneer fauna is similar to the faunal assemblage of the coral-dominated reefs (see chapter 4.2.2). The

branched mode of growth probably prevented corals from being covered by reworked mud sediment and enabled them to rise over the turbid bottom water that would have resulted in burial and reduction of light intensity. In addition, only clinger rudist-morphotypes and constructive rudist frameworks were able to exist in the mobile substrate. In contrast, isolated elevators are frequently tilted (Plate 4/7) at the reef base. The tilting was caused by water currents or wash out of the stabilizing substrate, and rudists were subsequently covered by sediment (Götz, 2001). The pioneer fauna stabilized the substrate and generated an elevated reef topography, which allowed the development of a more diverse coral-rudist fauna in the reef core, unaffected by reworked sediment, burial, or reduction of light intensities. The diverse reef fauna indicates excellent environmental conditions for a successful co-existence of corals and rudists. In the reef core, corals stabilize rudists and prevent a tilting of individuals. The hard substrate provided by rudist shells and coral skeletons allowed the development of a diverse coral assemblage (Götz, 2003a). Moderate to – probably episodic – high current energies are indicated by sorted bioclasts, high degree of fragmentation, and the occurrence of detrital quartz within the sediment of most coral-rudist reefs. These reefs probably grew above the fair-weather wave base in the lower shoreface. In contrast, few coral-rudist reefs developed in low energy protected lagoonal environments and are characterized by abundant miliolid foraminifera and rhodoliths, and minor amounts of shell fragments and detrital quartz (Plate 9/2).

In coral-dominated reefs, the low variety of coral growth forms, the predominance of branching corals, the abundance of dasycladacean algae and peysonelliacean rhodoliths, and the absence of detrital quartz indicate reef growth on a soft and mobile substrate of protected areas (Chappell, 1980; Baron-Szabo, 1997). They developed in protected areas of the lower shoreface, probably proximal to the mixed coral-rudist reefs, as observed in many localities of the Tethyan realm (e.g., Scott et al., 1990; Gili et al., 1995; Skelton et al., 1997; Sanders and Pons, 1999; Götz, 2001). Lime mud was baffled in the dense reef structure, and only episodic storm events led to reworking of corals and significant export of the muddy sediment. The branched mode of growth enabled corals to rise over the turbid bottom waters and permit the development of flat-shaped and massive corals on the resulting elevated reef, which was less affected by turbidity. In addition, the accumulation of coarse reef debris permitted a stable upward-growth of big elevator rudists in the reef core (Skelton and Gili, 1991; Götz, 2003a).

Delicate branching bryozoans, orbitoidacean foraminifera, and serpulids characterize deeper water of the offshore transition zone (Smith, 1995; Aguilar et al., 2002). In this environment, isolated individuals of *Exogyra costata* and *Arctostrea aguilerae* flourished. These taxa favored a soft substrate and inhabited deeper environments, less affected by water currents (Carter, 1968; Stenzel, 1971; LaBarbera, 1981; Seilacher et al., 1985). Sporadically intercalated bioclastic packstone layers are interpreted as storm deposits and contain mixed bioclasts from shoreface (oysters, corallinacean algae) to offshore settings (branching bryozoans, benthic and planktic foraminifera, serpulid worm tubes) (Plate 11/4).

Further offshore**,** siltstone and marl contain abundant planktic foraminifera and calcispheres and rare echinoids and pectinid bivalves.

5 Depositional facies of the Tabaco Formation

Conspicuous red-colored conglomerate, arenite**,** silt-, and claystone characterize the Tabaco Formation, but outcrops are scarce.

Conglomerate layers are unsorted and contain coarse sand- to cobble-sized, rounded to sub-angular clasts (Plate 11/6) of arenite, silt-, and limestone.

Limestone clasts derived from the Cardenas Formation and consist of reef limestone, peloidal and corallinacean algal grainstone, and marly wackestone containing planktic foraminifera and calcispheres. Reef limestone consists of a packstone with radiolitid and hippuritid fragments and benthic foraminifera. Corallinacean algal grainstone contains abundant spheroidal to hemispheroidal corallinacean algae and benthic foraminifera. In some grainstones, bioclasts and intragranular pores are coated by hematite. Arenite and siltstone clasts consist of carbonate and quartz. They are either unfossiliferous and correspond to the red arenite and siltstone lithologies of the Tabaco Formation as described below, or they lack the red color and contain fragments of radiolitids, non-rudist bivalves, and benthic foraminifera (*Sulcoperculina*, orbitoidacean foraminifera). These latter clasts must be derived from the underlying Cardenas Formation. The conglomerate matrix consists of quartz and carbonate clasts, but also contains fragments of rudists, benthic foraminifera (*Sulcoperculina*, orbitoidacean foraminifera), and corallinacean algae. Boring of lithophagid bivalves is common in shell fragments, and rims of the bioclasts contain calcite crystals of *Microcodium* (Plate 11/9). Grainsize varies from middle to coarse sand. The interstitial spaces are filled by spar cement.

The arenite in the Tabaco Formation is fine-grained and lithology is similar to the siltstone (Plate 11/8). Grains are weakly rounded to angular and consist of quartz, hematite, and carbonate, as well as sparse fragments of benthic foraminifera. The hematite grains cause the red color of the sediments. Actaeonellid gastropods are present in the arenite and siltstone, and bioturbation is common (Plate 5/6).

5.1 Depositional setting

The red beds of the Cardenas Formation are interpreted to represent delta deposits similar to the red beds of the Difunta Group of northeastern Mexico (e.g., McBride, 1974; McBride et al., 1975). *Microcodium* in the limestone clasts indicate subaerial exposure of the source area (Scholle and Ulmer-Scholle, 2003). The detrital hematite in the sediments and the hematite coatings of the clasts derived from continental weathering (Tucker, 1985). The paleosoils indicate occasional emersion of the depositional area.

6 Sequence stratigraphy

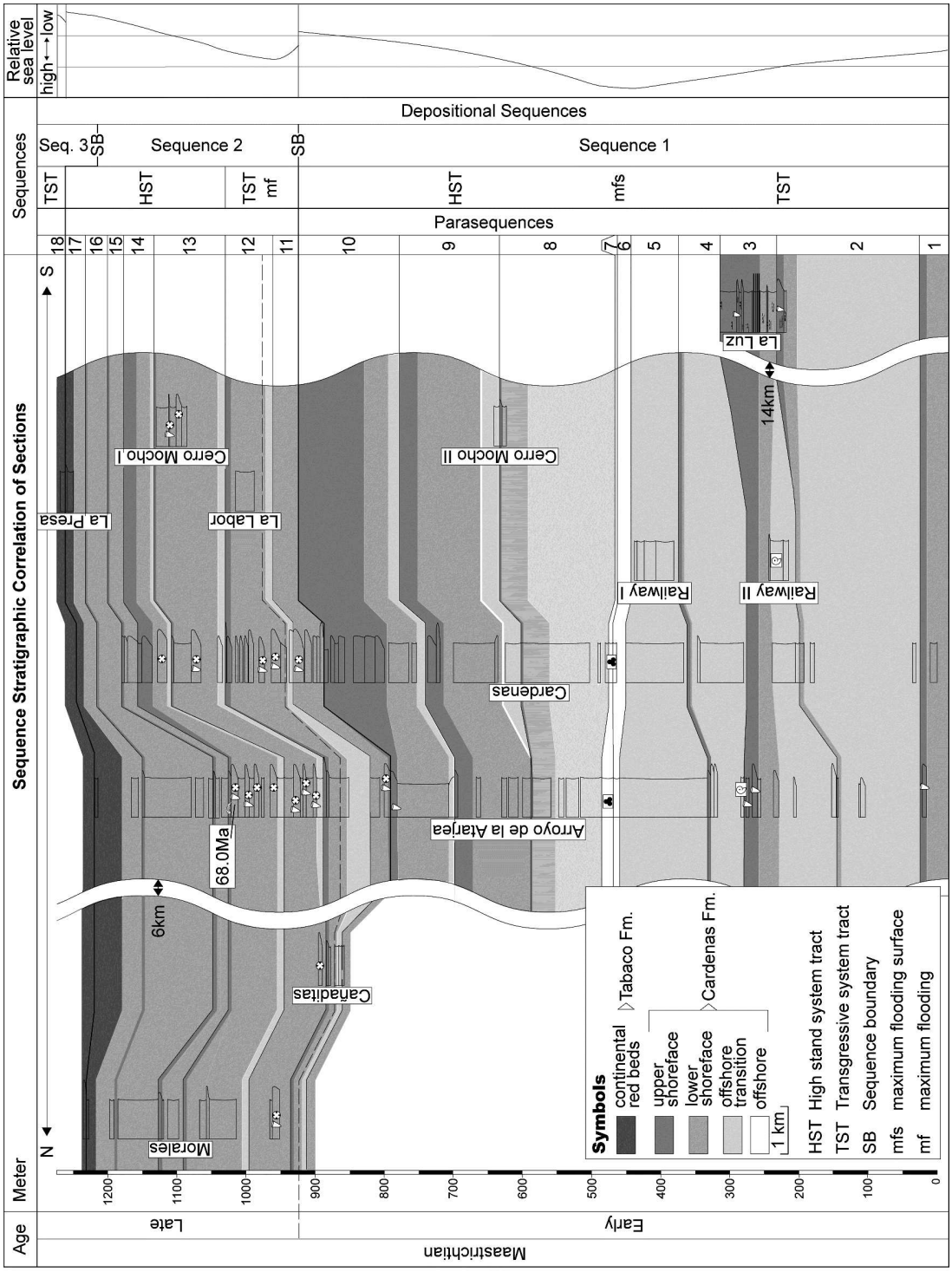

Figure 27: Sequence stratigraphic correlation of sections in the Cardenas area. Biostratigraphic markers are presented in boxes. The 68.0 Ma age resulted from Sr-isotope measurements. The position of the early/late Maastrichtian boundary is based on sequence stratigraphic correlation with the global sea-level chart provided by Hardenbol and Robaszynski, 1998 (see chapter 7.2). Datum is the mfs between parasequences 7 and 8. See text for discussion.

Sequence stratigraphic framework permits the correlation of sections of the Cardenas Formation by parasequences, which is otherwise hampered by the absence of marker horizons. In addition, sequence stratigraphic interpretation allows recognition of the evolution in time of the Cardenas area in terms of sea level changes and correlation of the investigated sequence with the sea level chart provided by Hardenbol and Robaszynski (1998).
Genetically related depositional facies (see chapter 4 and 5) are therefore summarized in elementary (Strasser et al., 1999; Bernaus et al., 2003) or parasequences (Van Wagoner et al., 1988; Coe and Church, 2003), which are in turn forming blocks of sequences or depositional sequences (e.g., Van Wagoner et al., 1988; Strasser et al., 1999; Coe and Church, 2003). Within the depositional sequences, changes in the rate of accommodation space or sediment supply are represented by low stand (LST), transgressive (TST), high stand (HST), and falling stage (FSST) system tracts (Van Wagoner et al., 1988; Coe and Church, 2003). A maximum flooding surface (mfs) marks the most landward extension of the shoreline during transgression, and a maximum water depth in the depositional area (Coe and Church, 2003; Schaefer, 2005). Sediments of the FSST usually occur during forced regression (Coe and Church, 2003), but due to the following emersion of the depositional area, they are frequently eroded. They are absent in the Cardenas and Tabaco formations.

6.1 Parasequences

In the investigated sections, 18 parasequences are recognized by the progradational stacking pattern of depositional facies. Their thickness reaches from 4 m to 180 m (Figure 27). The lower and upper parasequences (1, 2, 17, and 18) are poorly exposed. Parasequences 1 to 16 belong to the Cardenas Formation, whereas parasequence 17 encompasses the uppermost part of the Cardenas Formation and the lower part of the Tabaco Formation. Parasequence 18 only includes the Tabaco Formation. Composition of the parasequences is quite uniform and, offshore transitional facies passes into lower shoreface facies, which in turn underlies sediments of the upper shoreface or lagoon and continental red beds (parasequences 3, 4, 8, 9, 10, 12, 13, 14, 15). Parasequences 6 and 7 are exclusively composed of offshore facies, whereas parasequences 5 and 11 consist only of offshore transitional (parasequence 5), and upper shoreface (parasequence 11) depositional facies, respectively. The uppermost parasequences 15 to 18 only contain lower shoreface and upper shoreface/lagoonal or continental red bed facies.
Boundaries between the parasequences are sharp, and they are separated by marine flooding surfaces (Schaefer, 2005), marked by an abrupt change in facies from shallow (e.g., lower shoreface, upper shoreface/lagoonal facies) into deeper water facies (e.g., offshore transitional facies). The boundaries between parasequences 6, 7, and 8 consist of hardgrounds, which are characterized by the accumulation of pectinid bivalves and iron crusts (Plate 5/2).

6.2 Depositional sequences

3 depositional sequences (Figure 27) are recognized in the investigated area based on the vertical stacking pattern of the 18 parasequences described in the previous chapter as well as associated discontinuity surfaces. Only the uppermost sequence is poorly exposed.

Depositional sequence 1 is between 800 m and 880 m thick and consists of a TST and HST. The TST is characterized by a retrogradational stacking pattern of parasequences 1 to 5, which mainly consist of offshore transitional facies, whereas lower and upper shoreface/lagoonal deposits are thin. The condensed parasequences 6 and 7 indicate a decreasing rate of sedimentation and deepening of the depositional area. These parasequences consist only of offshore facies and are separated by hardgrounds, which indicate sediment starvation and maximum water depth in the depositional area. The uppermost hardground corresponds to a mfs, which separates the TST from the HST. The HST is formed by the progradational stacking pattern of parasequences 8 to 10: from the lower parasquence 8 to the upper parasequence, 10 thickness of offshore transitional facies decreases, whereas thickness of lower and upper shoreface/lagoonal facies increases.

Depositional sequence 2 is 370 m to 450 m thick and consists of a TST and HST. An aggradational to retrogradational stacking pattern of parasequences 11 and 12 characterizes the TST. Maximum water depths are indicated by thick offshore transitional facies in the basal parasequence 12, which contains sparse planktic foraminifera. Upsection, offshore transitional facies decreases in thickness from parasequence 13 to 14, whereas lower and upper shoreface/lagoonal facies increase. In addition, offshore transitional facies is absent in parasequences 15 to 18 resulting in a progradational pattern. A paleosoil horizon and continental red beds in the uppermost parasequence 17 indicate emersion of the depositional area.

Depositional sequence 3 is poorly exposed. The base consists of an unsorted conglomerate, interpreted as a transgression conglomerate (see chapter 5). Emersion of the source area is indicated by clasts derived from upper shoreface to offshore environments, and by *Microcodium* incised into the rims of the reef clasts. Upsection from the conglomerate, actaeonellid-bearing red claystone indicates deposition on the shoreface, but the red color suggests subsequent emersion of the depositional area (see chapter 5.1).

Considering the large-scale stacking pattern of the 3 depositional sequences, sequences decrease in thickness upsection, and continental red beds of the Tabaco Formation terminate the sediment succession. In consequence, the depositional sequences present a progradational pattern, which results in regression and emersion of the Cardenas area during the late Maastrichtian.

7 Discussion and conclusions

7.1 Geological history of the Cardenas area during the Maastrichtian

The Cardenas Formation and overlying Tabaco Formation form a 1250 m thick sediment sequence of wave-dominated shoreface delta sediments. They were deposited during the Maastrichtian, in the newly developed foreland of the Sierra Madre Oriental (Figure 28). Wave-dominated shoreface delta systems, such as the Cardenas Formation (see chapter 4.5),

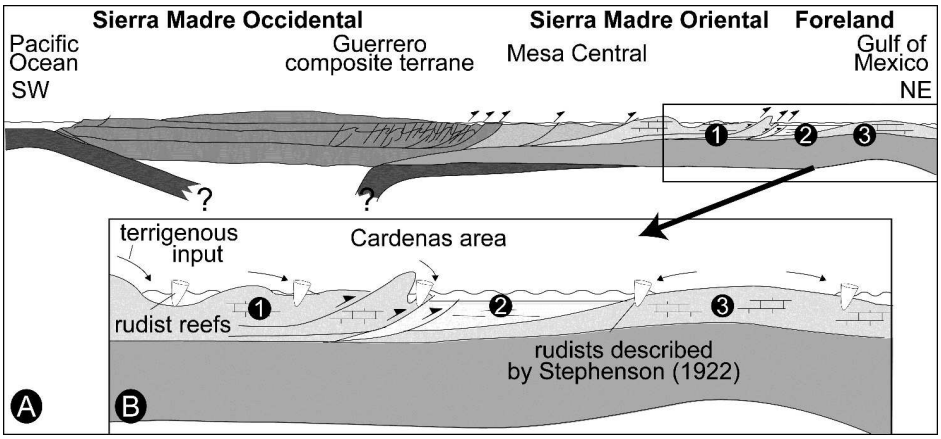

Figure 28: A) Southwest–northeast schematic cross section through central Mexico showing late Cretaceous paleogeography and tectonic framework (modified after Ye, 1997). B) Depositional model of Maastrichtian rudist frameworks on the inherited palaeorelief of the Valles-San Luis Potosí carbonate platform. East-central Mexico is dissected by thrust and folds resulting in emerged islands exposed to erosion. Rudist frameworks developed in small basins between the islands and were affected by terrigeneous input. (1) Valles-San Luis Potosí. carbonate platform, (2) Tampico-Misantla foredeep, (3) Tamaulipas arch. See also text for discussion.

are characteristic features of young orogenic belts, which lack established drainage systems during their uplift (Howell and Flint, 2003). In consequence, sediment is transported into the foreland basin by numerous small rivers. Sediments are easily reworked and redistributed along the coast in the delta systems of these foreland basins by wave processes and storm events (Howell and Flint, 2003). In the Cardenas Formation, the absence of tidal deposits and the presence of barrier islands indicate micro- to mesotidal regimes, similar to the present Gulf of Mexico (Elliott, 1986). In consequence, the depositional environment of the Cardenas Formation fits the tectonic models, which propose that initial uplift of the Sierra Madre Oriental began during the uppermost Cretaceous (see Figure 1; e.g., Sohl et al., 1991; Gray and Johnson, 1995; Ye, 1997; Antuñano et al., 2000).

The presence of shoreface deposits in the Cardenas and Tabaco formations indicates an extended shallow water area in the central Mexican foreland, which is otherwise predominated by deep water deposits of the Mendez Formation (see chapter 1.1). This shallow water area results from a palaeorelief inherited from the Valanginian to Campanian Valles-San Luis Potosí carbonate platform, which is indicated by corresponding depositional areas and a gradual transition between the Cardenas Formation and underlying Valles-San Luis Potosí platform carbonates (see chapter 1.1; Smith, 1986; Basáñez-Loyola et al., 1993). On this pa-

laeohigh, sediments of the shoreface predominate, whereas offshore facies only developed during major transgressive events (Figure 29).
The Sierra Madre Oriental uplift resulted in minor folding and thrusting of this palaeohigh (Ye, 1997) leading to small islands (Figure 28). These islands were exposed to erosion and the terrigenous sediment was transported into the sea by small wave-dominated delta systems, similar as known for the Cretaceous foreland basin of the southern Pyrenees (Spain)

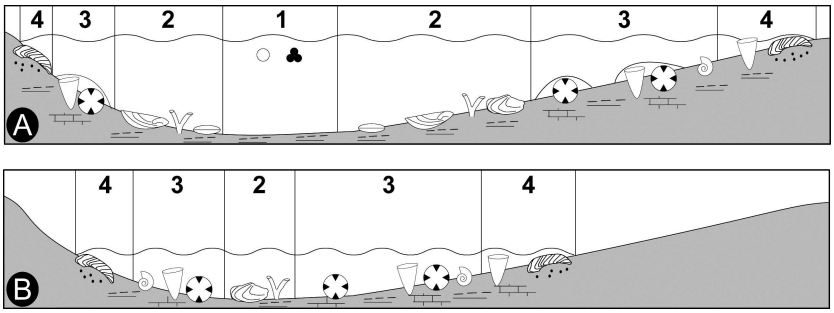

Figure 29: Depositional facies during sea level high-stand (A) and low-stand (B). (1) offshore, (2) offshore transition zone, (3) lower shoreface, (4) upper shoreface. See text for discussion.

(Puigdefàbregas et al., 1992). Stratigraphic data suggest a mean depositional rate of 55 cm/ka for the Cardenas Formation. As a result of this high terrigenous input, reef growth was probably restricted to areas between small delta fans, as observed today in the northern Red Sea (Roberts and Murray, 1988). Continental red beds of the Tabaco Formation result from the emersion of the Cardenas area due to enlargement of the foreland belt and probably a concomitant sea level lowstand (see chapter 7.2).
In east-central Mexico, rudists of Maastrichtian age are not restricted to the Cardenas Formation. They are also known to exist in outcrops of the Gulf Coast plain, approximately 200 km east of the investigated area (Figure 28; Stephenson, 1922) near the railway stations Manuel and Chocoy. The Manuel section represents the type locality of the genus *Tampsia* (Stephenson, 1922). Sediment consists of marl, assigned by Stephenson (1922) to the Mendez Formation, the deep water time equivalent of the Cardenas Formation. The occurrence of rudists, however, indicates a shallow water environment corresponding to the Cardenas Formation. Between these two outcrop areas of the Cardenas Formation and the rudist-bearing Mendez Formation, open marine deep water sediments of the Mendez Formation containing abundant planktic foraminifera are exposed. The presence of rudists close to the Gulf of Mexico coastline therefore supports the existence of a latest Cretaceous palaeohigh along the Tamaulipas Arch (Stinnesbeck et al., 1993; Stinnesbeck et al., 1996; Ye, 1997).

7.2 Age of the analyzed sequence

The formation of various scaled sequences (e.g., parasequences, depositional sequences) is attributed to a large variety of interrelated and interacting parameters, reaching from a local (e.g., tectonism, carbonate sediment production) to a global scale (e.g., climate, glacioeustasy; Bailey, 1998; Strasser et al., 1999). Sequences that coincide with the sequence stratigraphic pattern recognized in European basins (Hardenbol and Robaszynski, 1998), are considered as eustatic and provide additional age data on analyzed sections. However, ages of

the Maastrichtian sequences are not well constraint in the sea level chart, and Hardenbol and Robaszynski (1998) only describe a tentative sequence record.

Stratigraphic markers are rare in the Cardenas Formation, and makes determination of time ranges difficult. The maximum flooding surface (mfs) in sequence 1 is either within the range or close to the LAD of *Pachydiscus neubergicus*, in the upper foraminiferal zone CF6 or lower CF5. It coincides with the major transgressive event MA3 at 68.9 Ma described by Hardenbol and Robaszynski (1998). Using this transgressive event as datum for sequence stratigraphic correlation, the sequence stratigraphic pattern of the Cardenas Formation corresponds well with the Maastrichtian sea level record (Figure 30), which suggests, that depositional sequences of the Cardenas Formation represent eustatic sea level changes and are unrelated to regional tectonic movements. 6 Parasequences are intercalated between the mfs at 68.9 Ma and the 68.0 Ma stratigraphic marker derived from Sr-isotope stratigraphy, resulting in an average time span of 0.13 Ma for each parasequence (Figure 27). This corresponds to a fourth order cyclicity (Church and Coe, 2003). In consequence, depositional sequences correspond to 3d order cycles (Church and Coe, 2003). The exposed part of depositional sequence 1 corresponds to a period of 1.3 Ma, whereas sequence 2 spans a period of 0.9 Ma. The boundary between sequences 1 and 2 is at 68.5 Ma, and the boundary between sequences 2 and 3 at 67.6 Ma.

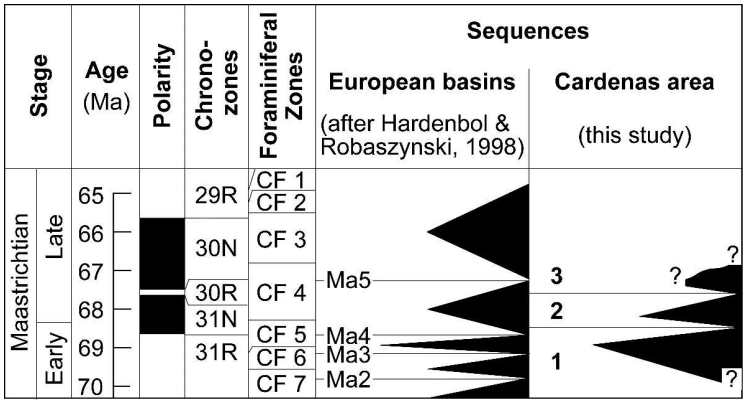

Figure 30: Maastrichtian sequence record of Hardenbol & Robaszynski (1998) compared to sequences recognized in the Cardenas and Tabaco formations. Black triangles indicate transgresssive events. See text for discussion.

In conclusion, stratigraphic correlation of sequence patterns in the Cardenas area and the sea level chart of Hardenbol and Robaszynski (1998) suggests an early Maastrichtian age for the exposed part of sequence 1 of the Cardenas Formation, spanning the foraminiferal zones CF7 to CF5 (lower part). Sequence 2 and the exposed part of sequence 3 are of early to middle late Maastrichtian age, corresponding to the foraminiferal zones CF5 (uppermost part) and CF4 (Figure 30). In summary, the age of the analyzed sequence of the Cardenas and Tabaco formations reaches from the early Maastrichtian (approx. 69.5 Ma) to the middle late Maastrichtian (approx. 67.2 Ma) resulting from the combination of Sr-isotope, bio-, and sequence stratigraphy.

7.3 Biozones of the Cardenas Formation

Myers (1968) subdivided the Cardenas Formation (from base to top) into the *Durania ojanchalensis*, the *Arctostrea aguilerae*, and the *Tampsia floriformis* biozones (see chapter 1.4). Based on observations in the Arrroyo de la Atarjea section, he considered the *Tampsia floriformis* zone as a new Maastrichtian biozone for the Gulf of Mexico, above the *Exogyra costata* zone (Myers, 1968). I agree with Myers (1968) regarding the biozonal subdivision of

the Cardenas Formation, but disagree regarding his interpretation on the evolution of these index fossils (Figure 6).

According to Myers (1968), changing depositional environments were responsible for the disappearance of *Durania ojanchalensis* in the upper part of the lower lithologic member. At Arroyo de la Atarjea, *Durania* is restricted to limestone units of the lower member representing protected lagoonal areas. At La Luz, however, *Durania* also occurs in siltstones and arenites of upper shoreface or lagoonal environments, where they build loose carpets of limited extent and with only few individuals. Similar depositional facies are scarce in the middle member of the Cardenas Formation, which is predominated by offshore transitional sediments. In the upper member of the Cardenas Formation, however, sediments reflecting the transition from lagoonal to lower shoreface environments are common, but neither *Durania* associations nor *Praebarrettia* assemblages have been observed. It appears, that these warm water adapted rudists may not have recovered after the late early Maastrichtian (foraminiferal zones CF5 and CF6) transgressive phase, which led to the ingression of cool waters into the Sierra Madre Oriental foredeep. These lower water temperatures are indicated by the diverse ammonite assemblage in the Mendez Formation (Ifrim et al., 2005), as well as by diverse planktic foraminiferal faunas (Li and Keller, 1998a) and the stable isotopes (Barrera et al., 1997).

Myers (1968) also proposed an extinction of *Arctostrea aguilerae* and *Exogyra costata* in the lower part of the upper member (see chapter 1.4), thereby delimitating the *Arctostrea aguilerae* biozone. However, *Exogyra costata* is still present in the upper part of the upper member, although rare. Both, *Arctostrea aguilerae* and *Exogyra costata* are soft bottom dwellers that inhabited deeper water less affected by currents (Carter, 1968; Stenzel, 1971; LaBarbera, 1981; Seilacher et al., 1985). Deeper water and more distal environments are common in the middle, but sparse in the upper member, which is predominated by shoreface environments. Hence, changing environmental conditions resulted in the decrease of *Arctostrea* and *Exogyra* in the upper member, and the *Tampsia floriformis* zone does not represent an additional Gulf Coast biozone as suggested by Myers (1968).

7.4 Rudist paleobiogeography in central Mexico and the Caribbean

9 rudist genera and 11 species (Table 3) are described from the Cardenas Formation (Böse, 1906; Myers, 1968; this paper). Those genera are well known from Campanian–Maastrichtian formations in the Caribbean and Gulf of Mexico area (Steuber, 2002). In addition, *Tampsia* and *Praebarrettia* characterize the Cretaceous Caribbean province defined by Kauffman and Sohl (1973).

Rudist genera of the Cardenas Formation have also been described from southern Mexico (Chiapas; e.g., Alencáster, 1971; Cros et al., 1998; Garcia-Barrera et al., 1998), Tamaulipas (Burckhardt, 1930), Guatemala (e.g., Scott, 1995; Fourcade et al., 1999), Cuba (e.g., Douville, 1926, 1927; Palmer, 1933; Mac Gillavry, 1935; Rutten, 1936; Thiadens, 1936; Vermunt, 1937; Chubb, 1961; Lupu, 1975; Rojas and Iturralde-Vinent, 1995) and Jamaica (e.g., Trechmann, 1924, 1927; Chubb, 1955, 1956a, b, 1971; Mitchell, 1999; Mitchell and Gunter, 2002). A similar paleobiogeographical pattern results from an analysis on species level: 7 out of the 11 rudist species of the Cardenas Formation (*Mitrocaprina* cf. *tschoppi*, *Coralliochama gboehmi*, *Durania ojanchalensis*, *Tampsia floriformis*, *Bournonia cardenasensis*, *Hippurites*

muelleriedi, *Praebarrettia sparcilirata*) are widespread south of the Cardenas area in Jamaica, Cuba, Puerto Rico, and Yucatan. Only *Biradiolites aguilerae*, *Tampsia poculiformis* and *Hippurites perkinsi* are so far restricted to the Cardenas Formation (Steuber, 2002). In addition, 94% of the coral genera and 56.3% of the species from the Cardenas Formation (Table 4) are also known from the Campanian–Maastrichtian units of Jamaica (Baron-Szabo, 2002; Baron-Szabo, in press). However, corals of the Cardenas Formation also show close affinities to the Coniacian to Santonian associations of France and Austria (Baron-Szabo, 2002).

Table 3: Rudist species described from the Cardenas Formation:

Rudist species:	**Author:**
Mitrocaprina cf. *tschoppi* Palmer, 1933	Schafhauser (this paper)
Coralliochama gboehmi Böse, 1906	Böse (1906), Myers (1968)
Durania ojanchalensis Myers, 1968	Myers (1968)
Macgillavryia nicholasi (Whitfield, 1897)	Schafhauser (this paper)
Biradiolites aguilerae Böse, 1906	Böse (1906), Myers (1968)
Bournonia cardenasensis Böse, 1906	Böse (1906), Myers (1968), Schafhauser (this paper)
Tampsia poculiformis Myers, 1968	Myers (1968), Schafhauser (this paper)
Tampsia floriformis Myers, 1968	Myers (1968)
Hippurites perkinsi Myers, 1968	Myers (1968), Schafhauser (this paper)
Hippurites muelleriedi (Vermunt, 1937)	Myers (1968)
?*Praebarrettia sparcilirata* (Whitfield, 1897)	Schafhauser (this paper)

During the Maastrichtian, rudist assemblages in southern Mexican and the Caribbean belong to the Yucatan carbonate platform and the Greater Antillean arc (Pindell and Barrett, 1990; Meschede and Frisch, 1998; Mann, 1999), which were both located south of Cardenas (Figure 31). North of Cardenas only *Coralliochama* is known to exist in the Difunta group (McBride et al., 1975; Johnson and Kauffman, 1996), whereas all other rudist and coral species appear to be absent. In contrast, non-rudist molluscs of the Cardenas Formation are common elsewhere in the northern Gulf of Mexico region (e.g., Myers, 1968; Wolleben, 1977; Vega et al., 1995). This distributional pattern suggests that unfavorable environmental conditions (e.g., climate, mean annual water temperatures, sea water chemistry) inhibited a presence of coral and rudist specimens further to the north. In this case, the Cardenas

Table 4: Coral species described from the Cardenas Formation by Baron–Szabo et al. (2006):

Coral species
Dictuophyllia conferticostata (Vaughan,1899)
Cladocora jamaicaensis Vaughan, 1899
Cladocora gracilis (d'Orbigny, 1850)
Antiguastrea cellulosa (Duncan, 1863)
Multicolumnastraea cyathiformis (Duncan, 1865)
Placocoenia major Felix, 1903
Siderastrea vancouverensis Vaughan, 1923
Siderastrea adkinsi (Wells, 1934)
Actinhelia elegans (Goldfuss, 1826)
Meandrophyllia oceani (De Fromentel, 1873)
Dermosmiliopsis orbignyi Alloiteau, 1952
Trochoseris catadupensis Vaughan, 1899
Cyathoseris formosa d'Achiardi, 1875
Actinacis parvistella Oppenheim, 1930
Actinacis haueri Reuss, 1854
Goniopora sp.

region may represent the northern boundary of tropical faunal assemblages during the Maastrichtian.

The rudist genus *Tampsia* is conspicuously diverse in east-central Mexico. The genus was defined by Stephenson (1922), who identified *Tampsia bishopi* and *Tampsia chocoyensis* in the presumably shallow water sediments of the "Mendez Formation" 100 km east of Cardenas (see chapter 7.1). In addition, *Tampsia floriformis* and *Tampsia poculiformis* are abundant in the Cardenas Formation (Myers, 1968). Further to the south, only *Tampsia floriformis* has been described by Alencáster (1971) in the Ocozocuautla Formation of Chiapas. The high diversity of *Tampsia* in east-central Mexico and the large number of individuals suggest an origin and evolution of the genus in this area. The scarcity of this rudist in the remaining Gulf of Mexico area and the Caribbean region supports the existence of a northward directed surface current pattern, as suggested by Johnson (1999). These currents may have prevented larval dispersal towards the south. Towards the north lower water temperatures probably restricted the presence of this tropical rudist genus.

7.5 Rudist decline in east-central Mexico

The Cardenas Formation contains one of the last known rudist assemblages worldwide, prior to their extinction at the K/P-boundary (Myers, 1968; Johnson and Kauffman, 1996), but no detailed analysis of their decline exists. Frequently, the absence of biostratigraphic index fossils hampers stratigraphic analysis in rudist bearing shallow water deposits, and data on rudist extinction are not precise. For instance, in the eastern Tethys a reduction in rudist diversity and abundance is noted as early as the Campanian, probably due to the loss of habitat (Steuber et al., 2002). In the western Tethys available data are scarce and Johnson and Kauffman (1996) and Steuber (2002) are the only authors that analyzed rudist extinction. Johnson and Kauffman (1996) proposed a stepwise extinction of rudists in Jamaica, probably caused by changes in the ocean-climate system (sea level changes, temperature, circulation). According to these authors, complex rudist frameworks disappeared during the late early Maastrichtian and were replaced by coral-algal, algal-echinoderm and oyster communities.

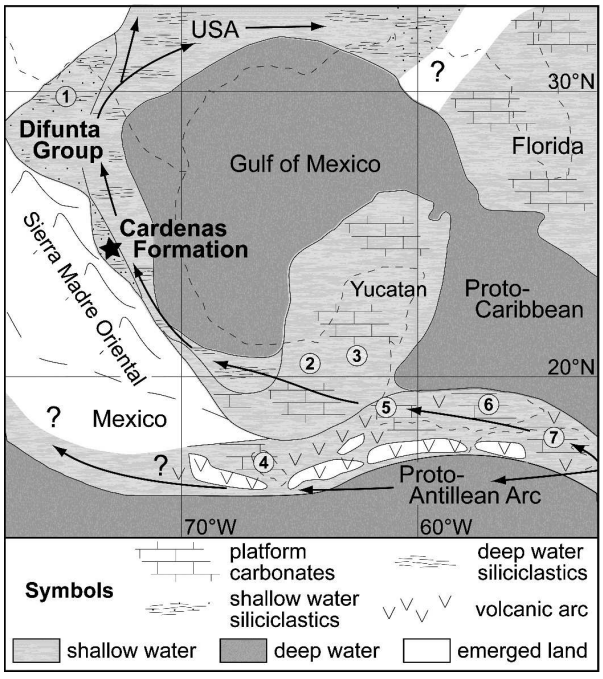

Figure 31: Surface current circulation pattern (arrows; after Johnson, 1999) and occurrences of Maastrichtian rudist species present in the Cardenas Formation in the Gulf of Mexico and Caribbean realm during the Maastrichtian: 1 Difunta Group, 2 Chiapas, 3 Guatemala, 4 Jamaica, 5 southwestern Cuba, 6 southern Cuba, 7 Puerto Rico. Asterisk marks the location of the Cardenas Formation. (Maastrichtian palaeogeography of the Gulf of Mexico and northern Caribbean after Pindell et al., 1988; Sohl et al., 1991; Goldhammer & Johnson, 2004). See text for discussion.

Only single non-reefal specimens and generalists persisted until within 100 ka to 250 ka prior to the K/P boundary (Johnson and Kauffman, 1996). Johnson and Kauffman (1996) suggested that the rudist extinction pattern in Jamaica correspond to that of east-central Mexico, comparing their analyzes from Jamaica with Myer´s (1968) description of the Cardenas Formation. In contrast, Sr-isotope stratigraphic data, provided by Steuber (2002), indicate an age of 65.8 Ma for the last rudists in Jamaica. Even though the age difference to the K/P boundary (65.0 Ma) is 800 ka, Steuber (2002) proposed a catastrophic extinction of Jamaican rudists, caused by an impact at the K/P boundary.
In the Cardenas Formation, I recognized 3 types of reefs: rudist, mixed coral-rudist, coral-dominated reefs. Reef development strongly depended on environmental conditions, such as water depth, current energy, substrate, and terrigenous input. Reefs thrived in a wave-dominated shoreface delta system in the foreland of the Sierra Madre Oriental. High sedimentation rates and unstable environments only permitted the existence of small bioherms (see chapters 4.5 and 7.1). Low diversity rudist reefs developed in low energy/lagoonal environments. Coral-rudist reefs grew in agitated water of the lower shoreface, affected by increased terrigenous input, whereas coral-dominated reefs flourished in protected areas characterized by soft substrate. Progradation of the foreland belt led to increased sediment input, which covered the rudist bioherms and prevented further rudist settlement. Sr-isotope stratigraphy indicates an early late Maastrichtian age (67.98 Ma) for the last reef (see chapter 2.3). The continuous progradation of the foreland belt and a decrease in sea level caused subaerial exposure of the area during the early late Maastrichtian, indicated by the continental red beds of the Tabaco Formation (see chapter 7.2). In consequence, rudist decline in the Cardenas Formation was not related to events at the K/P boundary, such as the Chicxulub impact, nor to changes in the ocean-climate system. Rather, emersion of the depositional area resulted in the total loss of rudist habitats.

7.6 Conclusions

1. The combination and correlation of biostratigraphic data based on the occurrence of ammonites and planktic foraminifera, Sr-isotope measurements and sequence stratigraphic interpretation indicates an early to middle late Maastrichtian age for the Cardenas and Tabaco formations.
2. The Cardenas and Tabaco formations represent a wave-dominated shoreface delta system, deposited in the foreland of the Sierra Madre Oriental. Shoreface facies predominated in the lower and upper members of the Cardenas Formation, whereas offshore transition facies are rare. The latter environments prevail in the middle member; a condensed unit deposited offshore indicates a transgressive event in the middle member during the late early Maastrichtian foraminiferal zones CF5 and CF6. Progradation of the Sierra Madre Oriental foreland belt led to the deposition of continental red beds, known as Tabaco Formation. These sediments conformably overlie the Cardenas Formation and indicate an emersion of the depositional area.
3. The Cardenas Formation represents the northernmost occurrence of Maastrichtian tropical rudist and coral species. Mono- to paucispecific rudist reefs grew in lagoons, whereas diverse coral and rudist assemblages thrived in high-energy environments, and coral-dominated assemblages in protected areas of the upper shoreface. The last

rudist assemblage in the Cardenas Formation, a coral-rudist reef, is of middle late Maastrichtian age (67.98 Ma). All bio-, isotope-, sediment-, and sequence stratigraphic data indicate, that the final decline of rudists in east-central Mexico is not related to events at the K/P boundary (e.g., changes in the ocean-climate system or the Chicxulub impact). Rather, progradation of the foreland belt led to increased sediment input and subsequent emersion of the Cardenas area, which resulted in the loss of rudist habitats approximately 3 Ma prior to the K/P boundary in the middle late Maastrichtian.

8 Taxonomy

All specimens described in this chapter are stored in the Colección Nacional de Paleontología der Universidad Autónoma de la Ciudad de México (registration: IMG).

Class. Gastropoda
Subclass. Caenogastropoda
Superfamily. Stromboidea
Family. Pugnellidae

Genus. *Pugnellus* Conrad, 1860
Type species. *Pugnellus densatus* Conrad, 1858

Pugnellus densatus Conrad, 1858
plate 13, figures 5–6

1858 *Pugnellus densatus* Conrad, p. 330, pl. 25, fig. 14.
1960 *Pugnellus* (*Pugnellus*) *densatus* Conrad?; Sohl, p. 114, pl. 14, fig. 8.
2000 *Pugnellus* (*Pugnellus) densatus* Conrad; Perrilliat et al., p. 13, figs. 6.1, 6.3.

Description: The body whorl contains eight S-shaped ribs, which are thickened in the central part and die out above and below. Almost the whole shell is covered with callus, so the spire is scarcely visible. The spire makes up about one quarter of the total shell height. The long rostrum (ro) is twisted to the right leading to an S-shaped anterior channel. The inner lip (li) contains a smooth S-shaped groove. The thickened shoulder (sh) bends towards the abapical side and ends at the rostrum. A deep groove separates the shoulder from the body whorl and a shallow groove is located between the shoulder and the outer lip (lo). The ab- and adapical ends of the outer lip terminate in two projections. In large specimens, a smoothed ridge (ri) broadens the outer lip abaxially. A shallow groove separates the outer lip from the shoulder.
Height: 56 mm; Width: 39 mm
Material: One well preserved specimen [IGM 8879] and several fragments.
Occurrence: Middle member of the Cardenas Formation (late Maastrichtian). In late Campanian to early Maastrichtian units of the western Tethys (e.g., Stephenson, 1941; Vega-Vera and Perrilliat, 1990; Kiel and Bandel, 1999).

Class. Bivalvia
Order. Hippuritoida

The following abbreviations are used in the taxonomical study of rudist bivalves (order Hippuritioida):

RV	right valve (in this study: attached valve)
LV	left valve (in this study: free valve)
ma	anterior myophore
mp	posterior myophore
1	anterior tooth in the LV
2	central tooth in the RV
2'	socket of the central tooth in the LV
3	posterior tooth in the LV
bc	body cavity
ac	accessory cavity extending ventrally from the central tooth (Caprinidae, Plagioptychidae)
s	dorso-ventral septum separating ac from bc (Caprinidae, Plagioptychidae)
Vb	ventral radial band (Radiolitidae)
Pb	posterior radial band (Radiolitidae)
Ib	interband between Vb and Pb (Radiolitidae)
P0	anterior pillar, “ligamental ridge” (Hippuritidae)
P1	central pillar (Hippuritidae)
P2	posterior pillar (Hippuritidae)

In transverse sections, the radiolitid shell consists of horizontal and vertical elements, called funnel plates and muri (see figure 32).

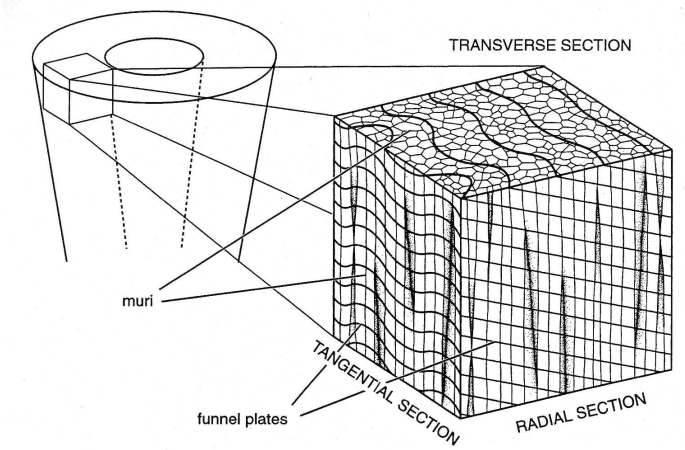

Figure 32: Scheme of the structure of the outer shell of radiolitidae consisting of horizontal funnel plates and vertical muri (after Steuber, 1999).

Family. Plagioptychidae
Genus. *Mitrocaprina* Böhm, 1895
Type species. *Coralliochama bayani* Douvillé, 1888

Mitrocaprina cf. *tschoppi* Palmer, 1933
plate 13, figures 3–4

* 1933 *Mitrocaprina tschoppi* Palmer, p. 103, pl. 10, figs. 1–4.
1937 *Mitrocaprina tschoppi* Palmer; Mac Gillavry, pp. 73, 158, pl. 5, fig. 7; pl. 7, figs. 1, 4–5, 7–8; pl. 8, figs. 4, 7.
v 1968 *Corallichama gboehmi* Böse; Myers, pp. 41–42, pl. 3, figs. 1–2.

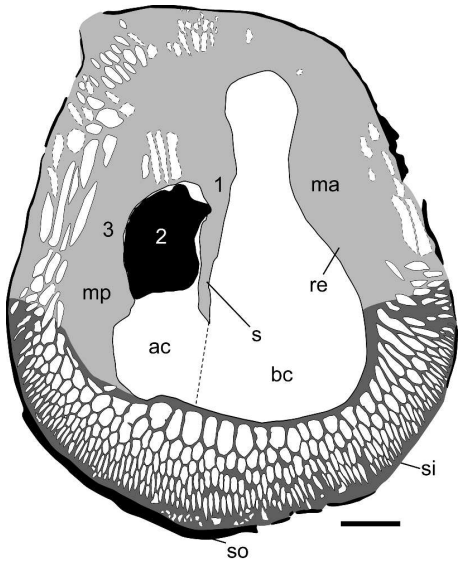

Figure 33: Transverse section of *Mitrocaprina* cf. *tschoppi* [IGM 8876] cutted 10 mm above the commissural plane. The inner shell consists of 3 to 5 rows of sub-rounded to polygonal canals. [so–outer shell; si–inner shell; re–recrystallized (light grey); other abbreviations, see text; scale bar 10 mm].

Description: The conical to spirogyrate RV is of oval to reniform outline. Heights of the RV reach from 50 mm to 105 mm and maximum commissural diameters vary between 45 mm and 50 mm. Rugose shell lamellae characterize the outer surface.

The coiled LV contains faint shell lamellae and equally spaced constrictions (Plate 13/3). The umbo protrudes 10 mm to 15 mm beyond the RV and is inclined towards the RV (Plate 13/3).

Transverse section: The outer shell of the LV is dark brown and 1 mm to 2 mm thick. The inner shell consists of one to three rows of sub-rounded to sub-polygonal pallial canals (Plate13/4). On the exterior side of the inner shell, one to three rows of elongated drop shaped to pyriform pallial canals follow, which are radially arranged. In transverse sections cutted 10 mm above the commissural plain, thickness of the inner shell increase, as well as the number of rows formed by sub-rounded to sub-polygonal canals (Figure 33). On the anterior and posterior sides of the LV, cells are more elongated and run parallel to the shell margin. S extends ventrally from the socket 2' and separates ac from the bc (Plate13/4). On the ventral side, s subsides into the LV.

Material: Two poorly preserved and small specimens, which reach maximum diameters of 45 mm [IGM 8875, IGM 8876]. Most of the outer shell is eroded and recrystallization obliterates most of the internal structures in both valves.

Discussion: Myers (1968) described a similar shell structure, but assigned the specimen (WSA 15583) to *Coralliochama gboehmi*. The pallial canals in *Mitrocaprina* are intraspecific variable (e. g., Douville 1888, Steuber, 1999), and the lack of internal structures prevents a definite assignment to *M. tschoppi*. The inner shell of *M. bayani* consists only of one inner row of sub-polygonal or sub-cylindrical pallial canals and the row is not continuous within the LV (Steuber, 1999). In *M. boeotica* diameter of the sub-polygonal canals of the inner shell differ and large canals characterize the posterior shell, whereas on the anterior side ca-

nals are small. In addition, sub-polygonal canals are absent on the ventral margin in many *M. boeotica* and only pyriform canals form the inner shell (Steuber, 1999). However, *M. tschoppi* resemble *M. vidali* and differences are not clearly defined. According to Mac Gillavry (1937), the RV of *M. vidali* is characterized by deeper posterior sockets, which are also more differentiated from the posterior myophore than in *M. tschoppi*. The recrystallized internal structures prevent an accurate determination of our specimens (Plate 13/4), but *M. vidali* is so far unknown from the western Tethyan region, so the presence of *M. tschoppi* in the Cardenas Fm. is more plausible.

Occurrence: Upper member of the Cardenas Formation (late Maastrichtian). Maastrichtian of Cuba (e.g., Palmer, 1933; Mac Gillavry, 1937).

Coralliochama gboehmi Böse, 1906
plate 13, figures 1–2

* 1906 *Coralliochama gboehmi* Böse, p. 46, pl. 5, fig. 5; pl. 6, figs. 1–2; pl. 7, fig. 1.
1971 *Plagioptychus agariciformis* n. sp. Alencaster, pp. 28–31, pl. 3, fig. 5; pl. 4, fig. 1; pl. 17, figs. 1–2.
1998 *Coralliochama gboehmi* Böse; Garcia-Barrera et al., pp. 128, 133, pl. 5, figs. 1-5.

Description: Rugose shell lamellae characterize the outer surface of the conical RV (Plate 13/1). The RVs are between 70 mm to 130 mm long and reach maximum commissural diameters between 55 mm and 120 mm.

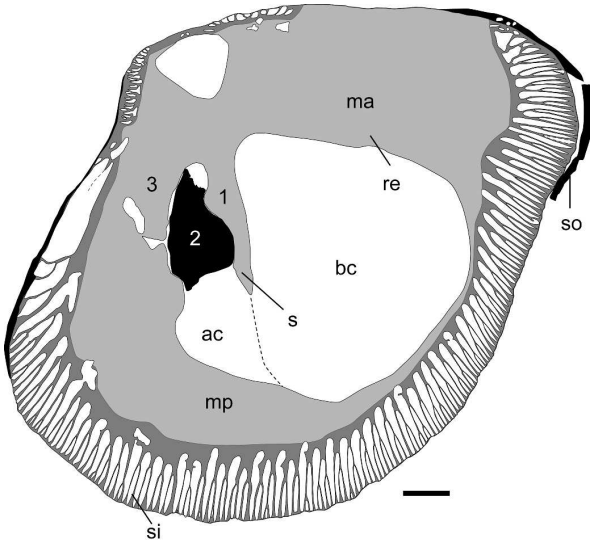

Figure 34; Transverse section of *Coralliochama gboehmi* [IGM 8878] showing the myocardinal apparatus and the row of radial pyriform canals in the inner shell [so–outer shell; si–inner shell; re–recrystallized (light grey); other abbreviations, see text; scale bar 10 mm].

The coiled LV is of triangular outline (Plate 13/2). Anterior–posterior diameter exceed the dorsal–ventral diameter in approximately 25%. The LV is characterized by faint shell lamellae (Plate 13/1). The umbo slightly overhangs the RV and is inclined towards the RV. The outer shell layers of RV and LV are dark brown, similar to *Mitrocaprina* cf. *tschoppi*.

Transverse section: In smaller specimens, tooth 2 is of sub-circular outline, whereas in large specimens it is more elongated.

In the LV, the laminated outer shell layer reaches maximum thicknesses of 3 mm. The inner shell consists one row of radial pyriform pallial canals formed by bifurcating radial partitionings (Plate 13/2). On the posterior side, pallial canals are irregular, more elongated and run parallel to the shell margin (Figure 34). Tooth 1 is a small bulge fitting into a round notch of tooth 2 of the RV (Plate 13/2). The shapes of the large subcircular ma and mp are obliterated by recrystallization. A small elongated notch separates

tooth 3 from mp (Plate 13/2). S extending ventrally from socket 2' separates an ac from the bc (Plate 13/2). On the ventral side, s subsides into the LV as it approaches the ventral margin.
Material: Two moderately preserved specimens [IGM 8877, IGM 8878]. Most parts of the outer shell are eroded. Internal structures recrystallized and cavities filled by calcite spar.
Discussion: C. gboehmi differs from *C. orcutti* by a thinner cellular inner shell layer in the RV (Myers, 1968) and by larger myophores in the LV (Böse, 1906).
Occurrence: Upper member of the Cardenas Formation (late Maastrichtian). Campanian–Maastrichtian of southern Mexico (Garcia-Barrera et al., 1998).

Family. Radiolitidae

Genus. *Macgillavryia* Rojas, Itturalde-Vinent and Skelton, 1995
Type species. *Radiolite*s (*Lapeirousia*) *nicholasi* (Whitfield, 1897)

Macgillavryia nicholasi (Whitfield, 1897)
plate 14, figures 1–4

* 1897	*Radiolite*s (*Lapeirousia*) *nicholasi* Whitfield, pp. 186–188, pls. 6–9.
1934	*Sphaerulites (Lapeirousia)* cf. *nicholasi* (Whitfield); Olsson, pp. 49–50, pl. 1, fig. 2; pl. 8, fig. 4.
1944	*Sauvagesia peruviana* n. sp. Olsson, pp. 206–208, pl. 8, figs. 1–5.
1971	*Durania nicholasi* (Whitfield); Chubb, pp. 199–201, pl. 43, fig. 6; pl. 44, fig. 1; pls. 45–46.
1971	*Durania nicholasi* (Whitfield); Alencaster, pp. 48–50, pl. 10, figs. 3–4.
1995	*Macgillavryia nicholasi* (Whitfield); Rojas, Itturalde-Vinent, and Skelton, pp. 285–288, pl. 3, figs. 1–3.
2004	*Macgillavryia nicholasi* (Whitfield); Philip and Jaillard, pp. 41–42, pl. 1.

Description: The RV is 180 mm long and the maximum commissural diameter is 490 mm. The circular bc is located at the posteroventral margin, close to Pb and Vb, and reaches a diameter of 40 mm (Plate 14/1). The outline of the RV is irregular oval to stellate. In the lower part of the RV, shell lammellae are steeply inclined, but inclination decreases rapidly towards the commissural plane resulting in a mushroom-like appearance of the RV (Plate 14/1); in the upper part of the RV, shell lamellae are orientated horizontally. Faint broad ribs and grooves characterize the upper part of the RV, which cause an irregular wavy commissural plane due to the horizontal orientation of the shell lamellae (Plate 14/2). Pb and Vb are rounded to angular grooves, and they are characterized by horizontal shell lamellae (Plate 14/1). On the anterior side, an irregular acute rib formed by V-shaped downfolds of the shell lamellae flanks Vb. Ib consists of a narrow acute irregular rib (Plate 14/1), which is characterized by a 2 mm broad median furrow formed by V-shaped downfolds of shell lamellae. LV is absent.
Transverse section: The inner shell layer is 0.8 mm thick. The dense undulating funnel plates are partially in contact. Funnel plates and muri form a rectangular network (Plate 14/3). A radial pattern of narrow bifurcating furrows formed by U-shaped funnel plates characterize

the commissural plain (Plate 14/4). These furrows have frequently been considered to represent vascular structures.
Material: One well preserved RV [IGM 8880] of the Estación Canoa section, which contains abundant bivalve borings.
Occurrence: Lower member of the Cardenas Formation (early Maastrichtian). Campanian to Maastrichtian of southern Mexico (Alencáster, 1971), northwest Peru (e.g., Olsson, 1934; Philip and Jaillard, 2004) and Caribbean province (e.g., Chubb, 1956a; Philip, 1999).

Genus. *Bournonia* Fischer, 1887
Type species. *Sphaerulites bournoni* des Moulins, 1826

Bournonia cardenasensis (Böse, 1906)
plate 16, figures 1–5

* 1906	*Biradiolites cardenasensis* Böse, pp. 59–60, pl. 11, fig. 3; pl. 12, fig. 3.
1906	*Biradiolites potosianus* n. sp. Böse, pp. 60–61, pl. 5, figs. 2–3; pl. 11, fig. 4; pl. 12, fig. 5.
1924	*Bournonia barreti* n. sp. Trechman, p. 405, pl. 26, figs. 2–2a.
v 1968	*Biradiolites cardenasensis* Böse; Myers, p. 45, pl. 4, figs. 1–4.
1971	*Bournonia cardenasensis* Böse; Alencaster, pp. 43–45, pl. 7, figs. 5–7; pl. 19, figs. 2–4.
1995	*Bournonia cardenasensis* Böse; Scott, p. 303, pl. 2, figs. 5–6; text-fig. 6E.
2003	*Bournonia barretti* Trechmann; Mitchell, pp. 151–152, pls. 1–2; pl. 3, figs. d–f; pl. 4, figs. a, c–d.

Description: The RVs are between 60 mm to 80 mm long and reach maximum commissural diameters between 40 mm and 60 mm. Prominent shell lamellae characterize the cylindrical to conical RV. Irregular U-shaped grooves separate pronounced triangular longitudinal ribs. The grooves are generally wider than the ribs (Plate 16/1). The anterior side is flattened and contains few weakly developed ribs or ribs are absent (Plate 16/2). Steep and triangular downfolds of the shell lamellae form the ribs and smooth and U-shaped upfolds the grooves. Pb and Vb are characterized by broad ribs separated by a shallow groove representing Ib (Plate 16/1, 2).
The LV is plano-convex with serrated to stellate outline (Plate 16/2). It covers most part of the top of the RV. The central part of the LV that covered the bc is smooth and contains faint concentric shell lamellae. Periphery of the LV consists of pronounced up-and downfolded shell lamellae. The up-and downfolds form radial ribs and grooves, which match the ribs and grooves of the RV. Pb and Vb are characterized by two large projecting ribs of the LV, which are separated by a less prominent rib (Plate 16/2).
Transverse section: Close to the bc funnel plates are steeply inclined, but in the ribs they are almost horizontal. Inner shell layer is up to 1.5 mm thick. Undulated funnel plates match the form of the marginal ribs (Plate 16/3). The inner margin of the funnel plates is spiny, characteristic for the genus *Bournonia* (Plate 16/5). The short spines are arranged in regular intervals and are either in point contact to the adjacent funnel plate mimicking a rectangular network, or they are without contact. In transverse sections of the ribs, these spines appear as

dots due to the horizontal orientation of the funnel plates (Plate 16/4). The ma of the LV is less robust than mp, that is connected to tooth 3 by a narrow neck (Plate 16/3).
Remarks: B. cancellata is thicker, conical and tapered. It broadens rapidly towards the commissural plane. The anterior side lacks ribs, but is characterized by a prominent furrow.
Mitchell (2003) distinguishes between *B. cardenasensis* and *B. barretti*. Based on the associated rudist fauna in Jamaica, he considered the two species as homeomorph and suggests, that *B. barretti* is a stratigraphic marker for the late Maastrichtian, whereas *B. cardenasensis* for the middle to late Campanian (Mitchell, 2003). However, in the Cardenas Formation, *B. cardenasensis* occurs in the uppermost reef limestone, which is dated as early late Maastrichtian in age by Sr-isotope stratigraphy. In consequence, *B. barretti* is not distinguishable from *B. cardenasensis*, and both species are summarized in *B. cardenasensis*, as suggested by Alencaster (1971).
Material: Three well preserved specimen [IGM 8883, IGM 8884, IGM 8885].
Occurrence: Upper member of the Cardenas Formation (late Maastrichtian). Campanian to Maastrichtian of southern Mexico (Chubb, 1959; Alencáster, 1971), Guatemala (Scott, 1995), and Caribbean province (e.g., Trechmann, 1924; Chubb, 1971; Mitchell, 1999).

Genus. *Tampsia* Stephenson, 1922
Type species. *Tampsia bishopi* Stephenson, 1922

Tampsia poculiformis Myers, 1968
plate 15, figures 1–10

v* 1968 *Tampsia poculiformis* n. sp. Myers, pp. 47–48, pl. 5, figs. 6–7; pl. 7, fig. 2.

Description: The cylindrical or conical RV is of round to irregular outline. Heights of the RV vary between 50 mm to 105 mm and maximum commissural diameters reach from 45 mm and 110 mm. U-shaped up- and downfolds of the shell lamellae form wide grooves and narrow and smooth costae. Costae and grooves are less developed in smaller specimens (Plate 15/6). In the upper part of the RV, pronounced rugose horizontal shell lamellae characterize the anterior and dorsal sides and costae are absent (Plate 15/2). Poorly developed to pronounced ribs and grooves consisting of large-scaled up- and downfolds characterize the area close to the radial bands (Plate 15/4). These ribs and grooves include several of the narrow costae. In many specimens, these ribs are generally less developed in the lower part of the RV, but prominent in the upper part. Ib is the most prominent rib of the shell and Pb and Vb are wide grooves (Plate 15/4). Pb is the deepest groove, is as broad as Vb or broader, and flanked by prominent ribs. Vb is a wide groove of varying depths with a narrow slit on the bottom. The slit is formed by sharply upfolded and V-shaped shell lamellae and characterizes the genus *Tampsia*.
On the top of the RV, shell lamellae are almost horizontal. Their up- and downfolds lead to a wavy commissural plane (Plate 15/1). Pb and Vb are the most prominent rises on the commissural plane and flanked by deep grooves. In most specimens Vb is more pronounced than Pb. Ib is the deepest groove on the commissural plane and depth of the grooves decreases gradually towards the anterior side (Plate 15/1). The slit of Vb is represented by a narrow ridge located in a semicircular to triangular depression with the top of the triangle pointing to

the exterior side (Plate 15/3). The commissural plain of many specimens contains a dentritic pattern of radial depressions (Plate 15/1). It consists of a row of rectangular cells that have often been interpreted to represent vessel structures.

The LV covered the whole surface of the attached valve and matches the wavy structure of the commissural plane of the RV. It is slightly convex and contains concentric growth lines on the surface. Faint radial rays characterize the marginal part of the LV (Plate 15/5).

Transverse section: A regular pattern of polygonal cells fills the broad space between the irregular and wavy funnel plates (Plate 15/8). The regular network of polygonal cells is similar to *Durania ojanchalensis* (Plate 15/ 8, 9, 10), but at Vb, funnel plates are sharply inclined towards the central cavity and form a V-shaped slit characteristic for the genus *Tampsia* (Plate 15/9). The slit extends from the bottom of the Vb -groove on the shell margin to a few millimeters before the circular bc. At the slit, the inner margin of the round central cavity smoothly arches inward or forms a straight line.

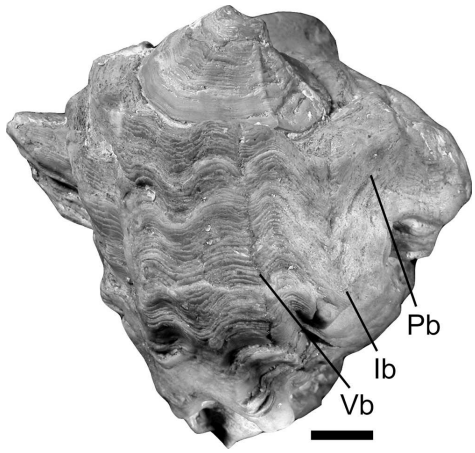

Figure 35: Posterior side of *Tampsia floriformis* [IGM 8890] with a jelly bag cap-like left valve (abbreviations, see text; scale bar 10 mm)

Discussion: The irregular and rugose shell lamellae and the irrgeluar and pronounced ribs and grooves, which characterize the area of the radial bands, distinguish *T. poculiformis* from *T. chococyensis* and *T. bishopi*. The latter species are characterized by regular rounded grooves of the radial bands and less pronounced and wavy shell lamellae. In smaller specimens of *T. poculiformis*, the ribs characterizing the zone of the radial bands and the location of the slit are poorly developed. However, the rises on the commissural plane, characterizing this zone, are clearly visible. Specimens of *T. poculiformis* with well developed ribs resemble much *T. floriformis*. However, the shell structure of *T. floriformis* vary within one specimen from parts characterized by denticulate funnel plates to areas consisting of a network of rectangular, sub-circular or polygonal cells (Alencáster, 1971). In addition, the LV of *T. floriformis* is tapered resulting in a jelly bag cap appearance in many specimens (Figure 35).

Material: Two well preserved specimens [IGM 8881, IGM 8882] and many poorly preserved specimen.

Occurrence: Upper member of the Cardenas Formation (late Maastrichtian).

Family. Hippuritidae Gray, 1848

Genus. *Hippurites* Lamarck, 1801
Type species. *Hippurites bioculata* Lamarck, 1801

Hippurites perkinsi Myers, 1968
plate 16, figures 8–9
v* 1968 *Hippurites perkinsi* n. sp. Myers, p. 43, pl. 4, figs. 5–6.

Description: RV is cylindrical, straight or slightly curved and gently tapering. The pronounced and narrow triangular ribs are separated by rounded grooves, which are wider than the ribs. On the external side, P0, P1, and P2 are marked by V-shaped grooves. The grooves characterizing P0 and P1 are wider than regular peripheral grooves, whereas the groove representing P2 is of similar width (Plate 16/8). The groove of P0 is the broadest and deepest inward fold on the shell, which is flanked by two prominent triangular ribs. In few specimens, these ribs are splitted by shallow and narrow furrows into smaller costae. The most prominent rib separates the grooves of P0 and P1. LV is not preserved.
Transverse section: P0 is a broad triangular inward fold. P1 is round, short and stumpy, and in one specimen slightly pinched. The ellipsoidal P2 is the longest pillar. It is thinner than P1 and contains a slightly pinched base. The inner margin of the shell is smoothly undulated and infoldes correspond to the grooves of the outer surface (Plate 16/8). The cellular structure of the outer shell mimics a radiolitid shell (Plate 16/9).
Discussion: The species *H. muelleriedi*, *H. ceibarum*, and *H. perkinsi* are poorly defined and difficult to distinguish. *H. muelleriedi* and *H. ceibarum* are distinguished by the sizes of individuals and angles between P0, P1, and P2 (Vermunt, 1937; Chubb, 1956b, 1971). However, the irregular outline of the pillars make accurate measurements of the angles impossible (Myers, 1968), and the intraspecific variability of pillars in hippuritids is documented by Vicens (1992) and Steuber (1999). In addition, the arrangement of the pillars and the cellular shell structure of *H. muelleriedi* correspond to *H. perkinsi* (Mac Gillavry, 1937; Myers, 1968). Only the pronounced narrow and triangular longitudinal ribs distinguish *H. perkinsi* from *H. muelleriedi* that is characterized by broad and round ribs (Myers, 1968). However, the strength, presence, or absence of ribs vary intraspecifically (Vicens, 1992) and depends on the interaction with associated fauna (ecophenotypes), but also on ontogenetic stages (Götz, 2003b). Hence, additional criteria and morphometric data are needed for a clear definition and distinction of *H. perkinsi*, *H. ceibarum*, and *H. muelleriedi*.
Material: One association of five specimens [IGM 8886] and many RVs of collapsed specimens.
Occurrence: Common in the upper member of the Cardenas Formation (late Maastrichtian).

Genus. *Praebarrettia* Trechmann, 1924
Type species. *Barrettia sparcilirata* Whitfield, 1897

Praebarrettia? *sparcilirata* (Whitfield, 1897)
plate 16, figure 6–7, 10

*	1897	*Barrettia sparcilirata* Whitfield, p. 245, pls. 36–37.
	1924	*Praebarrettia sparcilirata* (Whitfield); Trechmann, pp. 395–396, pl. 23, figs. 3–4.
	1926	*Praebarrettia sparcilirata* (Whitfield); Sánchez Roig, 1926, p. 98, pls. 3–4.
	1931	*Pseudobarrettia chiapasensis* n. sp. Muellerried, pp. 256–259, text-figs. 1a–b, 2a–b.
	1932	*Barrettia sparcilirata* (Whitfield); Boissevain and Mac Gillavry, p. 1303, text-figs. 1a–b, 2a–b, 3a.
	1933	*Praebarretia porosa* n. sp. Palmer, p. 99, pl. 6, figs. 3–6.
	1933	*Praebarreta sparcilirata* var. *cubensis* n. var. Palmer, p. 98, pl. 6, fig. 1-1.
	1936	*Barrettia sparcilirata* (Whitfield); Thiadens, pp. 1011–1013, text-fig. 2; text-figs. 3a–k.
	1971	*Praebarrettia sparcilirata* (Whitfield); Chubb, pp. 199, 215, pl. 57, figs. 1–2; pl. 58, fig. 1.
	1971	*Praebarrettia sparcilirata* (Whitfield); Alencaster 1971, pp. 70–78, pl. 14, figs. 1–6; pl. 15, figs. 2–3.
	1973	*Praebarrettia sparcilirata* (Whitfield); van Dommelen, p. 69, pl. 3, fig. 3; pl. 4, figs. 1–2; text-figs. 6a–b, 12, 20–21; table 8.

Description: The RVs are between 15 mm to 50 mm long and reach maximum commissural diameters between 15 mm and 40 mm. The straight or curved RV is cylindrical and flat, or long, slender and tapered.

Weak rounded ribs characterize the otherwise irregular surface. The ribs are separated by rounded and narrow grooves arranged in regular intervals (Plate 16/10).

LV is opercular, flat and covers the whole surface of the RV. The shell of the LV is upfolded above the pillars and pseudo-pillars of the RV (Plate 16/6). Most of these upfolds converge in a round central apex resulting in a radial symmetry of the LV. Only the round pronounced upfold above P2 and the two short upfolds flanking the upfold above P0 reach not to the central apex. P0, P1, P2 penetrate through the shell of the LV.

Transverse section: The structure of the outer shell of the RV consists of a cellular network, which is similar to *Hippurites perkinsi*. The outer shell reaches a maximum thickness of 1 mm and infolds of the shell form the exterior grooves. The inner shell is less than 1 mm thick and form pillars and pseudo-pillars at the infolds, which are connected by thin irregular tabulae (Plate 16/7). Most of the pseudo-pillars are short and stumpy, whereas thin elongated pseudo-pillars with ellipsoidal terminations are rare. P0 and P2 are long pillars that reach into the central cavity. P0 is the longest pillar with a weak terminal ellipsoidal swelling. P1 and P2 consist of a thin base. The pronounced termination of P1 is circular to ellipsoidal, whereas P2 broadens to an ellipsoidal termination. The interior of P1 and P2 consists of thin radial furrows that converge into a central cavity (Plate 16/7).

Discussion: Arrangement of the pillars and pseudo-pillars as well as the external and internal structure of the specimens correspond to *Praebarrettia sparcilirata* (e.g. Mac Gillavry, 1937; Alencáster, 1971; Van Dommelen, 1971) However, the Cardenas specimens are small compared to *Praebarrettia sparcilirata* described from southern Mexico or Jamaica (e.g., Mac Gillavry, 1937; Alencáster, 1971; Van Dommelen, 1971). In addition, according to Van Dommelen (1971), the LV of *Praebarrettia sparcilirata* contains rows of pores on each side of the upfolds, and these pores are connected by transverse furrows. He considered this structures as diagnostic for the genus *Praebarrettia* (Van Dommelen, 1971). The shell of the LVs of the Cardenas specimens is massive and lacks pores and canals. These features are so far unknown from multifold-hippuritids, such as *Praebarrettia, Barrettia,* or *Pironaea*. Therefore the assignment of the Cardenas specimens to *Praebarrettia* is questionable.

Material: Three well preserved specimens [IGM 8887, IGM 8888, IGM 8889] and many poorly preserved specimens. Erosion of the thin shell by boring organisms is very common and well preserved specimens are rare. In transverse sections, recrystallization by sparite obscures the internal structures and details of the cardinal apparatus are not visible.

Occurrence: Lower member of the Cardenas Formation (early Maastrichtian). Campanian to Maastrichtian of southern Mexico (Alencáster, 1971) and Caribbean province (e.g., Whitfield, 1897; Van Dommelen, 1971; Rojas and Iturralde-Vinent, 1995).

9 References

Aguilar, M., Bernaus, J. M., Caus, E., Hottinger, L., 2002. *Lepidorbitoides minima* Douville from Mexico, a foraminiferal index fossil for the Campanian. Journal of Foraminiferal Research, 32(2), 126–134.

Aguilera-Franco, N., 2003. Cenomanian–Coniacian zonation (foraminifers and calcareous algae) in the Guerrero-Morelos Basin, southern Mexico. Revista Mexicana de Ciencias Geológicas, 20(3), 202–222.

Alencáster, G., 1971. Rudistas de Cretácico Superior de Chiapas, Parte 1. Paleontología Mexicana, 34, 1–91.

Alencáster, G., Oviedo-García, A., 1998. Re-examination of the genera *Texicaprina* Coogan, *Mexicaprina* Coogan and *Kimbleia* Coogan (caprinid rudists) from the Albian of central Mexico. Revista de la Sociedad Mexicana de Paleontología, 8(2), 163–179.

Alencáster, G., Pantoja-Alor, J., 1998. Two new lower Cretaceous rudists (Bivalvia-Hippuritacea). GeoBios, 22, 16–28.

Alloiteau, J., 1952. Embranchment de Coelentérés. II. Madréporaires post-paleozoiques. In: J. Piveteau (Editor). Traité de Paléontologie, Masson, Paris, 1, 539–684.

Antuñano, S. E., García, M. A., Marrett, R., 2000. Tectónica de la Sierra Madre Oriental, México. Boletin de la Sociedad Geológica Mexicana, LIII(1), 1–26.

Bailey, R. J., 1998. Stratigraphy, meta-stratigraphy and chaos. Terra Nova, 10, 222–230.

Baron-Szabo, R., 1997. Die Korallenfazies der ostalpinen Kreide (Helvetikum: Allgäuer Schrattenkalk; Nördliche Kalkalpen: Brandenberger Gosau), Taxonomie, Palökologie. Zitteliana, 21, 3–97.

Baron-Szabo, R., 2002. Scleractinian Corals of the Cretaceous. A Compilation of Cretaceous Forms with Descriptions, Illustrations, and Remarks on their Taxonomic Position. Privately Published, Knoxville, 539 pp.

Baron-Szabo, R., Schafhauser, A., Götz, S., Stinnesbeck, W., 2006. Scleractinian corals from the Cardenas Formation, San Luis Potosí, Mexico. Journal of Paleontology, 80(6), [in press].

Barrera, E., Savin, S. M., Thomas, E., Jones, C. E., 1997. Evidence for thermohaline-circulation reversals controlled by sea-level changes in the latest Cretaceous. Geology, 25(8), 715–718.

Basáñez-Loyola, M. A., Fernández-Turner, R., Rosales-Domínguez, C., 1993. Cretaceous platform of Valles-San Luis Potosí, northeastern central Mexico. In: A. J. Simo, W. R. Scott and J.-P. Masse (Editors), Cretaceous Carbonate Platforms. AAPG Memoir, vol. 56, American Association of Petroleum Geologists (AAPG), Tulsa, 51–59.

Bernaus, J. M., Arnaud-Vanneau, A., Caus, E., 2003. Carbonate platform sequence stratigraphy in a rapidly subsiding area: the Late Barremian–Early Aptian of the Organyà Basin, Spanish Pyrenees. Sedimentary Geology, 159(3-4), 177–201.

Böse, E., 1906. La fauna de moluscos del Senoniano de Cárdenas, San Luis Potosí. Boletín del Instituto Geológico de México, 24, 1–95.

Böse, E., Cavins, O. A., 1927. The Cretaceous and Tertiary of southern Texas and northern Mexico. University of Texas Bulletin, 2784, 7–142.

Boissevain, H., Mac Gillavry, H. J., 1932. Some remarks on *Barrettia sparcilirata* Whitfield and *Chiapasella radiolitiformis* (Trechmann). Koninklijke Akademie van Wetenschappen te Amsterdam, Proceedings of the Section of Sciences, 35, 1303–1312.

Burckhardt, C., 1930. Etude synthétique sur le Mésozoique mexicain. Mémoires de la Société Paléontologique Suisse, 50, 125–280.

Carrillo-Bravo, J., 1971. La plataforma Valles-San Luis Potosí. Boletin de la Asociación Mexicana de Geólogos Petroleros, 23, 1–101.

Carter, R. M., 1968. Functional studies on the Cretaceous oyster *Arctostrea*. Palaeontology, 11(3), 458–485.

Caus, E., Tambareau, Y., Colin, J.-P., Aguilar, M., Bernaus, J.-M., Gomez-Garrido, A., Brusset, S., 2002. Upper Cretaceous microfauna of the Cárdenas Formation, San Luis Potosí, NE Mexico. Biostratigraphical palaeoecological, and palaeogeographical significance. Revista Mexicana de Ciencias Geológicas, 19(2), 137–144.

Cestari, R., Sartorio, D., 1995. Rudist and Facies of the Periadriatic Domain. Agip, Mailand, 207 pp.

Chappell, J., 1980. Coral morphology, diversity and reef growth. Nature, 286, 249–252.

Chubb, L. J., 1955. A revision fo Whitfield´s type specimens of the rudist molluska from the Cretaceous of Jamaica, British West Indies. American Museum Novitates, 1713, 2–15.

Chubb, L. J., 1956a. Rudist assemblages of the Antillean Upper Cretaceous. Bulletins of North American Paleontology, 37(161), 5–23.

Chubb, L. J., 1956b. Some rarer rudists from Jamaica, B.W.I. Palaeontographica Americana, 4(26), 2–31.

Chubb, L. J., 1959. Upper Cretaceous of central Chiapas, Mexico. AAPG Bulletin, 43, 725–756.

Chubb, L. J., 1961. Rudist assemblages in Cuba. Bulletins of American Paleontology, 43(198), 413–422.

Chubb, L. J., 1971. Rudists of Jamaica. Palaeontographica Americana, 7(45), 157–257.

Church, K. D., Coe, A. L., 2003. Processes controlling relative sea-level change and sediment supply. In: A. L. Coe (Editor), The Sedimentary Record of Sea-Level Change. Cambridge University Press, Cambridge, 99–117.

Coe, A. L., Church, K. D., 2003. Sequence stratigraphy and sea-level change. In: A. L. Coe (Editor), The Sedimentary Record of Sea-Level Change. Cambridge University Press, Cambridge, 57–98.

Conrad, T. A., 1858. Observations on a group of Cretaceous fossil shells found in Tippah County, Mississippi, with descriptions of fifty-six new species. Journal of the Academy of Natural Sciences of Philadelphia, 2(3), 323–336.

Conrad, T. A., 1860. Descriptions of new species of Cretaceous and Eocene fossils of Mississippi and Alabama. Journal of the Academy of Natural Sciences of Philadelphia, 2(4), 275–297.

Crame, J. A., McArthur, J. M., Pirrie, D., Riding, J. B., 1998. Strontium isotope correlation of the basal Maastrichtian stage in Antarctica to the European and US biostratigraphic schemes. Journal of the Geological Society, 156, 957–964.

Cros, P., Michaud, F., Fourcade, E., Fleury, J.-J., 1998. Sedimentological evolution of the Cretaceous carbonate platform of Chiapas (Mexico). Journal of South American Earth Sciences, 11(4), 311–332.

D'Achiardi, A., 1875. Coralli eocenici del Friuli. Atti della Societa Toscana di Scienze Naturali, 1, 67–86.

De Fromentel, E., 1873. Zoophytes, terrains crétacés. In: A. d'Orbigny (Editor), Paléontologie Francaise. Masson, Paris, 9, 385–432.

D'Orbigny, A., 1850. Prodrôme de Paléontologie Stratigraphique Universelle. Masson, Paris, 428 pp.

Douvillé, H., 1926. Quelques fossiles du Crétacé supérieur de Cuba. Bulletin de la Société Géologique de France, 26(1), 127–138.

Douvillé, H., 1927. Nouveaux rudistes du Crétáce de Cuba. Bulletin de la Société Géologique de France, 27(1), 49–56.

Douvillé, H., 1927. Les Orbitoides de la région pétrolifère du Mexique. Comptes Rendus des Séances, Société Géologique de France, 1, 34–35.

Duncan, P. M., 1863. On the fossil corals of the West Indian Islands. Quarterly Journal of the Geological Society of London, 19, 406–458.

Duncan, P. M., 1865. A notice of the geology of Jamaica, especially with reference to the district of Clarendon; with descriptions of the Cretaceous, Eocene and Miocene corals of the islands. Quarterly Journal of the Geological Society of London, 21, 1–14.

Dunham, R. J., 1962. Classification of carbonate rocks according to their texture. In: W. E. Ham (Editor), Classification of Carbonate Rocks – A Symposium. AAPG Memoir, vol. 1, American Association of Petroleum Geologists (AAPG), Tulsa, 108–121.

Einsele, G., 1992. Sedimentary Basins. Springer, Berlin, 628 pp.

Elliott, T., 1986. Siliciclastic shorelines. In: H. G. Reading (Editor), Sedimentary Environments and Facies. Blackwell Scientific Publications, Oxford, 155–188.

Embry, A. F., Klovan, J. E., 1971. A Late Devonian reef tract on northeastern Banks Island. Bulletin of Canadian Petroleum Geology, 19, 730–781.

Felix, J. P., 1903. Studien über die korallenführenden Schichten der oberen Kreideformation in den Alpen und in den Mediterrangebieten. Palaeontographica, 49, 163–359.

Flügel, E., 1978. Mikrofazielle Untersuchungsmethoden von Kalken. Springer, Berlin, 454 pp.

Flügel, E., 2004. Microfacies of Carbonate Rocks. Springer, Berlin, 976 pp.

Fourcade, E., Piccioni, L., Escribá, J., Rosselo, E., 1999. Cretaceous stratigraphy and palaeoenvironments of the Southern Petén Basin, Guatemala. Cretaceous Research, 20, 793–811.

Fuente-Navarro, M. J., 1964. Estudio geológico del area Cárdenas-Rio Verde, S. L. P., y Arroyo Seco, Querétaro, Mexico. Boletin de la Asociación Mexicana de Geólogos Petroleros, 16, 237–249.

Galloway, W. E., 1989a. Genetic stratigraphic sequences in basin analysis I: architecture and genesis of flooding-surface bounded depositional units. AAPG Bulletin, 73(2), 125–142.

Galloway, W. E., 1989b. Genetic stratigraphic sequences in basin analysis II: application to northwest Gulf of Mexico Cenozoic basin. AAPG Bulletin, 73(2), 143–154.

Garcia-Barrera, P., Avendaño, G. J., Omaña, L., Alencaster, G., 1998. *Antillocaprina trilobata* nov. sp. and upper Cretaceous associated fauna from Chiapas (southeast Mexico). Quatrième congrès international sur les rudistes, Geobios Mémoire spécial, vol. 22, 125–135.

Gili, E., Skelton, P. W., Vicens, E., Obrador, A., 1995. Corals to rudists – an environmentally induced assemblage succession. Palaeogeography, Palaeoclimatology, Palaeoecology, 119, 127–136.

Goldfuss, A., 1826. Petrefacta Germaniae. Arnz, Düsseldorf, 114 pp.

Goldhammer, R. K., Johnson, C. A., 2001. Middle Jurassic–Upper Cretaceous paleogeographic evolution and sequence-stratigraphic framework of the northwest Gulf of Mexico rim. In: C. Bartolini, R. T. Buffler and A. Cantú-Chapa (Editors), The Western Gulf of Mexico Basin. AAPG Special Memoir, vol. 75, American Association of Petroleum Geologists (AAPG), Tulsa, 45–82.

Götz, S., 2001. Rudisten-Assoziationen der keltiberischen Oberkreide SE-Spaniens: Paläontologie, Palökologie und Sediment-Organismus-Wechselwirkungen. PhD Thesis, Bayerische Akademie der Wissenschaften Abhandlungen, Naturwissenschaftliche Klasse, Neue Folge, vol. 171, Verlag der Bayerischen Akademie der Wissenschaften, München, 112 pp.

Götz, S., 2003a. Biotic interaction and synecology in a Late Cretaceous coral-rudist biostrome of southeastern Spain. Palaeogeography, Palaeoclimatology, Palaeoecology, 193, 125–138.

Götz, S., 2003b. Larval settlement and ontogenetic development of *Hippuritella vasseuri* (DOUVILLÉ) (Hippuritoidea, Bivalvia). Geologia Croatica, 56(2), 123–132.

Gradstein, F. M., Ogg, J. G., Smith, A. G., Bleeker, W., Lourens, L. J., 2004. A new Geologic Time Scale, with special reference to Precambrian and Neogene. Episodes, 27(2), 83–100.

Gray, G. G., Johnson, C. A., 1995. Structural and tectonic evolution of the Sierra Madre Oriental, with emphasis on the Saltillo-Monterrey corridor. In: G. G. Gray and C. A. Johnson (Editors), Structural and Tectonic Evolution of the Sierra Madre Oriental,

with Emphasis on the Saltillo-Monterrey Corridor. Field guidebook, American Association of Petroleum Geologists (AAPG), Houston, 1–20.

Greenstein, B. J., Pandolfi, J. M., 2003. Taphonomic alteration of reef corals: effects of reef environment and coral growth form II: The Florida Keys. Palaios, 18, 495–509.

Hardenbol, J., Robaszynski, F., 1998. Introduction to the Upper Cretaceous. In: P.-C. De Graciansky, J. Hardenbol, T. Jacquin and P. R. Vail (Editors), Mesozoic and Cenozoic Sequence Stratigraphy of European Basins. SEPM Special Publication, vol. 60, Society for Sedimentary Geology (SEPM), Tulsa, 329–332.

Heim, A., 1940. The front ranges of the Sierra Madre Oriental, México, from Ciudad Victoria to Tamazunchale. Eclogae Geologicae Helveticae, 33, 313–352.

Höfling, R., 1989. Substrate-induced morphotypes and intraspecific variability in Upper Cretaceous scleractinians of the eastern Alps (West Germany, Austria). In: P. A. Jell (Editor), 5th International Symposium on Fossil Cnidaria including Archaeocyatha and Spongiomorphs. Association of Australasian Paleontologists Memoir, vol. 8, Association of Australasian Paleontologists, Brisbane, 51–60.

Höfling, R., 1997. Eine erweiterte Riff-Typologie und ihre Anwendung auf kretazische Biokonstruktionen. Bayerische Akademie der Wissenschaften Abhandlungen, Naturwissenschaftliche Klasse, Neue Folge, vol. 169, Verlag der Bayerischen Akademie der Wissenschaften, München, 127 pp.

Howarth, R. J., McArthur, J. M., 1997. Statistics for strontium isotope stratigraphy. A robust LOWESS fit to the marine Sr-isotope curve for 0–206 Ma, with look-up table for the derivation of numerical age. Journal of Geology, 105, 441–456.

Howell, J. A., Flint, S. S., 2003. Tectonic setting, stratigraphy and sedimentology of the Book Cliffs. In: A. L. Coe (Editor), The Sedimentary Record of Sea-Level Change. Cambridge University Press, Cambridge, 135–157.

Ifrim, C., Stinnesbeck, W., López-Oliva, J. G., 2004. Maastrichtian cephalopods from Cerralvo, north-eastern Mexico. Palaeontology, 47(6), 1575–1627.

Ifrim, C., Stinnesbeck, W., Schafhauser, A., 2005. Maastrichtian shallow-water ammonites of northeastern Mexico. Revista Mexicana de Ciencias Geológicas, 22(1), 48–64.

Imlay, R. W., 1944. Cretaceous formations of central America and Mexico. AAPG Bulletin, 28, 1005–1045.

Johnson, C. C., 1999. Evolution of Cretaceous surface current circulation patterns, Caribbean and Gulf of Mexico. In: E. Barrera and C. C. Johnson (Editors), Evolution of Cretaceous Ocean-Climate System. GSA Special Paper, vol. 332, Geological Society of America (GSA), Colorado, 329–343.

Johnson, C. C., Kauffman, E. G., 1996. Maastrichtian extinction patterns of Caribbean province rudistids. In: N. MacLeod and G. Keller (Editors), Cretaceous-Tertiary Mass Extinctions: Biotic and Environmental Changes. Norton, W. W. & Company, New York, 231–273.

Kauffman, E. G., 1973. Cretaceous Bivalvia. In: A. Hallam (Editor), Atlas of Paleobiogeography. Elsevier, Amsterdam, 353–383.

Kauffman, E. G., Sohl, N. F., 1973. Structure and evolution of Antillean Cretaceous rudist frameworks. Verhandlungen der Naturforschenden Gesellschaft Basel, 84, 400–467.

Keller, G., Stinnesbeck, W., Adatte, T., Stüben, D., 2002. Multiple impacts across the Cretaceous-Tertiary boundary. Earth Science Reviews, 1283, 1–37.

Kiel, S., Bandel, K., 1999. The Pugnellidae, a new stromboidean family (Gastropoda) from the Upper Cretaceous. Paläontologische Zeitschrift, 73(1/2), 47–58.

LaBarbera, M., 1981. The ecology of Mesozoic *Gryphaea, Exogyra* and *Ilymatogyra* (Bivalvia: Mollusca) in a modern ocean. Paleobiology, 7(4), 510–526.

Lawton, T., Shipley, K. W., Aschoff, J. L., Giles, K., Vega, F., 2005. Basinward transport of Chicxulub ejecta by tsunami-induced backflow, La Popa Basin, northeastern Mexico, and its implications for distribution of impact-related deposits flanking the Gulf of Mexico. Geology, 33(2), 81–84.

Lawton, T. F., Vega, F. J., Giles, K. A., Rosales-Dominguez, C., 2001. Stratigraphy and origin of the La Popa Basin, Nuevo León and Coahuila, Mexico. In: C. Bartolini, R. Buffler and A. Cantú-Chapa (Editors), The Western Gulf of Mexico Basin: Tectonic, Sedimentary Basins, and Petroleum Systems. AAPG Memoir, vol. 75, American Association of Petroleum Geologists (AAPG), Tulsa, 219–240.

Li, L., Keller, G., 1998a. Abrupt deep-sea warming at the end of the Cretaceous. Geology, 26(11), 995–998.

Li, L., Keller, G., 1998b. Maastrichtian climate, productivity and faunal turnovers in planctic foraminifera on South Atlantic DSDPsites 525A and 21. Marine Micropaleontology, 33, 55–86.

Li, L., Keller, G., Stinnesbeck, W., 1999. The Late Campanian and Maastrichtian in northwestern Tunisia: palaeoenvironmental inferences from lithology, macrofauna and benthic foraminifera. Cretaceous Research, 20, 231–252.

Lopez-Ramos, E., 1985. Geologia de Mexico, II. Instituto Nacional de Estadística Geografía e Informática (INEGI), Ciudad de Mexico, 454 pp.

Lupu, D., 1975. Faune Sénonienne á rudistes de la province de Pinar del Rio (Cuba). Dari de Seama ale Sedintelor, 61, 223–254.

Mac Gillavry, H. J., 1935. Remarks on rudists. Koninklijke Akademie van Wetenschapen te Amsterdam Proceedings, 38(5), 558–565.

Mac Gillavry, H. J., 1937. Geology of the Province of Camaguey, Cuba, with Revisional Studies in Rudist Paleontology. PhD Thesis, University of Utrecht, Utrecht, 168 pp.

Mann, P., 1999. Caribbean sedimentary basins: classification and tectonic setting from Jurassic to present. In: P. Mann (Editor), Caribbean Basins. Sedimentary Basins of the World, vol. 4, Elsevier, Amsterdam, 3–31.

Masse, J.-P., Philip, J., 1981. Cretaceous coral-rudist buildups of France. In: D. F. Toomey (Editor), European Fossil Reef Models. Society for Sedimentary Geology (SEPM), Tulsa, 399–426.

McArthur, J. M., 1994. Recent trends in strontium isotope stratigraphy. Terra Nova, 6, 331–358.

McArthur, J. M., Crame, J. A., Thirlwall, M. F., 2000. Definition of Late Cretaceous stage boundaries in Antarctica using strontium isotope stratigraphy. Journal of Geology, 108, 623–640.

McArthur, J. M., Howarth, R. J., Bailey, R. J., 2001. Strontium isotope stratigraphy: LOWESS version 3: best-fit to the marine Sr-isotope curve for 0–509 Ma and accompanying look-up table for deriving numerical age. Journal of Geology, 109, 155–170.

McBride, E. F., 1974. Significance of color in red, green, purple, olive, brown, and grey beds of Difunta Group, northeastern Mexico. Journal of Sedimentary Petrology, 44(3), 760–773.

McBride, E. F., Weidie, A. E., Wolleben, J. A., 1975. Deltaic and associated deposits of the Difunta Group (Late Cretaceous to Paleocene), Parras and La Popa basins, northeastern Mexico. In: M. L. S. Broussard (Editor), Deltas. Houston Geological Society, Houston, Texas, 485–522.

McBride, E. F., Weidie, A. E., Wolleben, J. A., Laudon, R. C., 1974. Stratigraphy and structure of the Parras and La Popa basins, northeastern Mexico. GSA Bulletin, 84, 1603–1622.

Meschede, M., Frisch, W., 1998. A plate-tectonic model for the Mesozoic and early Cenozoic history of the Caribbean plate. Tectonophysics, 296, 269–291.

Miall, A. D., 1997. The Geology of Stratigraphic Sequences. Springer, Berlin, 433 pp.

Mitchell, S. F., 1999. Stratigraphy of the Guinea Corn Formation (Upper Cretaceous) at its type locality in the Rio Minho between Grantham and Guinea Corn, northern Clarendon, Jamaica. Journal of the Geological Society of Jamaica, 33, 1–12.

Mitchell, S. F., 2003. Morphology, microstructure, and stratigraphy of some late Cretaceous radiolitid rudists from Jamaica. Geologia Croatica, 56(2), 149–172.

Mitchell, S. F., Gunter, G. C., 2002. Biostratigraphy and taxonomy of the rudist *Chiapasella* in the *Titanosarcolites* Limestones (Maastrichtian) of Jamaica. Cretaceous Research, 23, 473–487.

Moran-Zenteno, D., 1994. The Geology of the Mexican Republic. AAPG Studies in Geology, vol. 39, American Association of Petroleum Geologists (AAPG), Tulsa, 160 pp.

Muellerried, F. K., 1931. Sobre una anomalía en las invaginaciones de las valvas de algunas Hippuritidae. Anales del Instituto de Biología, 2, 255–261.

Muellerried, F. K., 1941. La Sierra Madre Oriental en México. Revista Mexicana de Geografía, 2, 13–52.

Myers, R. L., 1968. Biostratigraphy of the Cardenas Formation (Upper Cretaceous) San Luis Potosí, Mexico. Paleontología Mexicana, 24, 1–89.

Olsson, A. A., 1934. Contributions to the paleontology of northern Peru: The Cretaceous of the Amotape region. Bulletin of American Paleontology, 20(69), 1–104.

Olsson, A. A., 1944. Contributions to the paleontology of northern Peru part VII. The Cretaceous of the Paita region. Bulletin of American Paleontology, 28(111), 5–147.

Oppenheim, P., 1930. Die Anthozoen der Gosauschichten in den Ostalpen. Privately Published, Berlin-Lichterfelde, 604 pp.

Palmer, R. H., 1933. Nuevos rudistas de Cuba. Revista de Agricultura, Comercio y Trabajo, 14, 95–125.

Perrilliat, M. C., Vega, F. J., Corona, R., 2000. Early Maastrichtian mollusca from the Mexcala Formation of the state of Guerrero, southern Mexico. Journal of Paleontology, 74(1), 7–24.

Pettijohn, F. J., Potter, P. E., Siever, R., 1984. Sand and Sandstone. Springer, Berlin, 552 pp.

Philip, J., 1999. Description of well-preserved specimens of *Macgillavryia* Rojas, Itturalde-Vinent and Skelton, from the early Campanian of Filim (Eastern Oman): systematics and palaeobiogeographic implications. Fifth International Congress on Rudists, Erlanger Geologische Abhandlungen, Sonderband, 3(53), [in press].

Philip, J., Jaillard, E., 2004. Revision of the Upper Cretaceous rudists from northwestern Peru. Journal of South American Earth Sciences, 17, 39–48.

Pindell, J. L., Barrett, S. F., 1990. Geological evolution of the Caribbean region; a plate tectonic synthesis. In: G. Dengo and J. E. Case (Editors), The Caribbean Region. The Geology of North America, vol. H, GSA Boulder, Geological Society of America (GSA), Colorado, 405–432.

Puigdefàbregas, C., Muñoz, J. A., Vergés, J., 1992. Thrusting and foreland basin evolution in the southern Pyrenees. In: K. R. McClay (Editor), Thrust Tectonics. Chapman & Hall, London, 247–254.

Reuss, A. E., 1854. Beiträge zur Charakteristik der Kreideschichten in den Ostalpen, besonders im Gosauthale und am Wolfgangsee. Denkschriften der kaiserlichen Akademie der Wissenschaften, Mathematisch-Naturwissenschaftliche Classe, 7, 73–133.

Riding, R., 2002. Structure and composition of organic reefs and carbonate mud mounds: concepts and categories. Earth Science Reviews, 58, 163–231.

Roberts, H. H., Murray, S. P., 1988. Gulfs of the northern Red Sea: depositional settings of abrupt siliciclastic-carbonate transitions. In: L. J. Doyle and H. H. Roberts (Editors), Carbonate-Clastic Transitions. Developments in Sedimentology, vol. 42, Elsevier, Amsterdam, 99–142.

Rojas, R., Iturralde-Vinent, M., 1995. Checklist of Cuban rudist taxa. Revista Mexicana de Ciencias Geológicas, 12(2), 292–293.

Rojas, R., Iturralde-Vinent, M., Skelton, P. W., 1995. Stratigraphy, composition, and age of Cuban rudist-bearing deposits. Revista Mexicana de Ciencias Geológicas, 12(2), 272–291.

Rutten, M. G., 1936. Rudistids from the Cretaceous of northern Santa Clara Province, Cuba. Journal of Paleontology, 10(2), 134–142.

Samankassou, E., Strasser, A., Gioia, E., Rauber, G., Dupraz, C., 2003. High-resolution record of lateral facies variations on a shallow carbonate platform (Upper Oxfordian, Swiss Jura Mountains). Eclogae Geologicae Helveticae, 96, 425–440.

Sanchez y Roig, M., 1926. La fauna cretácica de la región central de Cuba. Memorias de la Sociedad Cubana de Historia Natural "Felipe Poey", 7, 83–102.

Sanders, D., Baron-Szabo, R., 1997. Coral-rudist bioconstructions in the Upper Cretaceous Haidach section (Gosau Group; Northern Calcareous Alps, Austria). Facies, 36, 69–90.

Sanders, D., Pons, J. P., 1999. Rudist formations in mixed siliciclastic-carbonate depositional environments, Upper Cretaceous, Austria: stratigraphy, sedimentology, and models of development. Palaeogeography, Palaeoclimatology, Palaeoecology, 148, 249–284.

Schaefer, A., 2005. Klastische Sedimente. Elsevier, Amsterdam, 414 pp.

Schafhauser, A., Götz, S., Baron-Szabo, R., Stinnesbeck, W., 2003. Depositional environment of coral-rudist associations in the Upper Cretaceous Cardenas Formation (central Mexico). Geologia Croatica, 56(2), 187–198.

Scholle, P. A., Ulmer-Scholle, D. S., 2003. A Color Guide to the Petrography of Carbonate Rocks: Grains, Textures, Porosity, Diagenesis. AAPG Memoir, vol. 77, American Association of Petroleum Geologists (AAPG), Tulsa, 474 pp.

Schulte, P., 2003. The Cretaceous-Paleogene Transition and Chicxulub Impact Ejecta in the Northwestern Gulf of Mexico: Paleoenvironments, Sequence Stratigraphic Setting, and Target Lithologies. PhD Thesis, University of Karlsruhe, Karlsruhe, 204 pp.

Schulte, P., Stinnesbeck, W., Stüben, D., Kramar, U., Berner, Z., Keller, G., Adatte, T., 2003. Fe-rich and K-rich mafic spherules from slumped and channelized Chicxulub ejecta deposits in the northern La Sierrita area, NE Mexico. International Journal of Earth Sciences, 92, 114–142.

Schumann, D., 2000. Paleoecology of late Cretaceous rudist settlements in Central Oman. In: S. Alsharhan-Abdulrahman and R. W. Scott (Editors), Middle East Models of Jurassic/Cretaceous Carbonate Systems. SEPM Special Publications, vol. 69, Society for Sedimentary Geology (SEPM), Tulsa, 143–153.

Scott, R. W., 1995. Cretaceous rudists of Guatemala. Revista Mexicana de Ciencias Geológicas, 12(2), 294–306.

Scott, R. W., Fernández-Mendiola, P. A., Gili, E., Simo, A. J., 1990. Persistence of coral-rudist reefs into the Late Cretaceous. Palaios, 5(2), 98–110.

Seilacher, A., Matyja, B. A., Wierzbowski, A., 1985. Oyster beds: morphologic response to changing substrate conditions. In: U. Bayer and A. Seilacher (Editors), Sedimentary and evolutionary cycles. Lecture Notes in Earth Sciences, vol. 1, Springer, Berlin, 421–435.

Simone, L., Carannante, G., Ruberti, D., Sirna, M., Sirna, G., Laviano, A., Tropeano, M., 2003. Development of rudist lithosomes in the Coniacian–Lower Campanian carbonate shelves of central-southern Italy: high-energy vs low-energy settings. Palaeogeography, Palaeoclimatology, Palaeoecology, 200, 5–29.

Skelton, P. W., 1979. Preserved ligament in a radiolitid rudist bivalve and its implication of mantle marginal feeding in the group. Paleobiology, 5(2), 90–106.

Skelton, P. W., Gili, E., 1991. Palaeoecological classification of rudist morphotypes. 1st International Conference on Rudists, Serbian Geological Society Special Publication [preprint issued for unpublished volume], Belgrad, 265–287.

Skelton, P. W., Gili, E., Rosen, B. R., Valldeperas, F. X., 1997. Corals and rudists in the late Cretaceous: a critique of the hypothesis of competitive displacement. Boletin de la Real Sociedad Española de Historia Natural, Sección Geológica, 92(1-4), 225–239.

Smith, A. M., 1995. Paleoenvironmental interpretation using bryozoans: a review. In: D. W. J. Bosence and P. A. Allison (Editors), Marine Palaeoenvironmental Analysis from Fossils. Geological Society Special Publication, vol. 83, Geological Society, London, 231–243.

Smith, B. A., 1986. Upper Cretaceous Stratigraphy and the Mid-Cenomanian Unconformity of East Central Mexico. PhD Thesis, University of Texas, Austin, 200 pp.

Soegaard, K., Giles, K., Vega, F., Lawton, T., 1997. Structure, Stratigraphy and Paleontology of Late Cretaceous-Early Tertiary Parras-La Popa Foreland Basin near Monterrey, Northeast Mexico. AAPG Field Trip, vol. 10, American Association of Petroleum Geologists (AAPG), Dallas, 135 pp.

Soegaard, K., Ye, H., Halik, N., Daniels, A. T., Arney, J., Garrick, S., 2003. Stratigraphic evolution of latest Cretaceous to early Tertiary Difunta foreland basin in northeast Mexico: influence of salt withdrawal on tectonically induced subsidence by the Sierra Madre Oriental fold and thrust belt. In: C. Bartolini, R. Buffler and J. Blickwede (Editors), The Circum-Gulf of Mexico and the Caribbean: Hydrocarbon Habitats, Basin Formation and Plate Tectonics. AAPG Memoir, vol. 79, American Association of Petroleum Geologists (AAPG), Tulsa, 364–394.

Sohl, N. F., 1960. Archeogastropoda, Mesogastropoda and Stratigraphy of the Ripley, Owl Creek, and Prairie Bluff Formations. U.S. Geological Survey Professional Paper, vol. 331-A, U. S. Geological Survey, Washington, 151 pp.

Sohl, N. F., Martínez, E. R., Ureña-Salmeron, P., Jaramillo-Soto, F., 1991. Upper Cretaceous. In: A. Salvador (Editor), The Gulf of Mexico Basin. The Geology of North America, vol. J, GSA Boulder, Geological Society of America (GSA), Colorado, 205–244.

Stenzel, H. B., 1971. Oysters. Treatise on Invertebrate Paleontology, vol. 3, part N. Geological Society of America (GSA) & The University of Kansas, Colorado, 271 pp.

Stephenson, L. W., 1922. Some upper Cretaceous shells of the rudistid group from Tamaulipas, Mexico. Proceedings U.S. National Museum, 61(2422), 1–13.

Stephenson, L. W., 1941. The Larger Invertebrate Fossils of the Navarro Group of Texas. The University of Texas Publication, vol. 4101, University of Texas, Austin, 624 pp.

Steuber, T., 1999. Cretaceous Rudists of Boeotia, Central Greece. Special Papers in Palaeontology, vol. 61, The Palaeontological Association, London, 229 pp.

Steuber, T., 2001. Strontium isotope stratigraphy of Turonian–Campanian Gosau-type rudist formations in the Northern Calcareous and Central Alps (Austria and Germany). Cretaceous Research, 22, 429–441.

Steuber, T., 2002. List of occurrences of rudist bivalves (Hippuritoidea) in the Americas. Geological Society of America, Data Repository Item 2002022, 1–71.

Steuber, T., 2003. Strontium isotope stratigraphy of Cretaceous hippuritid rudist bivalves: rates of morphological change and heterochronic evolution. Palaeogeography, Palaeoclimatology, Palaeoecology, 200, 221–243.

Steuber, T., Mitchell, S. F., Buhl, D., Gunter, G., Kasper, H. U., 2002. Catastrophic extinction of Caribbean rudist bivalves at the Cretaceous-Tertiary boundary. Geology, 30(11), 999–1002.

Stinnesbeck, W., Barbarin, J. M., Keller, G., López-Oliva, J.-G., Pivnik, D. A., Lyons, J. B., Officer, C. B., Adatte, T., Graup, G., Rocchia, R., Robin, E., 1993. Deposition of channel deposits near the Cretaceous-Tertiary boundary in northeastern Mexico: Catastrophic or "normal" sedimentary deposits?. Geology, 21(7), 797–800.

Stinnesbeck, W., Keller, G., 1996. K/T boundary coarse-grained siliciclastic deposits in northeastern Mexico and northeastern Brazil: evidence for mega-tsunami or sea-level changes?. In: G. Ryder, D. Fastovsky and S. Gartner (Editors), The Cretaceous-Tertiary Boundary Event and other Catastrophes in Earth History. GSA Special Paper, vol. 307, Geological Society of America (GSA), Colorado, 197–209.

Stinnesbeck, W., Keller, G., Adatte, T., López-Oliva, J.-G., MacLeod, N., 1996. Cretaceous-Tertiary boundary clastic deposits in NE Mexico: Bolide impact or sea-level lowstand?. In: N. MacLeod and G. Keller (Editors), The Cretaceous-Tertiary Boundary Mass Extinction: Biotic and Environmental Events. W.W. Norton & Co, New York, 471–517.

Stinnesbeck, W., Schulte, P., Lindenmaier, F., Adatte, T., Affolter, M., Schilli, L., Keller, G., Stüben, D., Berner, Z., Kramar, U., Burns, S., López-Oliva, J.-G., 2001. Late Maas-

trichtian age of spherule deposits in northeastern Mexico: implication for Chicxulub scenario. Canadian Journal of Earth Sciences, 38(2), 229–238.

Strasser, A., Pittet, B., Hillgärtner, H., Pasquier, J.-B., 1999. Depositional sequences in shallow carbonate-dominated sedimentary systems: concepts for a high-resolution analysis. Sedimentary Geology, 128, 201–221.

Suter, M., 1987. Structural traverse across the Sierra Madre Oriental in east-central Mexico. GSA Bulletin, 98, 249–264.

Thiadens, A. A., 1936. Rudistids from southern Santa Clara, Cuba. Koninklijke Akademie van Wetenschappen te Amsterdam, Proceedings of the Section of Sciences, 39, 1010–1019.

Torre, H. C., 1964. Estudio geológico del area Cerritos-Cárdenas. Boletin de la Asociación Mexicana de Geólogos Petroleros, 16, 221–235.

Trechmann, C. T., 1924. The Cretaceous limestones of Jamaica and their mollusca. Geological Magazine, 61(9), 385–410.

Trechmann, C. T., 1927. The Cretaceous shales of Jamaica. Geological Magazine, 64, 27–42.

Tucker, M. E., 1985. Einführung in die Sedimentpetrologie. Enke, Stuttgart, 262 pp.

Tucker, M. E., 1990. Shelf margin sand bodies. In: M. E. Tucker and V. P. Wright (Editors), Carbonate Sedimentology. Blackwell Scientific Publications, Oxford, 127–136.

Vail, P. R., Audemard, F., Bowman, S. A., Eisner, P. N., Perez-Cruz, C., 1991. The stratigraphic signatures of tectonics, eustasy and sedimentology – an overview. In: G. Einsele, W. Ricken and A. Seilacher (Editors), Cycles and Events in Stratigraphy. Springer, Berlin, 617–659.

Vail, P. R., Mitchum, R. M. J., 1977. Seismic stratigraphy and global changes of sea level. In: C. E. Payton (Editor), Seismic Stratigraphy – Applications to Hydrocarbon Explorations. AAPG Memoir, vol. 26, American Association of Petroleum Geologists (AAPG), Tulsa, 51–52.

Van Dommelen, H. , 1971. Ontogenetic, phylogenetic and taxonomic studies of the American species of *Pseudovaccinites* and of *Torreites* and the multiple-fold hippuritids. PhD Thesis, University of Amsterdam, Amsterdam, 125 pp.

Van Wagoner, J. C., 1995. Overview of sequence stratigraphy of foreland basin deposits: terminology, summary of papers, and glossary of sequence stratigraphy. In: J. C. Van Wagoner and G. T. Bertram (Editors), Sequence Stratigraphy of Foreland Basin Deposits: Outcrop and Subsurface Examples from the Cretaceous of North America. AAPG Memoir, vol. 64, American Association of Petroleum Geologists (AAPG), Tulsa, 9–21.

Van Wagoner, J. C., Mitchum, R. M., Campion, K. M., Rahmanian, V. D., 1990. Siliciclastic Sequence Stratigraphy in Well Logs, Cores and Outcrops. Methods in Exploration Series, vol. 172, American Association of Petroleum Geologists (AAPG), Tulsa, 55 pp.

Van Wagoner, J. C., Posamentier, H. W., Mitchum, R. M., Vail, P. R., Sarg, J. F., Loutit, T. S., Hardenbol, J., 1988. An overview of the fundamentals of sequence stratigraphy and key definitions. In: C. K.,Wilgus, B. S. Hastings, C. A. Ross, H. W. Posamentier, J. C. Van Wagoner, C. G. S. C. Kendall (Editors), Sea-Level Changes: An Integrated Approach. SEPM Special Publications, vol. 42, Society for Sedimentary Geology (SEPM), Houston, 39–45.

Vaughan, T. W., 1899. Some Cretaceous and Eocene corals from Jamaica. Bulletin of the Museum of Comparative Zoology, 34, 227–250.

Vaughan, T. W., 1923. Fauna of the Sooke Formation, Vancouver Island, description of a new coral. Publications of Geology of the University of California, 14, 175–176.

Vega, F. J., Feldmann, R. M., 1991. Fossil crabs (Crustacea, Decapoda) from the Maastrichtian Difunta Group, northeastern Mexico. Annals of Carnegie Museum, 60(2), 163–177.

Vega, F. J., Feldmann, R. M., Sour-Touvar, F., 1995. Fossil crabs (Crustacea, Decapoda) from the late Cretaceous Cárdenas Formation, east-central Mexico. Journal of Paleontology, 69(2), 340–350.

Vega, F. J., Perilliat, M. C., Mitre-Salazar, L. M., 1999. Paleocene ostreids from the Las Encinas Formation (Parras basin, Difunta Group), northeastern Mexico; stratigraphic implications. In: C. Bartolini, J. L. Wilson and T. F. Lawton (Editors), Mesozoic Sedimentary and Tectonic History of North-Central Mexico. GSA Special Paper, vol. 340, Geological Society of America (GSA), Colorado, 105–110.

Vega, F. J., Perrilliat, M. C., 1995. On some Paleocene invertebrates from the Potrerillos Formation (Difunta Group), northeastern Mexico. Journal of Paleontology, 69(5), 862–869.

Vega-Vera, F. J., Perrilliat, M. C., 1990. Moluscos del Maastrichtiano del la Sierra de la Antrisco estado de Nuevo León. Paleontología Mexicana, 55, 1 - 42.

Veizer, J., 1983. Trace elements and isotopes in sedimentary carbonates. In: R. J. Reeder (Editor), Carbonates: Mineralogy and Chemistry. Reviews in Mineralogy, vol. 11, Mineralogical Society of America, Washington, 265–299.

Vermunt, L. W. J., 1937. Cretaceous rudistids of Pinar del Rio Province, Cuba. Journal of Paleontology, 11(4), 261–275.

Vicens, E., 1992. Intraspecific variability in hippuritidae in the southern Pyrenees, Spain: taxonomic implications. 2nd International Conference on Rudists, Geologica Romana, 28, 119–161.

Vogel, K., 1975. Endosymbiotic algae in rudists?. Palaeogeography Palaeoclimatology Palaeoecology, 17, 327–332.

Wade, B., 1926. The fauna of the Ripley Formation on Coon Creek, Tennessee. U. S. Geological Survey Professional Paper, vol. 137, U. S. Geological Survey, Washington, 272 pp.

Wells, J. W., 1934. Some fossil corals from the West Indies. Proceedings of the U. S. Natural Museum, 83, 71–110.

Whitfield, R. P., 1897. Observations on the genus *Barrettia* Woodward, with descriptions of two new species. Bulletin of the American Museum of Natural History, 9, 233–246.

Wilgus, C. K., Hastings, B. S., Kendall, C. G. S. C., Posamentier, C. A., Ross, C. A., Van Wagoner, J. C., 1988. Sea-Level Changes: An Integrated Approach. SEPM Special Publication, vol. 42, Society for Sedimentary Geology (SEPM), 407 pp.

Wilson, J. L., Ward, W. C., 1995. Early Cretaceous carbonate platforms of northeastern and east-central Mexico. In: A. J. Simo, R. W. Scott and J.-P. Masse (Editors), Cretaceous carbonate platforms. AAPG Memoir, vol. 56, American Association of Petroleum Geologists (AAPG), Tulsa, 35–49.

Wolleben, J. A., 1977. Paleontology of the Difunta Group (Upper Cretaceous-Tertiary) in northern Mexico. Journal of Paleontology, 51(2), 373–398.

Wright, P. V, 1992. A revised classification of limestones. Sedimentary Geology, 76, 177–186.

Wright, P. V., 1990. Carbonate sediments and limestones: constituents. In: M. E. Tucker and P. V. Wright (Editors), Carbonate Sedimentology. Blackwell Scientific Publications, Oxford, 1–27.

Ye, H., 1997. The arcuate Sierra Madre Oriental orogenic belt, NE Mexico: tectonic infilling of a recess along the southwestern North American continental margin. In: K. Soegaard, K. Giles, F. J. Vega and T. Lawton (Editors), Structure, Stratigraphy and Paleontology of Late Cretaceous-Early Tertiary Parras–La Popa Foreland Basin near Monterrey, Northeast Mexico. AAPG Field Trip, vol. 10, American Association of Petroleum Geologists (AAPG), Dallas, 82–115.

10 Plates

Plate 1: Lithologies of the Cardenas Formation

1 Planar laminated arenite deposited in the upper shoreface. Arroyo de la Atarjea section, middle member (diameter of the coin: 2 cm).

2 Conglomerate deposited in the upper shoreface. Arroyo de la Atarjea section, middle member (hammer width: 12 cm).

3 *Durania* reef representing lagoonal environments (see also plate 1/5). Arroyo de la Atarjea section, lower member.

4 Trough cross-stratified arenite deposited in the upper shoreface. Arroyo de la Atarjea section, middle member (diameter of the coin: 2 cm).

5 *Durania* reef containing abundant imbricated left (free) valves of *Durania* (see also plate 1/3). Arroyo de la Atarjea section, middle member.

6 Reworked specimen of *Durania* in the shoreface arenite. La Luz section, lower member (hammer width: 16 cm).

7 Sandy limestone containing small reworked radiolitids deposited in the upper shoreface. Arroyo de la Atarjea section, upper member (diameter of coin: 2 cm).

Plate 1

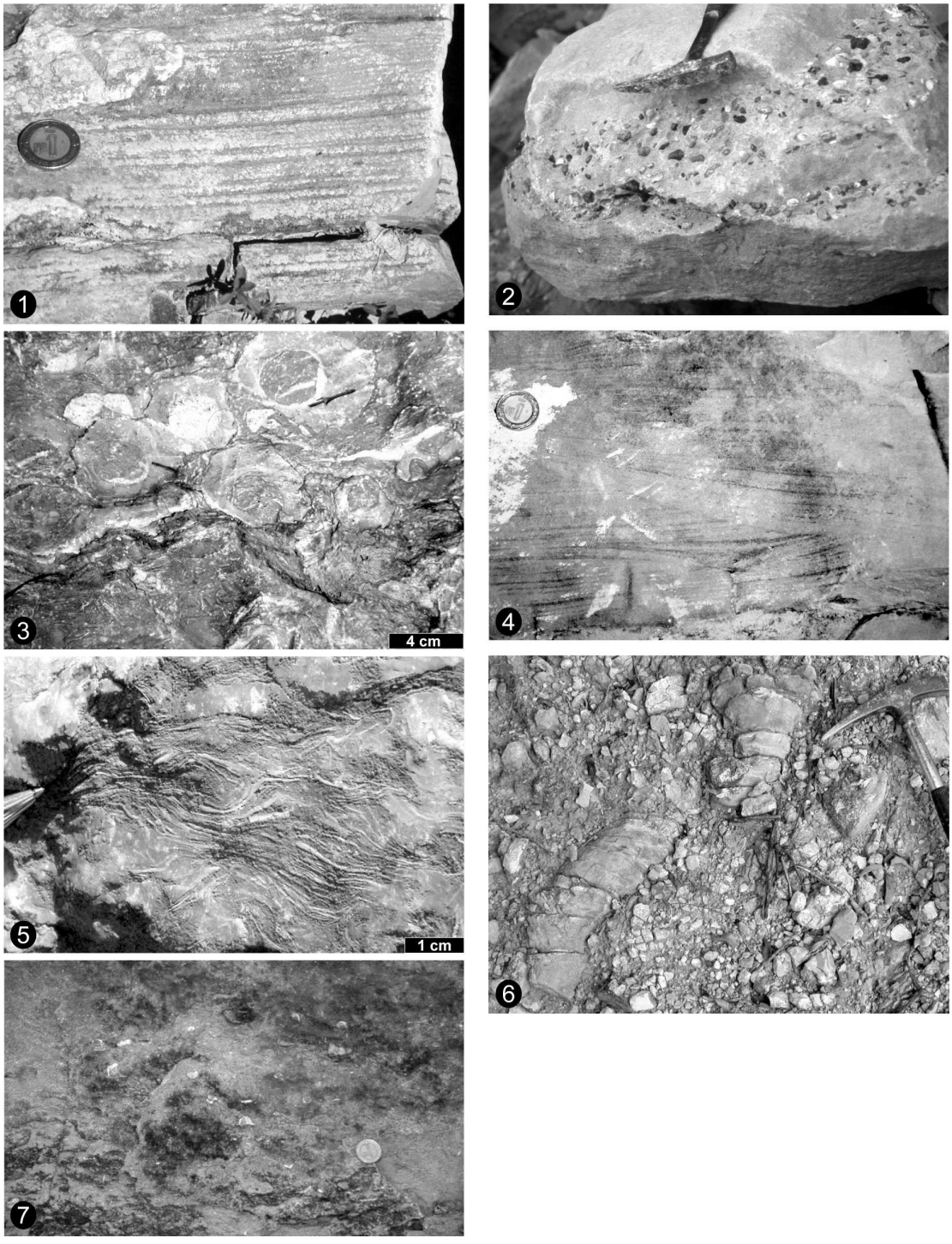

Plate 2: Lithologies of the Cardenas Formation

1 *Praebarrettia* reef in the transition between lagoonal and lower shoreface environments. La Luz section, lower member (length of pocket rule: 11 cm).

2 *Praebarrettia* reef. La Luz section, lower member (height of the kneeling person: approximately 0.9 m).

3 *Macgillavryia nicholasi* reef. Estación Canoa section, lower member (length of pocket rule: 11 cm).

4 *Macgillavryia nicholasi* (see also plate 2/3). Estación Canoa section, lower member (hammer length: 28 cm).

5 Basal part of a mixed coral-rudist reef. Clinger morphotypes of *Coralliochama* (white arrows) represent a pioneer fauna, which settled in erosional cavities of the underlying arenite. Upsection, branching corals follow. Arroyo de la Atarjea section, upper member (hammer length: 28 cm).

6 Hippuritid thicket at the margin of a coral-rudist reef. Arroyo de la Atarjea section, upper member (hammer length: 28 cm).

Plate 2

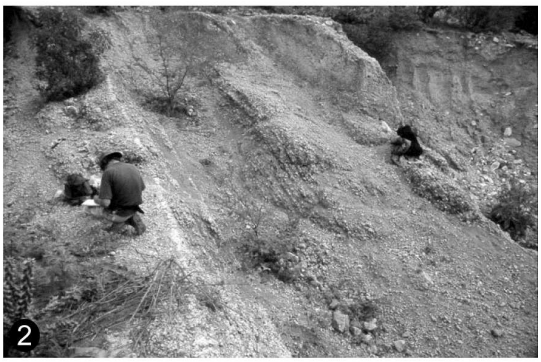

Plate 3: Lithologies of the Cardenas Formation

1 Coral-rudist reefs (black arrows) exposed in the Arroyo de la Atarjea. Arroyo de la Atarjea section, upper member (height of the backpack: approx. 60 cm).

2 Coral-rudist reef in the Cardenas section. Reefs in the lower upper member are generally thicker than in the Arroyo de la Atarjea, and reef sediment contains less marl and detrital quartz. Cardenas section, upper member (diameter of the coin: 2 cm).

3 Coral-rudist reefs intercalated in sandy marls. Cardenas section, upper member (hammer length: 28 cm).

4 Coral-rudist reef containing hippuritids (A), radiolitids (black arrow), branched (B) and massive (white arrow) corals. Arroyo de la Atarjea section, upper member (length of pocket rule: 11 cm).

5 Margin of small coral-rudist reef (above pocket rule) intercalated in sandy marl. Sediment contains abundant actaeonellid gastropods (see also plate 3/3). Cardenas section, upper member (length of pocket rule: 11 cm).

6 Base of a coral-rudist reef, with branched corals (A) and plagioptychid rudists (black arrow), overlain by hippuritids, radiolitids, and massive corals (white arrow). Section Arroyo de la Atarjea, upper member (length of pocket rule: 11 cm).

Plate 3

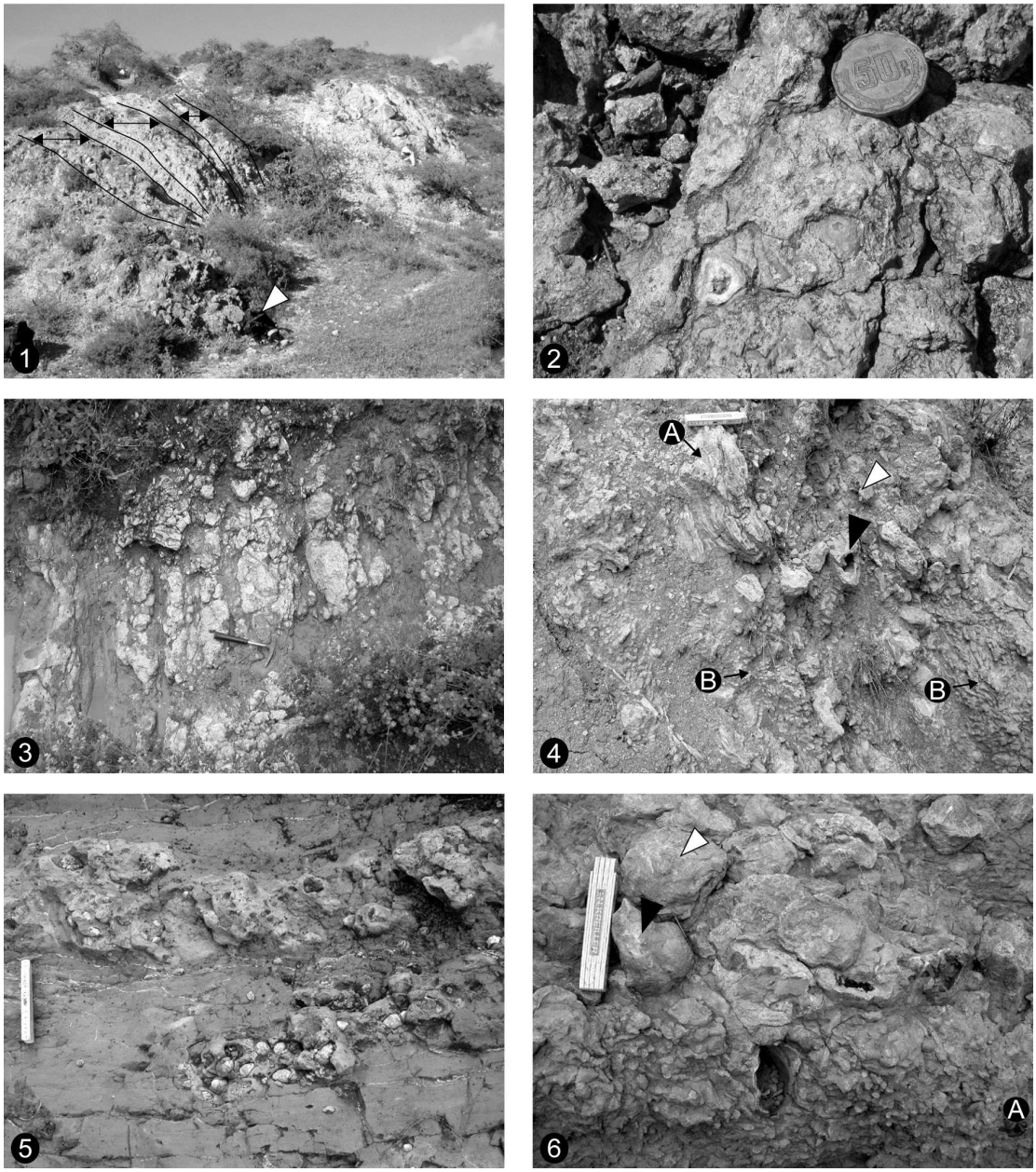

Plate 4: Lithologies of the Cardenas Formation

1 Branched corals (*Multicolumnastraea*) at the base of a coral-dominated reef. Arroyo de la Atarjea section, upper member.

2 Reef core of a coral-dominated reef containing big massive corals. Arroyo de la Atarjea section, upper member (length of pocket rule: 11 cm).

3 Upper part of a coral-dominated reef consisting of interlayered reef limestone and marl. Arroyo de la Atarjea section, upper member (hammer length: 28 cm).

4 Serpulid worm tubes in siltstone of outer shelf environments. Arroyo de la Atarjea section, middle member (diameter of the coin: 2 cm).

5 Reef core of a coral-dominated reef containing sparse rudists (white arrow). Cardenas section, upper member (hammer length: 28 cm).

6 Actaeonellid limestone deposited in the transition between upper and lower shoreface. Cardenas section, upper member (hammer width: 16 cm).

7 Base of a coral-dominated reef consisting of branched corals. Underlying marl contains reworked single elevator rudists. Cardenas section, upper member (length of pocket rule: 11 cm).

Plate 4

Plate 5: Lithologies of the Cardenas Formation

1 Big radiolitids in the core of a coral-dominated reef. Cardenas section, upper member (length of pocket rule: 11 cm).

2 Condensed horizon in offshore sediments, marked by the accumulation of pectinid bivalves and iron crusts. Arroyo de la Atarjea section, middle member (hammer length: 28 cm).

3 *Exogyra* nest in marl of the offshore transition zone. Arroyo de la Atarjea section, middle member (length of the hammer peak: 10 cm).

4 Paleosoil horizon (black arrow) in the Tabaco Formation. Arroyo de la Atarjea section, Tabaco Formation (length of pocket rule: 11 cm).

5 Branched bryzoans in arenite of the offshore transition zone. Cardenas section, middle member (hammer width: 12 cm).

6 Bioturbation on arenite surface in the Tabaco Formation. La Presa section, Tabaco Formation (diameter of coin: 2 cm).

Plate 5

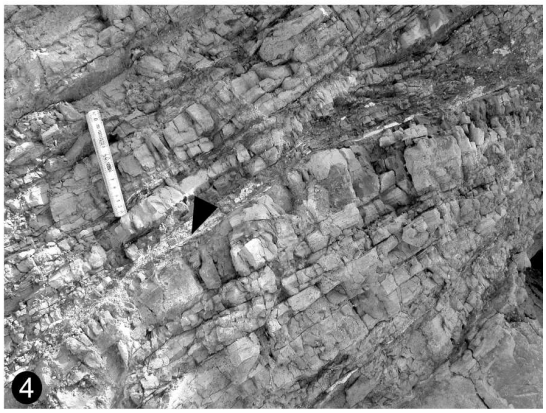

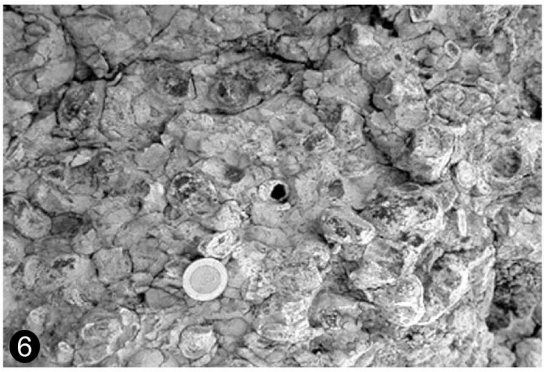

Plate 6: Microfacies of the Cardenas Formation

1 Lagoonal foraminiferal packstone. Bioclasts are predominated by miliolid and textulariid foraminifera [e.g., *Textularia* (black arrow), *Dicyclina* (white arrows)]. Arroyo de la Atarjea section, lower member.

2 Lagoonal wackestone containing miliolid foraminfera and dasycladacean algae (white arrow).

3 Lagoonal foraminiferal cementstone. Bioclasts are predominated by miliolid foraminifera. The matrix was initially micritic and later recrystallized into poikilotopic blocky spar during diagenesis. Arroyo de la Atarjea section, lower member.

4 Sediment of rudist reefs consisting of radiolitid cementstone. Larger bioclasts (>2 mm) consist of radiolitid fragments; internal sediment is a foraminiferal cementstone similar to the one described in plate 6/3. Arroyo de la Atarjea section, lower member.

5 Conglomerate representing sediment bars of the upper shoreface. Clasts consist of chert (A) and pelagic wackestones (B) containing calcispheres and planktic foraminifera. The arenitic matrix contains oyster fragments (black arrow) and sparse orbitoidacean foraminifera (white arrow). Cardenas section, middle member.

6 Lagoonal foraminiferal cementstone. Bioclasts consist almost exclusively of miliolid foraminifera. The previously micritic matrix is recrystallized into pseudospar. Arroyo de la Atarjea section, lower member.

7 Sediment of an oyster reef. Larger bioclasts (>2 mm) consist of oyster fragments. The packstone matrix contains ostracods (white arrow) and miliolid foraminifera. Oyster reefs of the Cardenas Formation developed in areas affected by terrigenous input, indicated by a high amount of detrital quartz in the reef sediment. La Luz section, lower member.

Plate 6

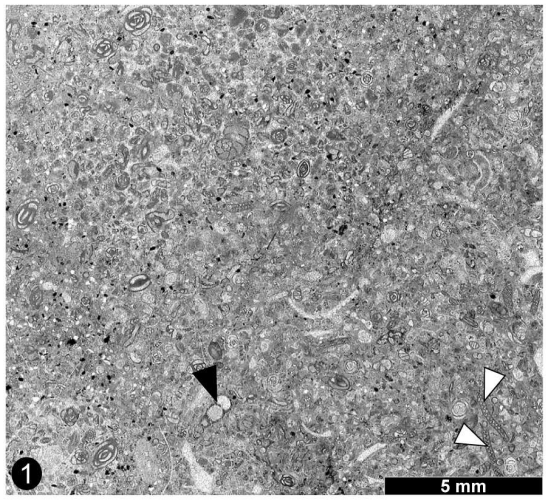

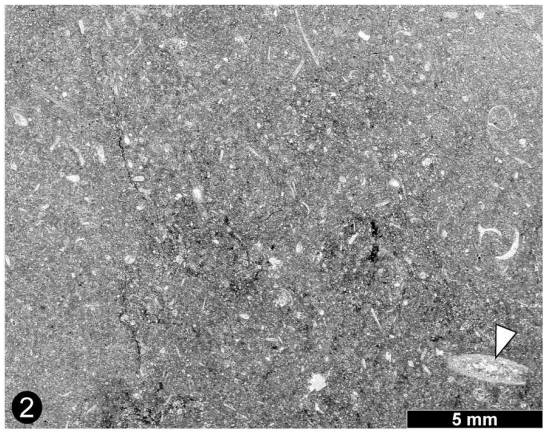

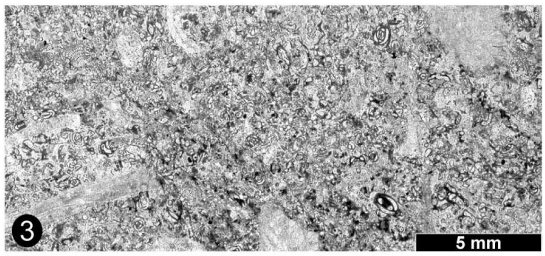

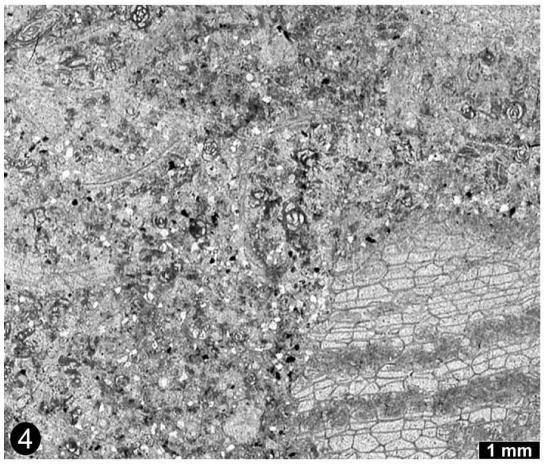

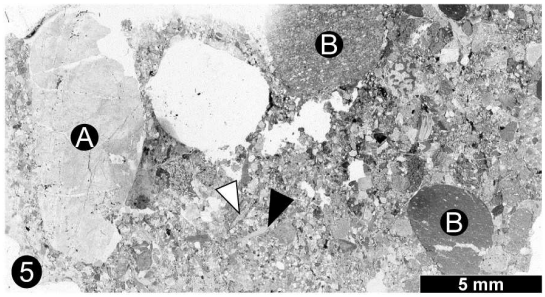

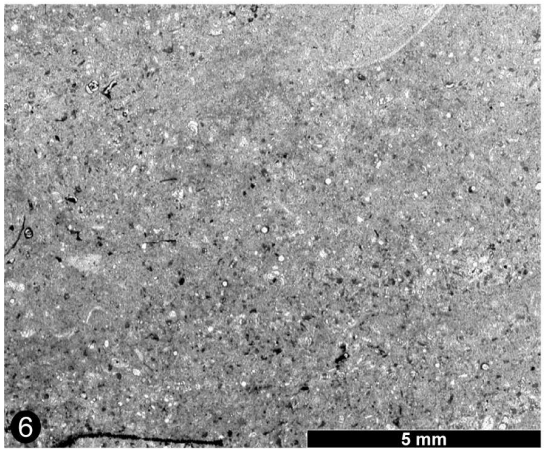

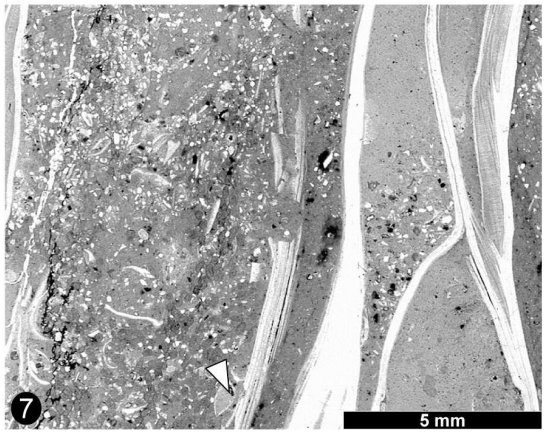

Plate 7: Microfacies of the Cardenas Formation

1 Well sorted unfossiliferous arenite of the upper shoreface, containing silt matrix. Arroyo de la Atarjea section, middle member.

2 Marly packstone containing coated bivalve fragmens (A), coral fragments (B), miliolid and texulariid foraminifera (black arrow), intraclasts (white arrow), peloids, as well as abundant detrital quartz. The packstone is interpreted to represent a storm layer deposited in the transition between the upper and lower shoreface. La Luz section, lower member.

3 Internal sediment of *Durania/Coralliochama* rudist floatstone. Larger bioclasts (>2 mm) are *Coralliochama* fragments. Bioclasts in the packstone matrix are predominated by miliolid and textulariid foraminifera, but also contain actaeonellid gastropods (white arrow) and sparse corals (black arrow). La Luz section, lower member.

4 Lagoonal packstone containing abundant dasycladacean algae (black arrows), calcispheres (charophytes(?), white arrow), miliolid foraminifera, and detrital quartz. All bioclasts are recrystallized into blocky spar. Arroyo de la Atarjea section, upper member.

5 Conglomerate at the base of parasequence 18. Bioclasts are predominated by oyster shells, but gastropods (black arrow), branching bryozoans (white arrow), and orbitoidacean foraminifera (A) are also present. Bigger clasts are calcimudstones (B) containing sparse planktic foraminifera of outer shelf environment. The arenitic matrix consists of quartz and lime clasts. Cardenas section, upper member.

6 Sandy radiolitid packstone of the upper member. Bioclasts consist only of fragmented radiolitids and sparse miliolid foraminifera. Internal sediment within radiolitids consists of calcimudstone indicating a protected lagoonal environment. The sandy packstone resulted from shallowing of the depositional area, which caused reworking of the radiolitids and increased terrigenous input. Arroyo de la Atarjea section, upper member.

7 Bioturbated lagoonal siltstone containing ostracods (white arrow) and miliolid foraminifera. Arroyo de la Atarjea section, upper member.

8 Reef sediment of *Macgillavryia nicholasi* reef. Sediment consists of packstone that contains abundant left (free) valves of *Macgillavryia* (white arrow), miliolid foraminifera, and peysonneliacean and corallinacean algae, arranged as rhodoliths around a pelsparitic nucleus (black arrow). Estación Canoa section, lower member.

9 Marly packstone of *Praebarrettia* reef. Sediment contains ostracods, miliolid foraminifera, and dasycladacean algae (white arrow). La Luz section, lower member.

10 Encrusting foraminifera on the right (attached) valve of *Praebarrettia*. La Luz section, lower member.

Plate 7

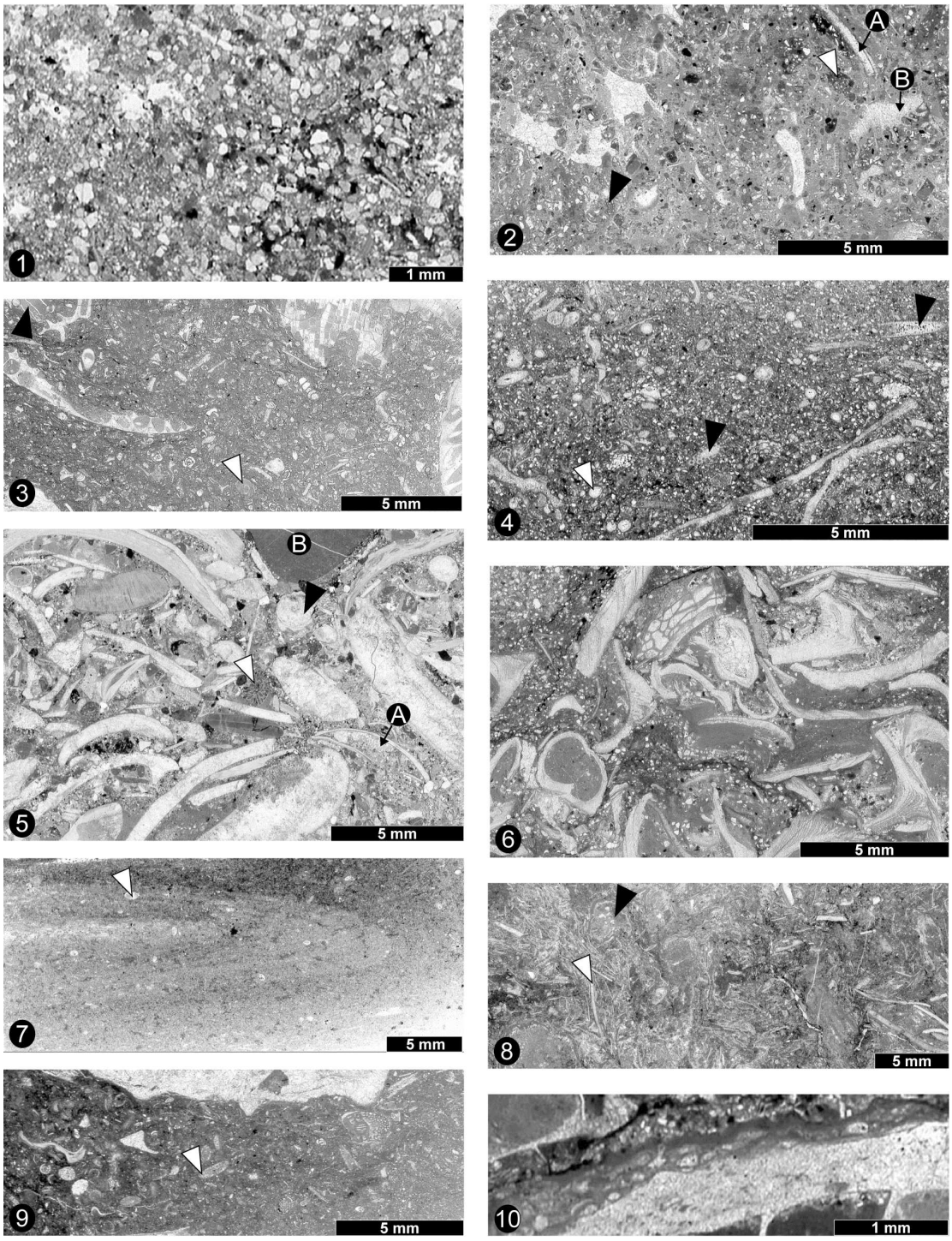

Plate 8: Microfacies of the Cardenas Formation

1 The textulariid foraminifera *Textularia* in sediment of the *Praebarrettia* reef. Section La Luz, lower member.

2 Fine-grained and well-sorted arenite. This sediment is very common in upper and lower shoreface environments. Arroyo de la Atarjea section, upper member.

3 The textulariid foraminifer *Dicyclina* in sediment of the *Praebarrettia* reef. La Luz section, lower member.

4 Siltstone containing actaeonellid gastropod. This microfacies is characteristic for the transition between the upper and lower shoreface. Arroyo de la Atarjea section, upper member.

5 Sorted packstone in the *Praebarrettia* reef. Bioclasts comprise recrystallized fragments of the right (attached) (A) and left (free) valves (black arrow) of rudists, orbitoidacean foraminifera (white arrows), and calcareous algae. This packstone is interpreted to represent storm deposits within the rudist reef. La Luz section, lower member.

6 Sandy packstone deposited in the lower shoreface. Bioclasts consist of gastropods, fragments of *Coralliochama* (white arrow) and corals, as well as ostracods, miliolid and textulariid foraminifera. Bioerosion by lithophagid bivalves is common in the shells (black arrows). Arroyo de la Atarjea section, upper member.

7 Oolitic grainstone consisting of single superficial ooids and coated grains. Nuclei of the ooids are shell fragments and detrital quartz. Allochems are well rounded and sorted. The sediment is interpreted to represent sand shoals of the lower shoreface. Arroyo de la Atarjea section, upper member.

Plate 8

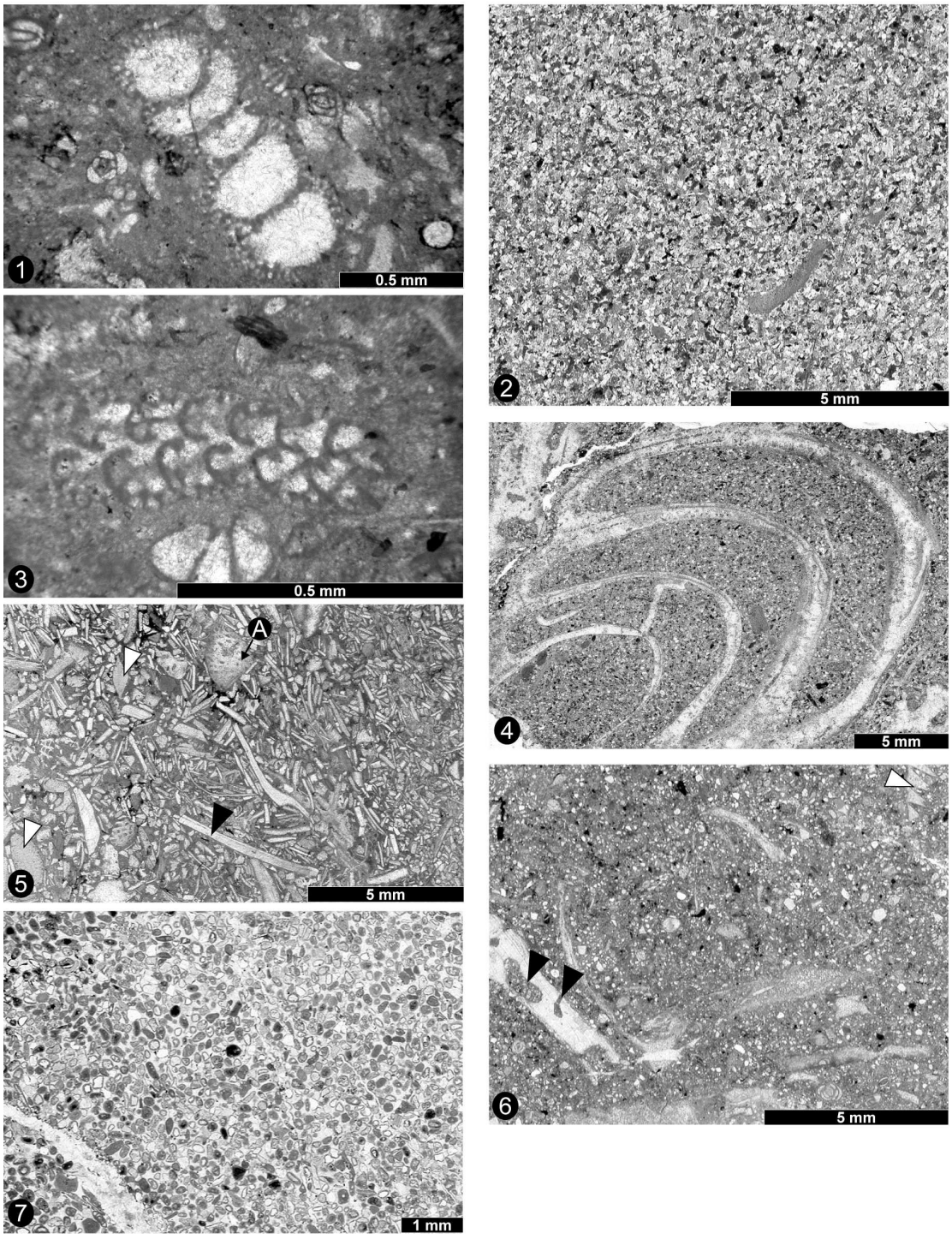

Plate 9: Reefal microfacies of the Cardenas Formation

1 Radiolitid floatstone of a radiolitid-reef. The bioclasts are exclusively composed of radiolitids indicating reef growth in a restricted lagoon. Arroyo de la Atarjea section, upper member.

2 Foraminiferal packstone of a coral-rudist reef. Sediment contains rudist (A) and coral fragments (white arrow) as well as dasycladacean algae (black arrow). This reef is characterized by the abundance of miliolid and textulariid foraminifera, and the absence of detrital quartz. It likely developed in a protected area of the lower shoreface. Arroyo de la Atarjea section, upper member.

3 Placopsilinid foraminifera on a rudist shell in the *Praebarrettia* reef. La Luz section, lower member.

4 Coral-bafflestone of a coral-dominated reef. Larger bioclasts (>2 mm) consist of coral fragments and peysonneliacean algae. The latter form rhodoliths (A) or encrusted rudists and corals. Packstone matrix contains ostracods, miliolid foraminifera (black arrow), and dasycladacean algae (white arrows). The absence of detrital quartz and little sorted bioclasts indicate, that reefs were not exposed to high terrigenous input and current energy. Abundance of calcareous algae indicates a reef development in a well-illuminated environment. Coral-dominated reefs likely developed in protected areas of the lower shoreface. Arroyo de la Atarjea section, upper member.

5 Sorted rudstone of the core of a coral-rudist reef. Larger bioclasts (>2 mm) consist of coral (A) and rudist fragments (black arrow). Packstone matrix contains miliolid foraminifera and fragments of dasycladacean algae (white arrow). Sorted bioclasts indicate increased current energy and reef growth in the proximal lower shoreface. Arroyo de la Atarjea section, upper member.

6 Rudstone of the margin of a coral-rudist reef. Larger bioclasts (>2 mm) are rudist and coral (A) fragments. The sorted packstone matrix contains peysonneliacean (black arrow) and dasycladacean (white arrows) algae. In contrast to the sediment of the reef core (Plate 9/5), abundant detrital quartz indicates exposure to terrigenous input. Coral-rudist reefs grew in agitated water of the lower shoreface. Arroyo de la Atarjea section, upper member.

7 Storm layer in *Praebarrettia* reef. This rudist rudstone contains bioclasts (>2 mm) of rudists (*Praebarrettia*, black arrow), which are filled by micritic internal sediment. The packstone matrix contains rudist fragments, sparse bryozoans (white arrow), calcareous algae, and abundant detrital quartz. La Luz section, lower member.

Plate 9

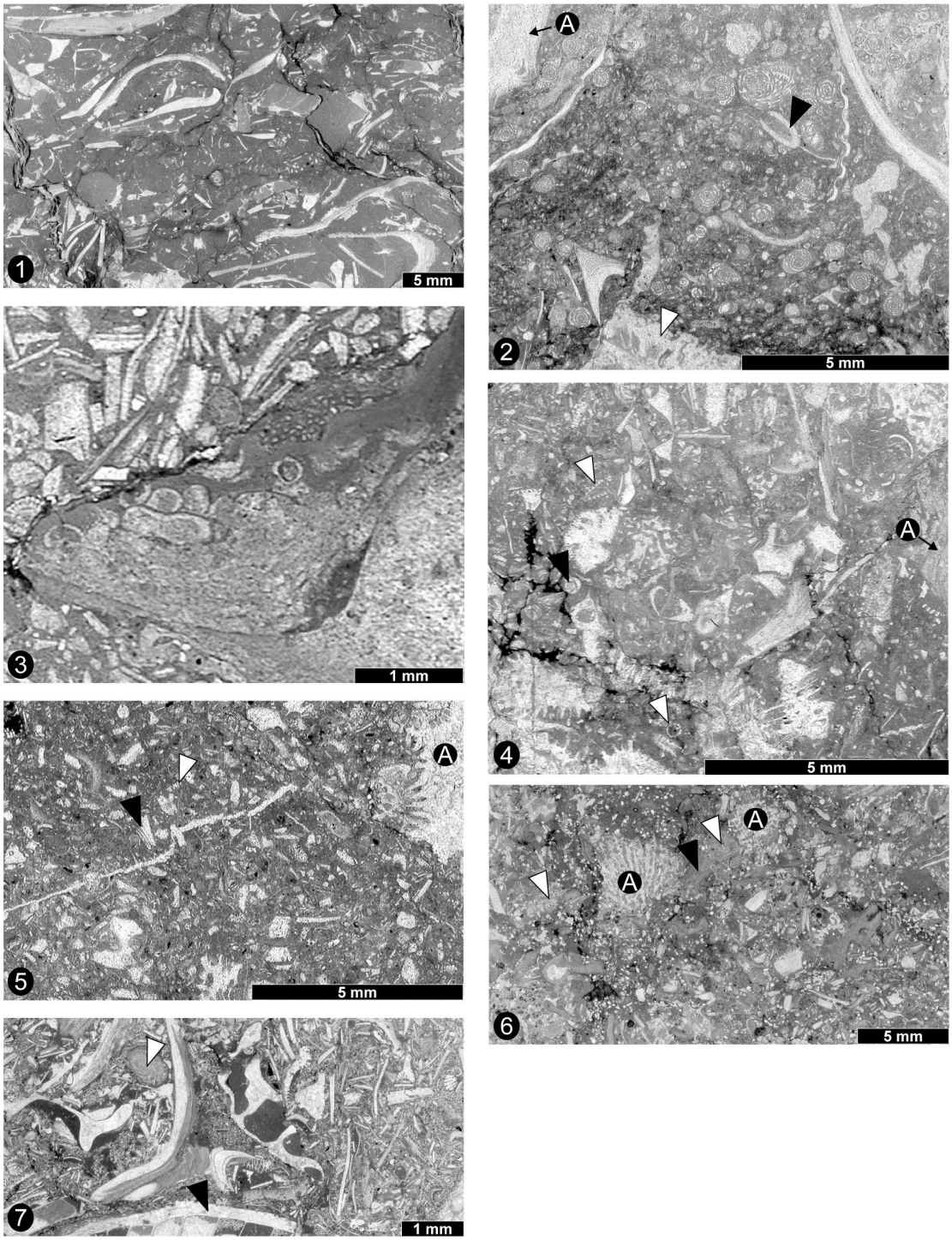

Plate 10: Microfacies of the Cardenas Formation

1 Peysonneliacean rhodoliths in a coral-rudist reef. Nuclei consist of gastropods (white arrow), rudist shells (black arrows), and peloidal grainstones (A). Arroyo de la Atarjea section, upper member.

2 Lagoonal bioclastic packstone containing recrystallized ostracods, miliolid foraminifera, and dasycladacean algae. Arroyo de la Atarjea section, lower member.

3 Siltstone of the offshore transition zone, containing benthic foraminifera (black arrow), calcified serpulid (white arrow) and recrystallized spirobid worm tubes (A). Railway 2 section, middle member.

4 Arenite of the offshore transition zone, containing branching bryozoans (A), agglutinated sabellariid worm tubes (white arrow), and fragments of calcified serpulid worm tubes (black arrows). Arroyo de la Atarjea section, middle member.

5 Arenite of the offshore transition zone, containing benthic foraminifera: *Ayalaina* (white arrow), orbitoidaceans (black arrow), and miliolids (A). Arroyo de la Atarjea section, upper member.

6 Lagoonal bioclastic packstone containing recrystallized ostracods, miliolid foraminifera, dasycladacean algae, and peloids. Arroyo de la Atarjea section, lower member.

7 Unfossiliferous arenite of the upper shoreface. Quartz and lime clasts are well-sorted and moderately rounded to rounded. Arroyo de la Atarjea section, lower member.

8 Oolithic packstone containing gastropods (A), benthic foraminifera (e.g., orbitoidaceans, white arrow), coated grains (black arrow), intraclasts (B), and abundant detrital quartz. Nuclei of the ooids consist of echinoderm fragments, benthic foraminifera, calcareous algae, and intraclasts. Pores are rare and filled by calcite spar. Sediment is interpreted as storm deposit in the lower shoreface. Section Arroyo de la Atarjea, middle member.

9 Packstone of the lower shoreface, containing miliolid foraminifera, recrystallized spirobid worm tubes, and abundant detrital quartz. Arroyo de la Atarjea, middle member.

Plate 10

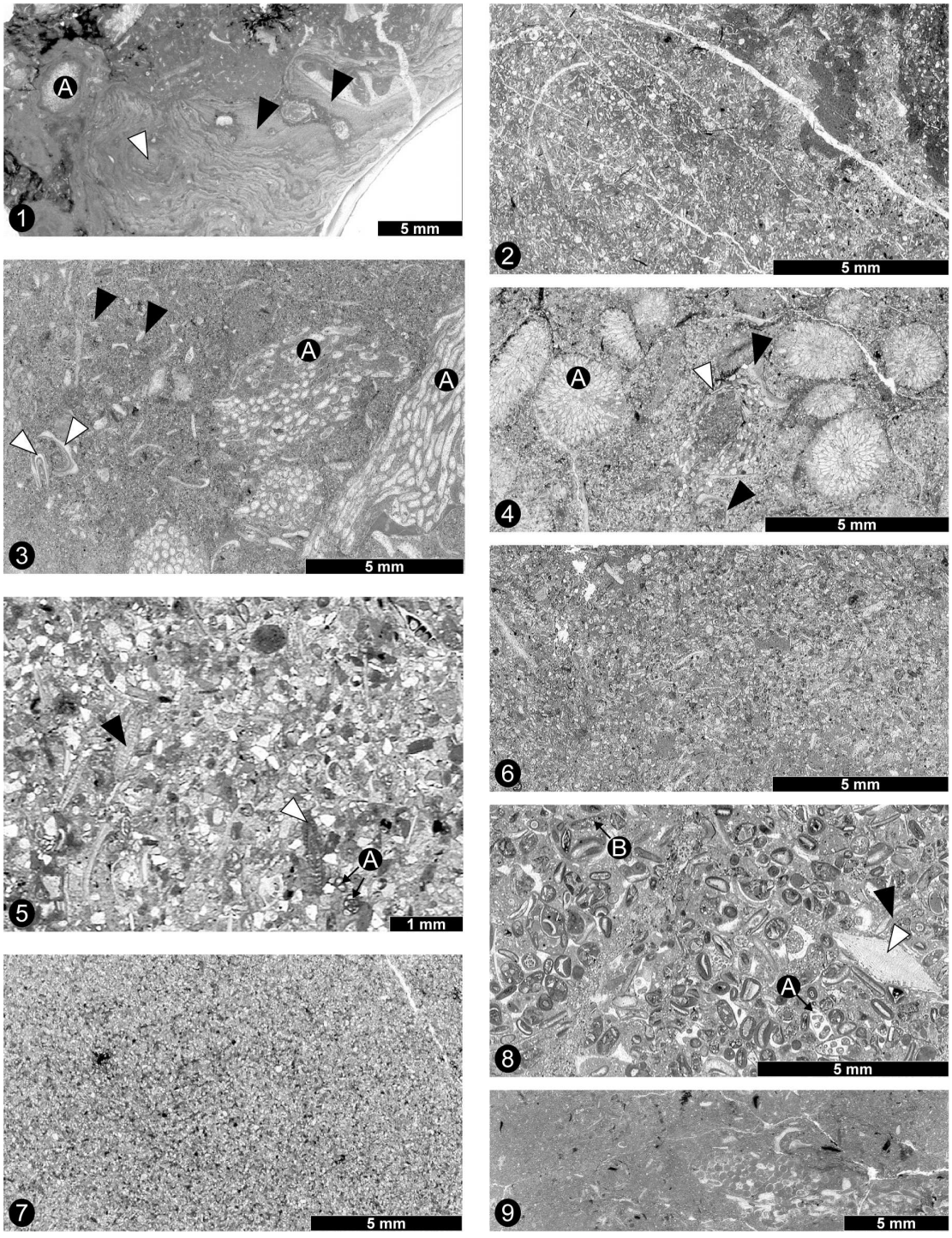

Plate 11: Microfacies of the Cardenas and Tabaco formations

1 Marly packstone of the offshore transition zone, containing benthic foraminifera (*Sulcoperculina*), sparse planktic foraminifera, and calcispheres. Railway II section, middle member.

2 Offshore siltstone, containing benthic foraminifera (orbitoidaceans), abundant planktic foraminifera and calcispheres. Arroyo de la Atarjea section, middle member.

3 Offshore siltstone, containing echinoderm fragments, planktic foraminifera, and abundant calcispheres. Arroyo de la Atarjea section, middle member.

4 Bioclastic packstone, containing gastropods (A), oyster shells (B), bryzoans (white arrow), serpulid worm tubes (black arrow), corallinacean algae (C), sparse planktic foraminifera, and abundant detrital quartz. Differing geopetal fabrics within the gastropods and serpulid tubes indicate reworking of the bioclasts. The bioclasts derived from lower shoreface to offshore environments, and sediment is interpreted as storm deposit in the offshore transition zone. Arroyo de la Atarjea section, middle member.

5 *Sulcoperculina* in offshore transitional sediment. Railway II section, middle member.

6 Conglomerate of the Tabaco Formation. Clasts consist of rudist fragments (A), red arenite and siltstone (B), peloidal (C) and corallinacean algae grainstone (white arrows). Shell fragments are bored by lithophagid bivalves, and rims of clasts are carved by *Microcodium* indicating exposure to the vadose zone (black arrow, see also Plate 11/9). The middle to coarse sand matrix consists of lime and quartz clasts, benthic foraminifera (*Sulcoperculina*, orbitoidaceans), and fragments of calcareous algae. Morales section, Tabaco Formation.

7 *Lepidorbitoides* in offshore transitional sediment. Railway II section, middle member.

8 Red sandstone of the Tabaco Formation. The fine-grained quartz and carbonate clasts are coated by hematite. Morales section, Tabaco Formation.

9 *Microcodium* in a massive rudist shell of the conglomerate of the Tabaco Formation (see also Plate 11/6). Morales section, Tabaco Formation.

Plate 11

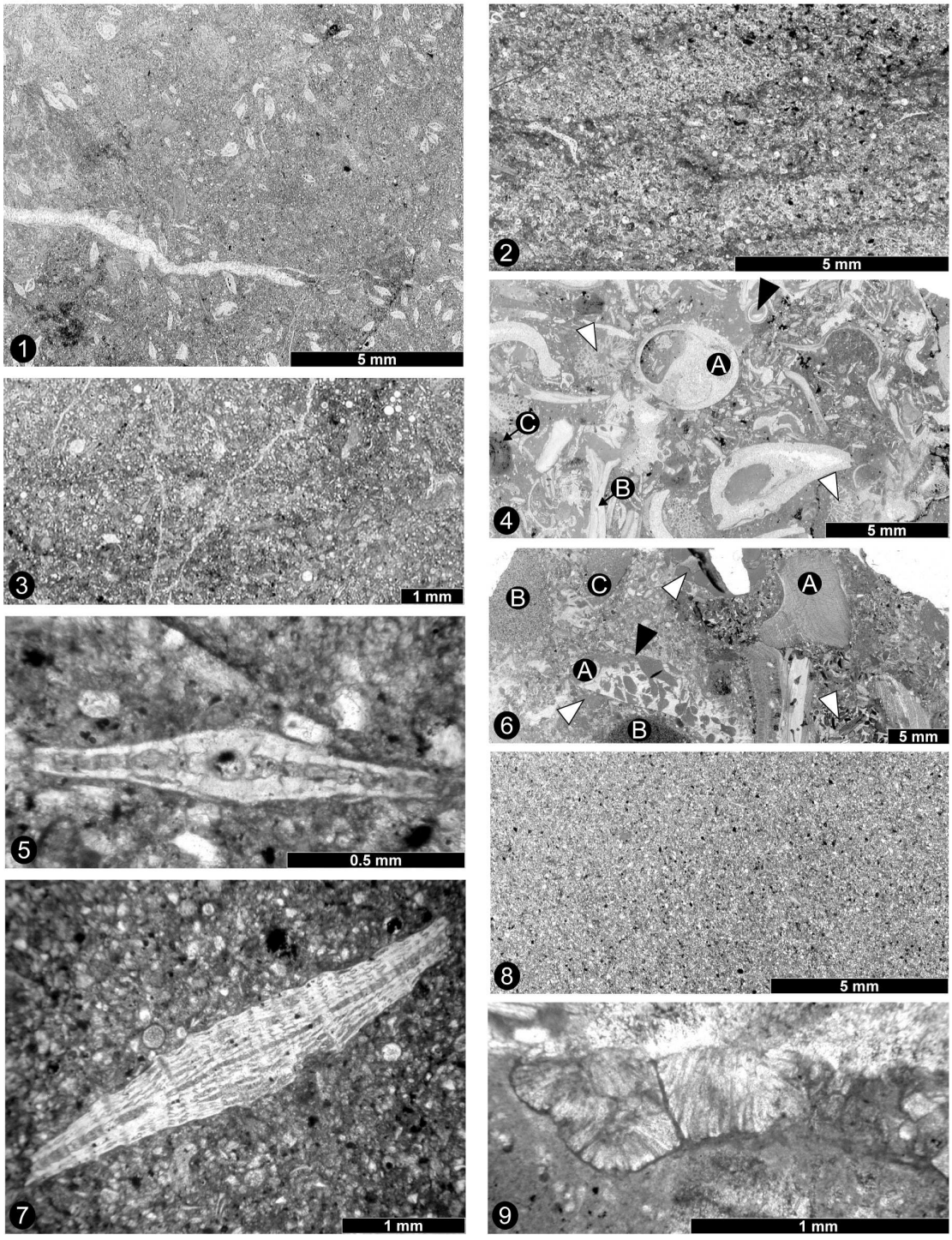

Plate 12: Planktic foraminifera of the Cardenas Formation

1 *Globotruncana arca*. Cardenas section, middle member.

2 *Globotruncana arca*. Cardenas section, middle member.

3 *Globotruncana stuarti*. Cardenas section, middle member.

4 *Globotruncana linneiana*. Arroyo de la Atarjea section, middle member.

5 *Globotruncana aegyptiaca*. Cardenas section, middle member.

6 *Globotruncana dupeublei*. Arroyo de la Atarjea section, middle member.

7 *Globotruncana linneiana*. Arroyo de la Atarjea section, middle member.

8 *Archaeocretacea cretacea*. Arroyo de la Atarjea section, middle member.

9 *Globotruncanella petaloidea*. Arroyo de la Atarjea section, middle member.

10 *Globotruncana linneiana*. Arroyo de la Atarjea section, middle member.

11 *Gansserina gansseri*. Arroyo de la Atarjea section, middle member.

12 *Rugoglobigerina rugosa*. Cardenas section, middle member.

13 *Rugoglobigerina pennyi*. Arroyo de la Atarjea section, middle member.

14 *Hedbergella monmouthensis*. Cardenas section, middle member.

15 *Rugoglobigerina rugosa*. Cardenas section, upper member.

16 *Hedbergella monmouthensis*. Cardenas section, upper member.

17 *Globigerinelloides aspera*. Arroyo de la Atarjea section, middle member.

18 *Heterohelix globulosa*. Arroyo de la Atarjea section, middle member.

19 *Guembelitria cretacea*. Cardenas section, middle member.

20 Chambers of *Rugoglobigerina rugosa*. Arroyo de la Atarjea section, middle member.

21 Chamber of *Globotruncana* sp. Cardenas section, middle member.

22 Unidentified benthic foraminifera. Arroyo de la Atarjea section, middle member.

23 Unidentified benthic foraminifera. Cardenas section, middle member.

Plate 12

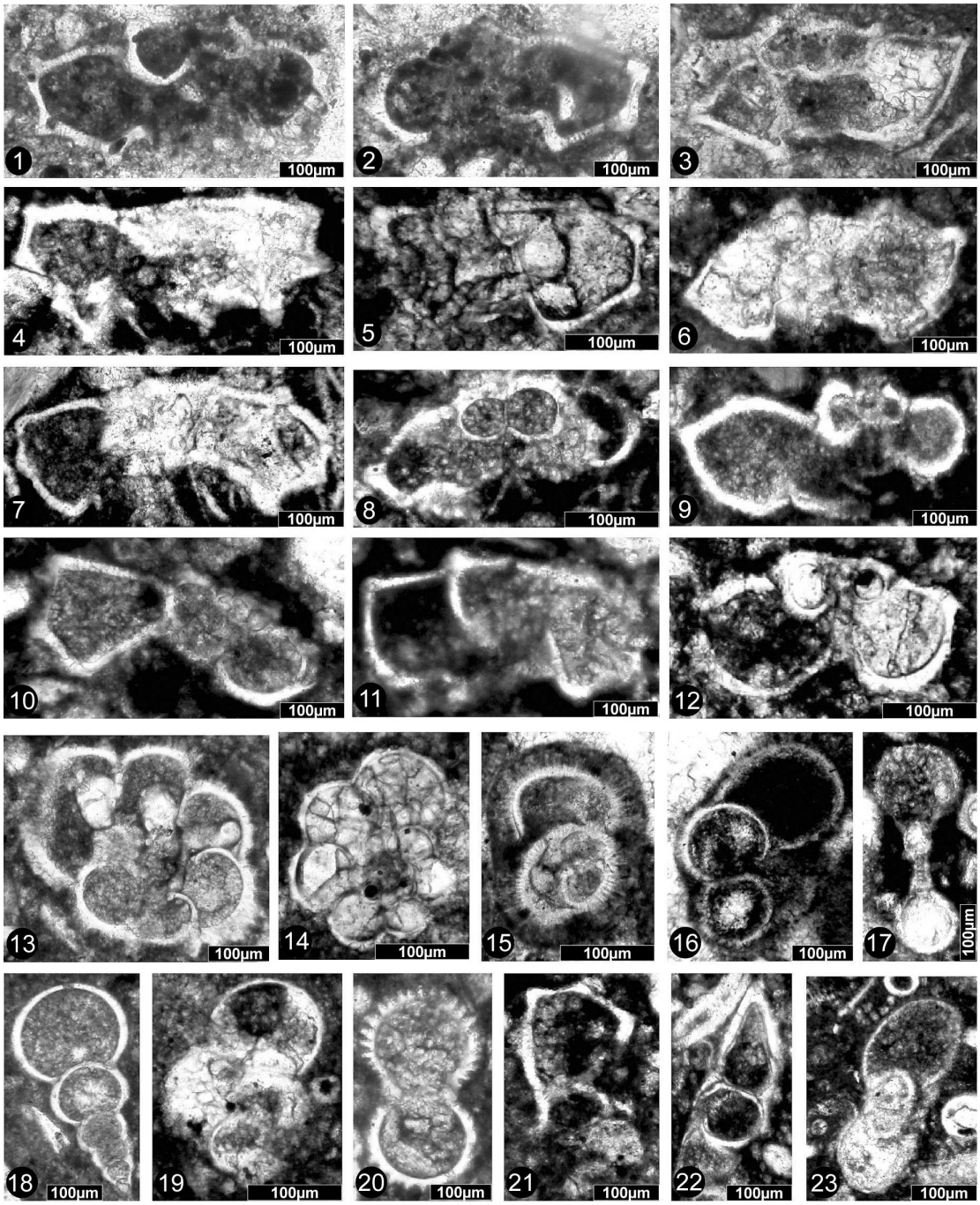
1
100µm
2
100µm
3
100µm
4
100µm
5
100µm
6
100µm
7
100µm
8
100µm
9
100µm
10
100µm
11
100µm
12
100µm
13
100µm
14
100µm
15
100µm
16
100µm
17
100µm
18
100µm
19
100µm
20
100µm
21
100µm
22
100µm
23
100µm

Plate 13: Taxonomy (scale bar: 10 mm)

1 Posterior side of *Coralliochama gboehmi* showing the constrictions and the protruding umbo of the left (free) valve as well as the rugose shell lamellae of the right valve [IGM 8877].

2 Transverse section of the left (free) valve of *Coralliochama gboehmi* (1–anterior tooth, 2–central tooth of the right valve, 3–posterior tooth, ac–accessory cavity, ma–anterior myophore, mp–posterior myophore) [IGM 8878].

3 Posterior side of *Mitrocaprina* cf. *tschoppi* showing the constrictions and the protruding umbo of the left (free) valve [IGM 8875].

4 Transverse section of the left (free) valve of *Mitrocaprina* cf. *tschoppi* (1–anterior tooth, 2–central tooth of the right valve, 3–posterior tooth, ac–accessory cavity, ma–anterior myophore, mp–posterior myophore) [IGM 8875].

5 Dorsal view of *Pugnellus densatus* showing the S-shaped ribs and the thickened shoulder (sh) [IGM 8879].

6 Ventral view of *Pugnellus densatus* (li–inner lip, lo–outer lip, ri–ridge, ro–rostrum) [IGM 8879].

Plate 13

1

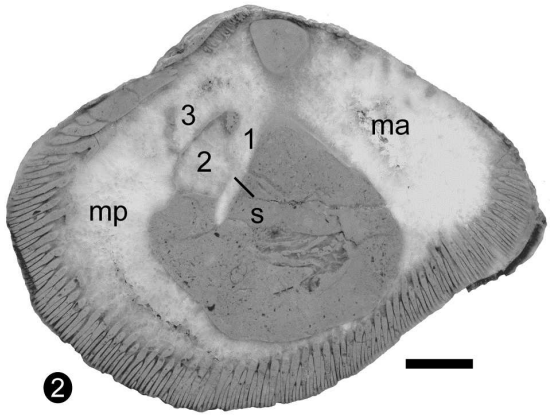

2

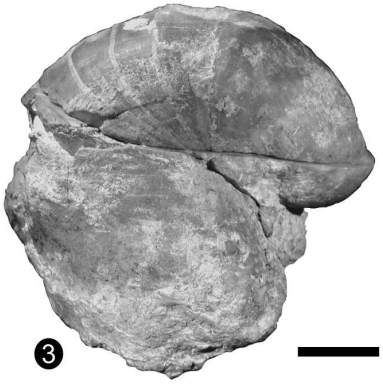

3

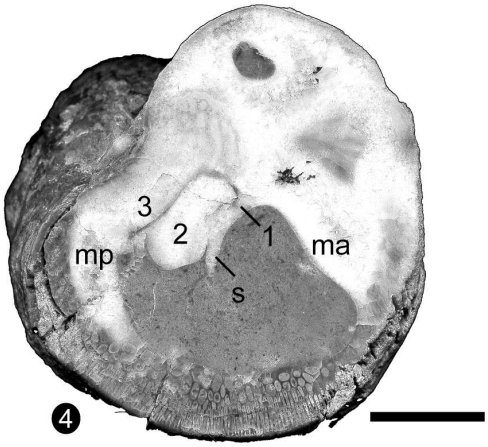

4

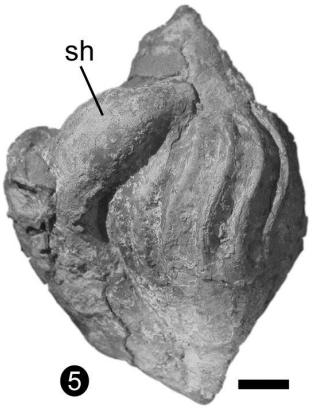

5

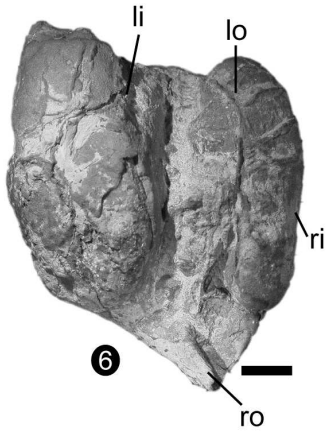

6

Plate 14: Taxonomy (Vb–ventral radial band, Pb–posterior radial band, Ib–interband between Vb and Pb; scale bar 10 mm)

1 Posteroventral aspect of *Macgillavryia nicholasi* showing the radial bands [IGM 8880].

2 Top of the right (attached) valve of *Macgillavryia nicholasi* [IGM 8880].

3 Detailed view of the polished section of the right (attached) valve of *Macgillavryia nicholasi* showing the rectangular network of the shell structure [IGM 8880].

4 Polished section of the right (attached) valve of *Macgillavryia nicholasi* with radial pattern of bifurcating U-shaped funnel plates [IGM 8880].

Plate 14

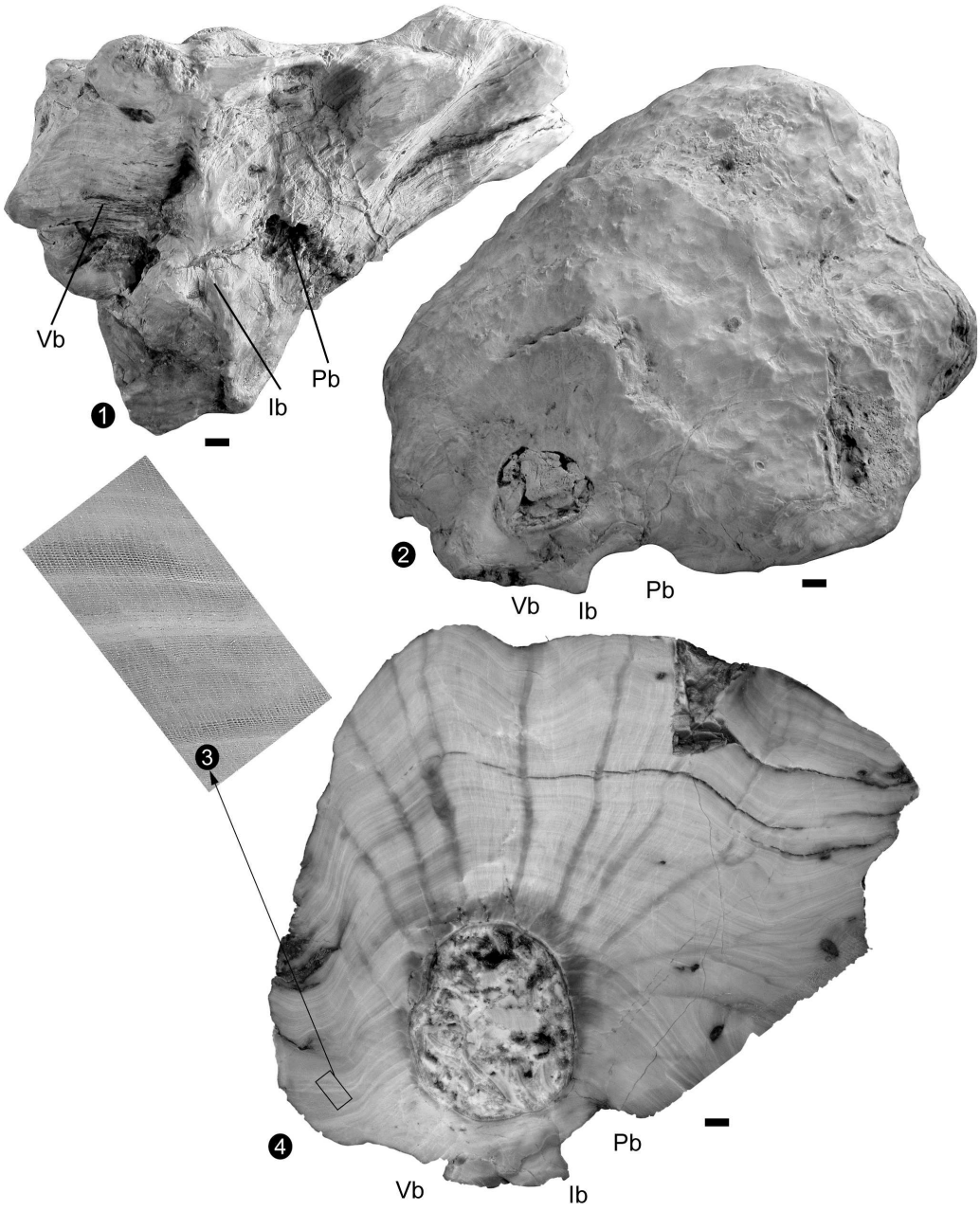

Plate 15: Taxonomy (Vb–ventral radial band, Pb–posterior radial band, Ib–interband between Vb and Pb; figures 1–9: scale bar 10 mm; figure 10: scale bar 5 mm)

1 Top of the right (attached) valve of *Tampsia poculiformis* showing the wavy commissural surface [IGM 8881].

2 Anterior aspect of *Tampsia poculiformis* showing the irregular shell lamellae [IGM 8881].

3 Narrow ridge on top of the right (attached) valve of *Tampsia poculiformis* The ridge is located in a triangular depression and marks the location of Vb [IGM 8881].

4 Posteroventral aspect of *Tampsia poculiformis* showing the radial bands [IGM 8881].

5 Top of the right (attached) valve of a small *Tampsia poculiformis*. Undulations are less pronounced than in bigger specimen, but prominent ribs show the location of the radial bands [IGM 8882].

6 Anterior side of *Tampsia poculiformis* showing the smooth grooves and costae in the upper part of the right (attached) valve [IGM 8882].

7 Posteroventral aspect of the right (attached) valve of *Tampsia poculiformis* showing the slit at Vb formed by sharp V-shaped upfolds of the shell lamellae and the pronounced rib representing Ib [IGM 8882].

8 Transverse section of the right (attached) valve of *Tampsia poculiformis* showing undulated funnel plates and the characteristic polygonal pattern of the muri [IGM 8882].

9 Detailed view of the slit at Vb of the right (attached) valve of *Tampsia poculiformis* formed by V-shaped funnel plates [IGM 8882].

10 Detailed view of the polygonal shell structure of the right (attached) valve of the paratype of *Tampsia poculiformis* described by Myers (1968), catalogue number WSA 14933.

Plate 15

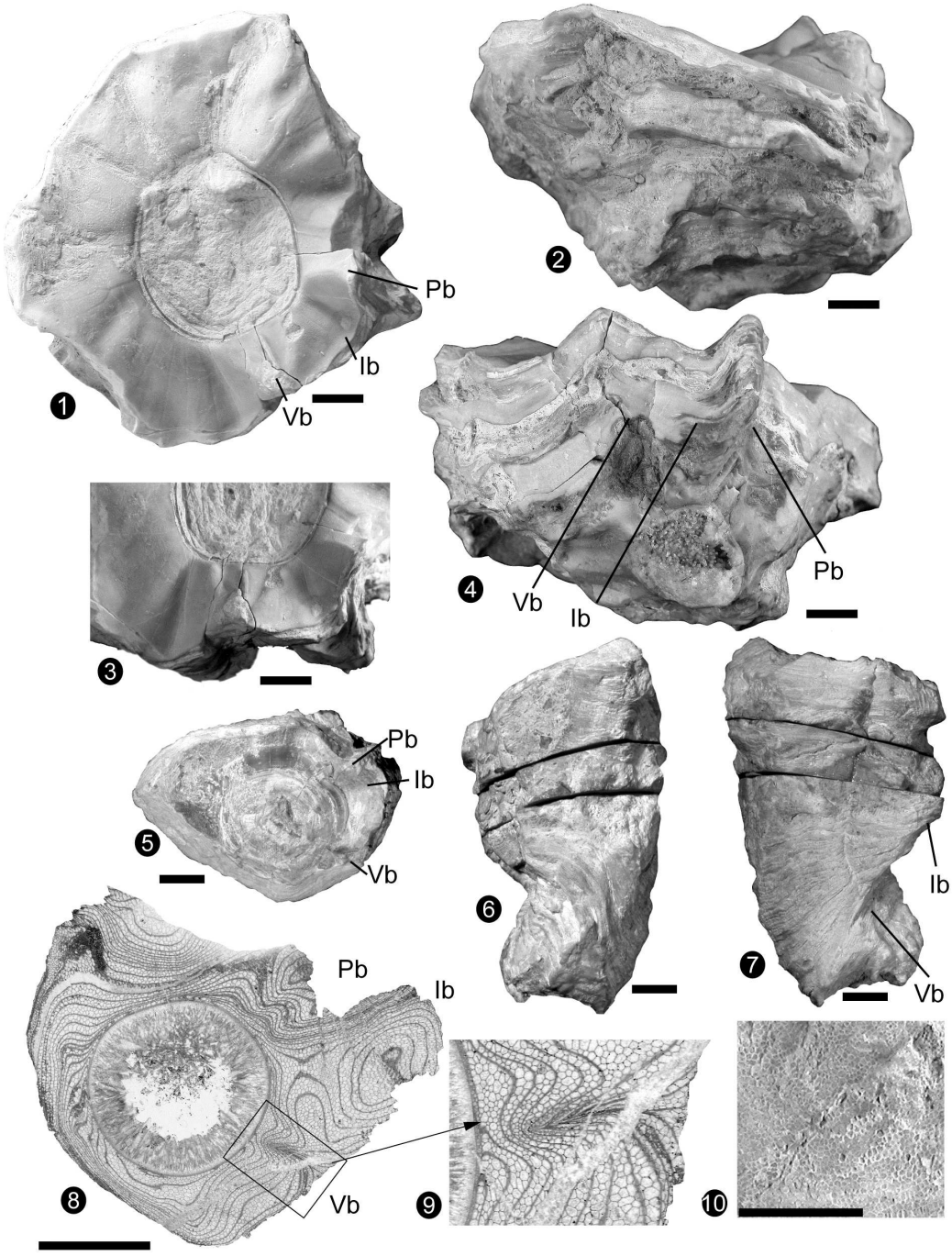

Plate 16: Taxonomy (scale bar 10 mm)

1 Posteroventral aspect of the right (attached) valve of *Bournonia cardenasensis* showing the pronounced ribs and grooves (Vb–ventral radial band, Pb–posterior radial band, Ib–interband between Vb and Pb) [IGM 8883].

2 Left (free) valve of *Bournonia cardenasensis* showing the projecting ribs of Vb and Pb (Vb–ventral radial band, Pb–posterior radial band, Ib–interband between Vb and Pb) [IGM 8884].

3 Transverse section of the right (attached) valve of *Bournonia cardenasensis* showing the myocardinal apparatus (1–anterior tooth, 2–central tooth of the right valve, 3–posterior tooth, ac–accessory cavity, ma–anterior myophore, mp–posterior myophore) [IGM 8885].

4 Transverse section cutted parallel to a horizontal funnel plate in a rib of the right (attached) valve *Bournonia cardenasensis* showing the top of the spines [IGM 8885].

5 Detailed view of the spiny funnel plates in the right (attached) valve of *Bournonia cardenasensis* [IGM 8885].

6 Left (free) valve of ?*Praebarrettia sparcilirata*. P0, P1 and P2 penetrate through the shell (P0–anterior pillar or “ligamental ridge”, P1–central pillar, P2–posterior pillar) [IGM 8888].

7 Tranverse section of the right (attached) valve of ? *Praebarrettia sparcilirata* showing the pillars and pseudo-pillars (P0–anterior pillar or “ligamental ridge”, P1–central pillar, P2–posterior pillar) [IGM 8887].

8 Transverse section through a bouquet of *Hippurites* cf. *perkinsi*. showing P0, P1, P2 in the right (attached) valves (P0–anterior pillar or “ligamental ridge”, P1–central pillar, P2–posterior pillar) [IGM 8886].

9 Detailed view of the cellular shell structure of the right (attached) valve of *Hippurites* cf. *perkinsi* [IGM 8886].

10 Right (attached) valve of ?*Praebarrettia sparcilirata* showing the rounded ribs and grooves [IGM 8889].

Plate 16